UNIVERSITÀ DI PARMA

UNIVERSITA' DEGLI STUDI DI PARMA

DOTTORATO DI RICERCA IN
" *Scienze Medico-Veterinarie*"

CICLO XXXIV°

"Valutazione con tomografia computerizzata dello sviluppo dell'articolazione del gomito: confronto tra Pastore tedesco e Labrador retriever"

"Computed tomographic assessment of elbow joint development: comparison between German shepherd and Labrador retriever"

Coordinatore:
Chiar.mo Prof. Donofrio Gaetano

Tutore:
Chiar.ma Prof.ssa Volta Antonella

Dottorando: Dott.ssa Fumeo Martina

Anni Accademici 2018/2019 – 2020/2021

INDEX

ABBREVIATIONS

AUC: Area Under the Curve

CED: Canine Elbow Dysplasia

CT: Computed Tomography

FCP: Fragmented Coronoid Process

GSDs: German Shepherd Dogs

IC: joint incongruity

ICC: Inter-Class Correlation

LRDs: Labrador Retriever Dogs

MCD: Medial Coronoid Disease

MCP: Medial Coronoid Process

MPR: Multiplanar Reconstruction

OC: Osteochondrosis

OCD: Osteochondritis Dissecans

ROC: Receiver Operating Characteristic

ROI: Regions of Interest

TNS: Trochlear Notch Sclerosis

UAP: Ununited Anconeal Process

ABSTRACT

La tomografia computerizzata, nonostante non sia la metodica diagnostica "gold standard" per la displasia del gomito, è stata proposta ed utilizzata con successo per la sua sensibilità e specificità elevate nei confronti di questo gruppo di patologie, soprattutto grazie alla possibilità di ottenere una ricostruzione multiplanare dell'articolazione del gomito, con il vantaggio di una bassa invasività.

Lo scopo di questo studio era ottenere una migliore comprensione della displasia del gomito esaminando, attraverso l'uso della tomografia computerizzata, gomiti sani e patologici in due diverse razze di cani in accrescimento, Pastore tedesco e Labrador retriever, proponendo un approccio alla patologia più orientato alla razza.

Le immagini tomografiche delle articolazioni del gomito di 34 Pastori Tedeschi e 20 Labrador retriever in accrescimento sono stati valutati a 6 e 12 mesi di età per descrivere le caratteristiche tomografiche di gomiti sani e patologici, mettendo in comparazione le due razze e raccogliendo misurazioni al fine di stabilirne un potenziale valore predittivo con l'obiettivo di ottenere una diagnosi precoce.

Nella popolazione in esame, la frammentazione del processo coronoideo/malattia del comparto mediale (FCP/MCD) è stata la condizione patologica più frequente in entrambe le razze. La misurazione dei valori di attenuazione del solco semilunare, in particolare nell'area distale, è risultata più significativa nel gruppo di cani di razza Labrador retriever; in questa razza la sclerosi subtrocleare era la principale manifestazione associata allo sviluppo della displasia, e l'osteocondrosi non articolare e la necrosi ossea la sospetta condizione patologica sottostante. Inoltre, sono stati rinvenuti valori HU molto più elevati in questa razza rispetto al Pastore tedesco. Nel gruppo di Pastori tedeschi, infatti, la presenza di uno step radio-ulnare e di un solco trocleare ulnare ellittico sono risultati significativamente associati allo sviluppo di displasia, mentre la sclerosi è risultata meno predittiva, per cui in questa razza l'incongruenza articolare potrebbe giocare un ruolo chiave nella patogenesi di questa complessa malattia.

Da questo studio possono essere ipotizzate quindi due diverse eziopatogenesi per la stessa patologia nei due gruppi di Pastori tedeschi e Labrador retriever, da tenere in considerazione in studi futuri su queste razze.

Un approccio maggiormente orientato alla razza potrebbe essere fondamentale nella realizzazione di ulteriori studi sulla displasia del gomito, in quanto potrebbe consentire una miglior caratterizzazione delle manifestazioni patologiche in relazione alla razza, in particolare in stadio precoce ed in accrescimento, e soprattutto per quanto riguarda l'eziopatogenesi della malattia e il trattamento.

ABSTRACT

Computed tomography (CT), despite not being the gold standard diagnostic technique for elbow dysplasia, has been proposed and largely used for its sensitivity and specificity towards this multifaceted disease, giving the possibility of a precise multiplanar reconstruction of the elbow joint with low invasiveness.

The aim of this study was to improve the current understanding of this pathology by studying through CT examination normal and affected elbow joints of growing dogs of two different breeds, German shepherd dogs and Labrador retriever dogs, proposing a more breed-oriented approach.

The elbow joints of 34 GSDs and 20 LRDs during growth have been evaluated at 6 and 12 months of age through CT by different operators, to describe tomographic findings in both healthy and affected joints, making comparisons between the two breeds and collecting several measurements with a potential predictive value in order to achieve an early diagnosis.

In the population of this study, fragmented coronoid process/medial compartment disease (FCP/MCD) was the most frequent form of elbow dysplasia in both breeds. Measurements of the attenuation values of the trochlear notch, especially in its distal area, were more useful in the LRDs; in this breed subtrochlear sclerosis was the main manifestation associated to the development of elbow dysplasia, with higher HU values in the subchondral bone, and non-articular osteochondrosis or bone necrosis was the suspected underlying pathologic condition. In the GSD, the presence of a radio-ulnar step and an elliptical ulnar trochlear notch were found significantly associated with CED, while sclerosis resulted less predictive, therefore in this breed joint incongruity could play a key role in the development of elbow dysplasia.

According to our results, two different etiopathogenesis could be hypothesized for the same disease in the two evaluated groups of German shepherds and Labrador retrievers, which should be taken into consideration in future studies on these breeds.

A more breed-oriented approach could be fundamental in further studies on CED and could allow to better characterize the breed dependent manifestations of these conditions, the etiopathogenesis and the potential treatment, especially during growth and at an early stage.

1. INTRODUCTION

Elbow dysplasia is a progressive, hereditary, polygenic, multifactorial, complex developmental disease, usually identified with a group of four pathologies, often occurring in combination: fragmented medial coronoid process (FCP), ununited anconeal process (UAP), osteochondrosis (OC) or osteochondritis dissecans (OCD), and incongruity (IC) of the elbow joint.

Elbow dysplasia is also described as every developmental abnormality, which progressively leads to osteoarthritis (OA).

A long-term goal, especially set by the International Elbow Working Group (IEWG), has been to reduce the prevalence of this pathology through early diagnosis and selective breeding, mostly basing on radiographic screening.

Computed tomography (CT) has often been proposed as a reliable diagnostic tool for the diagnosis of canine elbow dysplasia. CT is well known to have many advantages over radiography, including a full anatomic detail of the bony structures of the elbow joint, without any superimposition, as well as the possibility of computer reconstruction of multiplanar images.

CT could represent a valid support to radiology for the early diagnosis of canine elbow dysplasia, and above all an efficient diagnostic tool complementary to radiography, whenever this technique results unclear or in those subjects with secondary signs of pathology or potentially symptomatic, in alternative to the more invasive arthroscopy, currently considered as the gold standard.

An early diagnosis could be fundamental in leading to a correct treatment plan and/or prognosis. In human medicine, computed tomography is widely used to image joints of immature and mature patients for diagnostic purposes, surgical planning, and evaluation of therapeutic interventions.

This study will be focused on the use of computed tomography on the elbow joints, either healthy or affected, of two groups of growing dogs of different breeds, German shepherd dogs and Labrador retriever dogs, at 6 and 12 months of age. Morphologic features and specific measurements will be collected through CT examination in the two groups and evaluated in comparison.

The aim of this research is to describe tomographic features of healthy and affected elbow joints during growth in the two breeds, to improve current understanding of canine elbow dysplasia and to assess the usefulness of computed tomography for the early diagnosis of this pathology in dogs, determining its sensitivity and sensibility to early changes in different breeds, monitoring the progression of the disease. To detect the earliest signs of elbow dysplasia, specific measurements were taken in the two breeds groups, compared from 6 to 12 months of age and in relation to the assigned elbow dysplasia grades, to discover their eventual predictive values.

It could also be used as a reliable method to further investigate the development of canine elbow dysplasia in growing dogs of different breeds, allowing a deeper understanding of the evolution of this pathology, in particular regarding its etiopathogenesis, which still remains unclear. In fact, the purpose of this study is to make comparisons between two different breeds, and to observe if and how the development of elbow joints differs among them, comparing and studying the same characters in different breeds throughout their growth, showing differences and common features in the elbow joints; the main hypothesis is that there could be some feature or character representing a breed-dependent early sign of the pathology.

2. ELBOW JOINT

2.1. ANATOMY

The humero-radio-ulnar joint, or elbow joint (*articulatio cubiti*), is a synovial composite joint (Figures 1 - 2), hence constituted by three joints: the humeral condyle articulates with the head of the radius in the humero-radial joint (*articulatio humeroradialis*), and with the trochlear notch of the ulna in the humero-ulnar joint (*articulatio humeroulnaris*), lastly the proximal radio-ulnar joint (*articulatio radioulnaris proximalis*) connects to the humero-radial and humero-ulnar joints freely. (Evans & De Lahunta, 2013)

The distal articular surface of the humerus is divided in two portions (Martini, 2006): the medial portion is the trochlea humeri, which gives stability to the elbow joint, while the capitulum is the lateral part, and, according to Samoy et al. (2006), is accountable for more than 80% of the weight bearing. In vitro studies from Mason et al. (2005) demonstrated that the weightbearing load is then equally distributed to the antebrachium from the capitulum to the radial head and from the trochlea humeri to the ulnar trochlear notch.

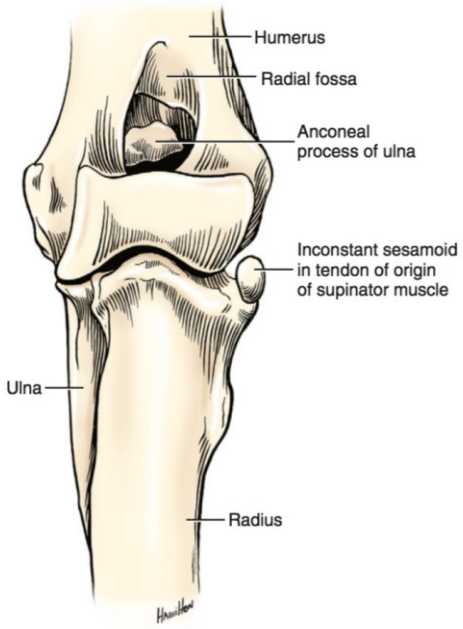

Figure 1. Left elbow joint, cranial view. From Miller's anatomy of the dog, 4th edition, p.132

The elbow joint is a perfect angular ginglymus with a high level of congruence (Martini, 2006), a typical hinge-joint with flexion and extension on the sagittal plane as the main range of motions and a limited range of rotation, therefore permitting a certain degree of supination and pronation at all levels of flexion and extension. (Burton and Owen, 2008)

In the dog, depending on the breed, the extension is possible between 100° and 140°. (König et al., 2004) In general, it is estimated that the normal range of motion of an elbow joint is approximately between 36° in flexion and 165° in extension, with a mean value of about 130°. (Tobias et al., 2013)

The contraction of the *triceps brachii* muscle, attached to the olecranon, with the contribution of the *anconeus* and the *tensor fasciae antebrachii* muscles (all innervated by the radial nerve), is accounted for achieving the extension of the elbow joint. (Tobias et al., 2013)

On the other hand, muscles localized to the anterior aspect of the limb, comprising mainly the *biceps brachii* and *brachialis* muscles, attached for the most part to the ulnar tuberosity and innervated by the musculocutaneous nerve, are responsible for flexion of the elbow joint. (Tobias et al., 2013)

Recent studies have suggested that these muscles could contribute to the development of elbow dysplasia by creating shear forces which could affect the medial coronoid process (Hulse et al, 2010).

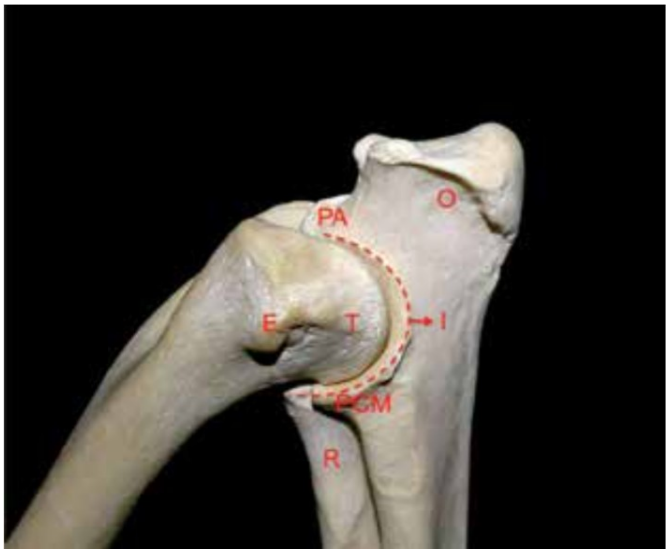

Figure 2. Elbow joint, media-lateral view. (PA) Anconeal Process; (O) Olecranon; (E) Medial Epicondyle; (T) Trochlea Humeri; (I) Semilunar, or trochlear, Notch; (PCM) Medial Coronoid Process; (R) Radius. From "La displasia di gomito nel cane: approccio preventivo", by A. Bonardi, C.J. Eid, F. Lusetti, AIVPA Journal, 2014, p.30

Lateral or rotational movements are avoided by the presence of prominent ridges and grooves on the trochlear surface and by the protrusion of the olecranon into the olecranon fossa of the humerus. (König et al., 2004)

Two separate synovial radio-ulnar articulations, the proximal radio-ulnar joint, formed by the articular circumference of the radius and the radial notch of the ulna, and the distal radio-ulnar joint, formed by the articular circumference of the ulna and the ulnar notch of the radius, are responsible for the capacity of rotational movements as pronation and supination. (König et al., 2004)

Although it is said that the rotational range of motion of the elbow joint varies greatly between individuals (Tobias et al., 2013), according to De Ryeke et al. (2002) generally the forepaws can be supinated approximately 90°, as enough rotational movement is permitted at the radio-ulnar and carpal joints. During supination and pronation, stabilization is provided mainly by the thick medial and lateral collateral ligaments and by the cranial extension of the anconeal process of the ulna into the deep olecranon fossa of the humerus. (Evans & De Lahunta, 2013; Tobias et al., 2013)

The elbow joint is stabilized by, in addition to the conforming shape of its articular surfaces, the joint capsule, thicker on the cranial flexor surface, the collateral ligaments, and the muscles and tendons, which give solidity to the cranial and caudal articular surfaces. (Barone, 2004) (Figure 3)

The joint capsule is common to all three articular parts and appears as a wide irregular sleeve. (Martini, 2006) It is tightly stretched on the sides, but it expands cranially and caudally. (Evans & De Lahunta, 2013)

On the cranial flexor surface the capsule attaches proximal to the coronoid fossa and the radial fossa, then under the basement of the lateral and medial epicondyles, not far from the articular surface, and, finally, it forms a loose, fat-covered synovial pouch above the olecranic fossa. (Barone, 2004)

The joint capsule proceeds distally between the radial notch of the ulna and the articular circumference of the radius (Evans & De Lahunta, 2013), close to the articular surfaces, and it proceeds to take part in the proximal radio-ulnar joint. (Barone, 2004)

However, in the dog the cranial part of the capsule attaches distally not on the radius but directly on the annular ligament (*lig. anulare radii)*, which strongly hooks this bone up to the ulna. (Barone, 2004) This ligament, running transversely around the radius and attached to the coronoid processes, has the function of stabilising the radio-ulnar joint, while allowing axial rotation of the elbow. (Evans & De Lahunta, 2013; Martini, 2006)

Proximally to the lateral epicondyle of the humerus the lateral collateral ligament (*lig. collaterale cubiti laterale*) is attached and divided distally into two crura, a slightly larger cranial one attached to the radius, and a flatter caudal crus which passes on the ulna. (Evans & De Lahunta, 2013) The function of this ligament is to prevent the adduction of the elbow. (Martini, 2006) At the level of the articular circumference the ligament blends with the annular ligament and, as described by Baum and Zietzschmann (1936), often contains a sesamoid bone.

The medial collateral ligament (*lig. collaterale cubiti mediale*) is thinner but longer than the lateral one, though quite similar. It attaches proximally to the medial epicondyle of the humerus, crosses the annular ligament distally, and divides into two crura. (Barone, 2004) The function of this ligament is to prevent the abduction of the elbow. (Martini, 2006)

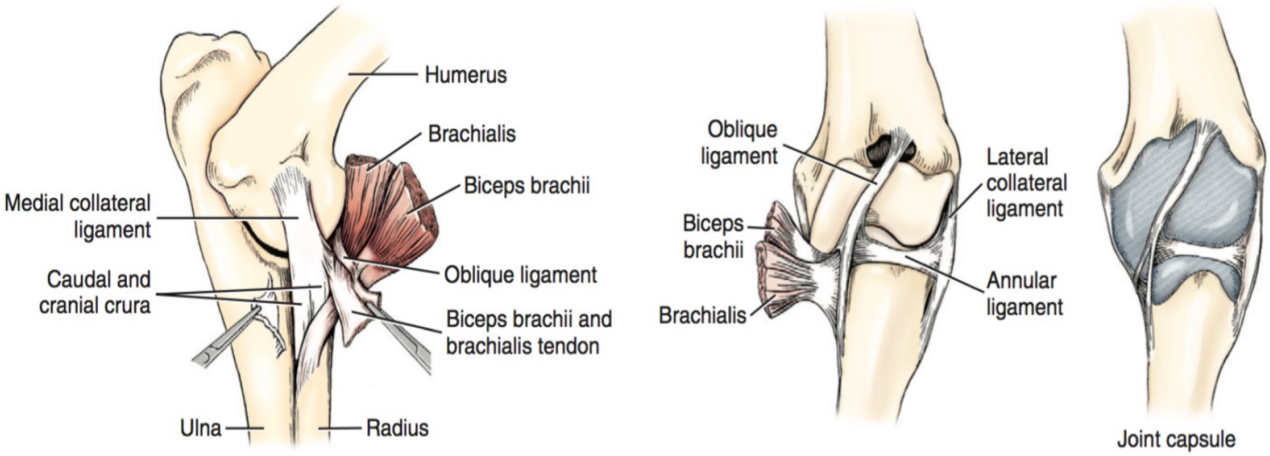

Figure 3. Medial aspect and cranial aspect of the left elbow joint of a dog. From Miller's anatomy of the dog, 4th edition, p. 170

Other contributors to the stability of the elbow are the olecranon ligament (*lig. olecrani*), placed between the craniomedial aspect of the olecranon to the medial border of the olecranon fossa, and the oblique ligament, a small branch of the joint capsule which connects to the medial collateral ligament. (Evans & De Lahunta, 2013)

2.2. ELBOW DEVELOPMENT

The thoracic limb-bud develops prior to the pelvic one, approximately on day 23 of gestation (about 5mm long embryo), as an oval paddle close at midbody. On day 25 (14 mm) the first signs of digit formation can be detected. Digits are quite distinct by day 30, when the thoracic limb has pronated and lengthened, followed by a further increase by day 35 (35 mm) in which the joints appear more delimited and digits develop claws. Meanwhile, in both limbs perichondral ossification of the long bones begins in the middle of the diaphysis, resulting in primary bone collars without endochondral involvement. (Evans & De Lahunta, 2013)

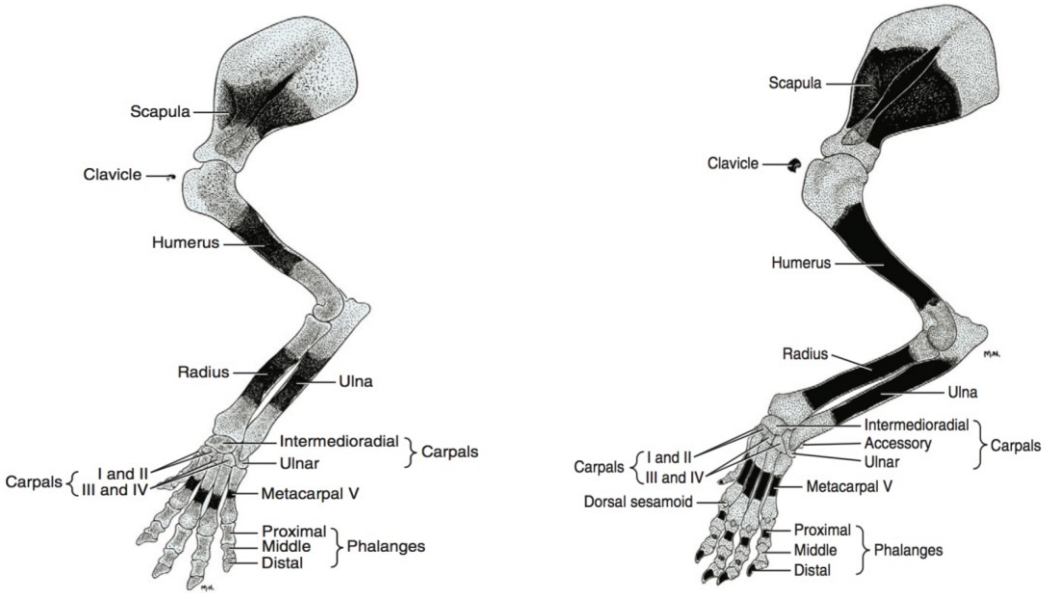

Figure 4. Ossification of the pectoral girdle and limb of a 55-mm (42-day) Beagle fetus and of a 93-mm (45-day) Beagle fetus. From Miller's Anatomy of the dog, 4th edition, p. 51

The humerus, radius, and ulna do not form epiphyses prior to birth. (Evans & De Lahunta, 2013) (Figures 4 – 5)

The humerus develops from a main ossification centre and six secondary ossification centres: two forming the proximal extremity, in particular the articular head (*caput humeri*) and the greater tubercle (*tuberculum majus*), and four forming the distal extremity (capitulum humeri, trochlea humeri, medial and lateral epicondyles). The lesser tubercle (*tuberculum minor*) in the dog develops by a simple expansion of the humeral head centre. The main ossification centre is present from the fourth week of gestation, while the secondary centres appear much later, some weeks after birth. The first to appear is the centre of the head, and the last one belongs to the lateral epicondyle. (Barone, 2004)

Distal epiphyses are the first to close in all the skeleton, from the seventh to the eighth month of life. On the other side, the proximal epiphyses appear to be the last ones, between 12 and 15 months old. (Barone, 2004)

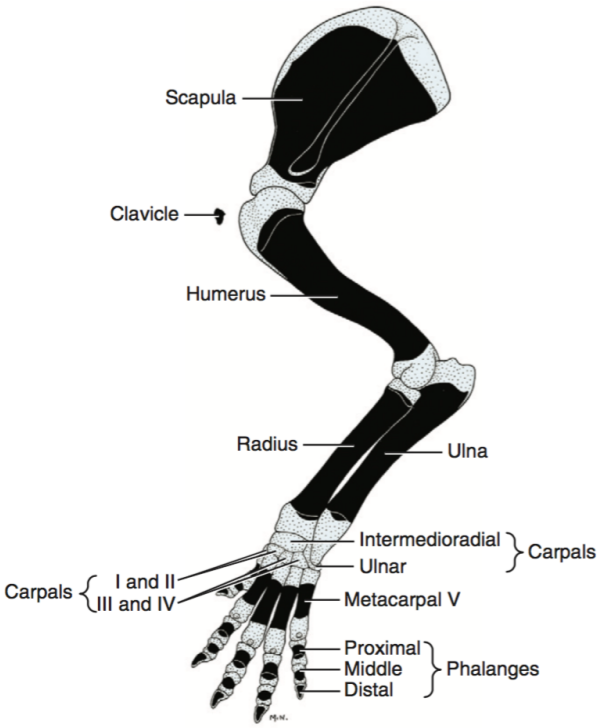

Figure 5. The thoracic limb and girdle at birth (60 days). From Miller's Anatomy of the dog, 4th edition, p.51

The radius develops from a primary ossification centre, which appears around the 4th week of gestation, and two secondary centres, one for the proximal extremity and the other for the distal extremity, both present from the fourth week after birth. The proximal epiphysis closes between 9 and 10 months old, while the distal epiphysis closes later, within 16 and 18 months old. (Barone, 2004)

The ulna similarly has one main ossification centre, forming at the same period than the radial primary centre, and two secondary centres, which develop usually later, around the 2nd week after birth. It's useful to remember that the proximal centre originates only the edge of the olecranon, and that the distal centre is not at the same level as the radius is, because of the difference in length. (Barone, 2004)

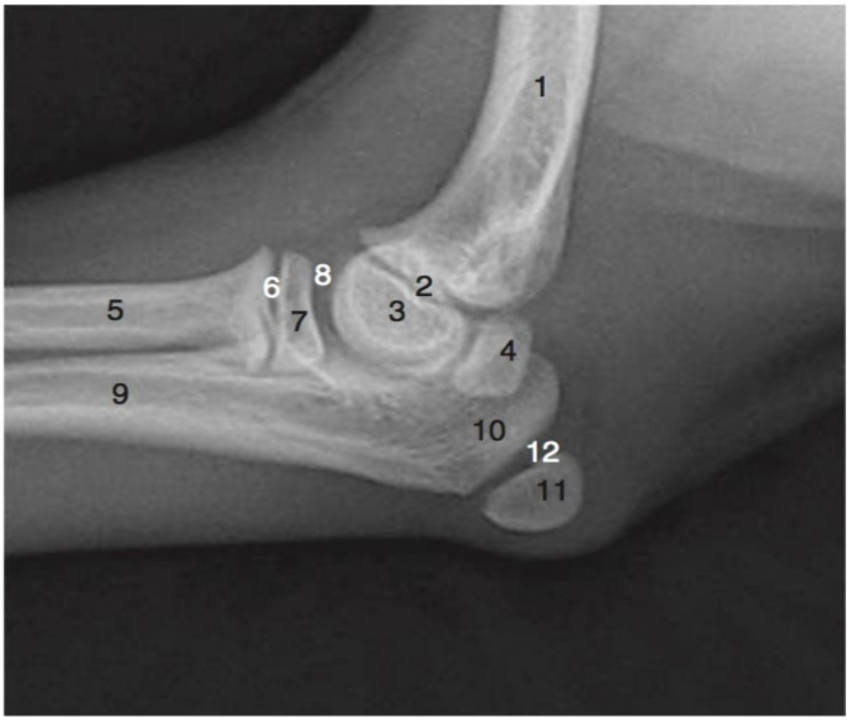

Figure 6. Lateral radiograph of a young dog's elbow: 1. Humerus, 2. Distal humeral physis, 3. Humeral condyle (distal epiphysis), 4. Medial epicondyle (apophysis), 5. Radius, 6. Proximal radial physis, 7. Head of radius (proximal epiphysis), 8. Radiohumeral joint, 9. Ulna, 10. Olecranon, 11. Olecranon tuber (apophysis), 12. Physis for olecranon tuber. From Miller's Anatomy of the dog, 4th edition, p.135

The two ulnar epiphyses close then in dogs between 7 and 11 months old. (Barone, 2004)

It has been esteemed that in the dog the 90% of the bones' growth in length is achieved during the first 6-7 months of life, with few variations mostly due to the animal's size. (Carmichael, 1998)
The epiphyseal plates responsible for the length growth of the forearm are essentially three: the proximal and distal plates of the radius and the distal plate of the ulna (while the proximal ulnar plate contributes poorly). (Figure 6) As a result, any interruption or disturbance during the growth of each one of these physes could lead to a shortening and angular deformation of the forearm, since radius and ulna are to be considered as a paired bone system, whose development must be synchronized. (Nardella, 2010)

2.3. BIOMECHANICS

In the recent years, biomechanical studies have gained growing interest among researchers, carrying out a variety of studies, including geometrical studies, transarticular joint forces mapping, joint contact patterns, joint development, subchondral bone density distribution, limb alignment and gait analysis. (Alves-Pimenta et al., 2019; Preston et al., 2000; Dickomeit et al., 2011; DeCamp et al., 1993; Burton et al., 2013; Carone et al., 2014, Lau et al., 2015)

Despite the great variety of conformations between breeds, even between those of similar size and weight, dogs generally carry about 60% of their weight in their forelimbs, and the remaining 40% in their hindlimbs during standing positions, with few differences between breeds when normalized to the weight of the dog. In a recent research by Humphries and colleagues (2020), kinematics and kinetics of 60 German shepherd dogs were evaluated after dividing the group according to their back conformation (levelled or sloped back). Sloped back dogs resulted in having an increased loading on the forelimbs compared to the other group, but still not as high as the result found by other researchers on a group of sound Labrador retrievers, in which about 69% of their weight was carried in the forelimbs. This feature was later confirmed in another research by Humphries et al. (2020), in which

a comparison between German shepherd dogs (GSDs) and Labrador retriever dogs (LRDs) biomechanics was carried out; in their study, higher vertical forces supported by the fore digital pads were noted in LRDs, along with increased weight bearings, while a more exaggerated hip extension and stifle and hock flexion angles were reported in the GSD. These findings seemed to indicate that the majority of the weight is borne on the forelimbs by LRDs, while moved between hindlimbs and forelimbs in GSDs.

According to literature, the assessment of the contact areas on the surface of a joint, whose size and position is dependent on both the forces acting on the joint and the conformation and geometry of articular surfaces, is often used to evaluate stress distribution. (Greenwald and Haynes, 1972; Bullough, Goodfellow and O'Connor, 1973; Miyanaga, Fukubayashi and Kurosawa, 1984; Eckstein et al., 1994)

However, measurements of the joint force and the size of the contact areas, since pressure distribution within these may not be uniform, could not assess the actual stress distribution. (Hehne 1983; Miyanaga et al 1984; Eckstein et al., 1994)

Preston et al. (2000) estimated the articular contact areas, along with the effects of axial load on their size and location, of radius and ulna proximal epiphysis in normal canine elbow joints. Particularly in large breed dogs, three specific areas of articular contact have been recognised, the caudo-medial aspect of the radial head, the medial coronoid process and the cranio-lateral aspect of anconeus. On the other hand, a lack of articular contact at the central trochlear notch was underlined. (Evans & De Lahunta, 2013; Alves-Pimenta et al., 2019)

Mason et al. (2005), studying transarticular forces maps, indicated how the proximal articular surface of the ulna contributes significantly to load transfer through the canine elbow joint, resulting, as previously reminded, in an equal distribution of weightbearing load between the ulna and the radius. (Evans & De Lahunta, 2013)

Several Authors state that incongruity of the elbow joint could lead to elbow dysplasia because of an increased pressure within the joint. (Samoy et al., 2005)

As it will be further discussed in the next chapters, elbow incongruity can occur during the joint development, due basically to a “short radius”, a “short ulna”, an elliptical trochlear notch or a growth deformity of the humerus.

Nevertheless, after Eckstein et al. in 1994 distinguished physiological from pathological incongruity in human elbow joints, and a similar theory was later demonstrated in dogs by Preston et al. in 2000, a small concave incongruity is generally accepted and considered as normal by several veterinary studies, as it is believed to optimize stress distribution during gait, thus ensuring better cartilage nutrition and lubrification. (Samoy et al. 2005; Wind et al. 1986; Alves-Pimenta et al., 2019)

3. CANINE ELBOW DYSPLASIA (CED)

3.1. DEFINITION, ETIOPATHOGENESIS AND SIGNALMENT

Carlson et al. in 1961 depicted for the first time an anomaly of the elbow joint, using the term "Canine Elbow Dysplasia" (CED); nowadays, this usually refers to a complex of pathologies and is commonly known as an abnormal development of the elbow, generally leading to osteoarthrosis, either clinically inapparent or provoking lameness and pain. (Kirberger and Fourie, 1998; Vezzoni and Benjamino, 2021)

According to the IEWG (International Elbow Working Group), it includes a group of developmental diseases: fragmented medial coronoid process (FCP), ununited anconeal process (UAP), osteochondrosis (OC) or osteochondritis dissecans (OCD), and incongruity (IC) of the elbow joint. (Kirberger and Fourie, 1998; Cook and Cook, 2009; Vezzoni and Benjamino, 2021)

All these disorders can appear individually or in combination of two or even three of them, and, being developmental conditions, are generally seen in young growing dogs of 4 – 7/8 months of age, of medium, large and giant breeds mostly (weighing over 20 kg).

Clinical signs are lameness of variable degrees and often external rotation of the distal forelimb, that are generally more difficult to recognize when the condition is bilateral. (Vezzoni and Benjamino, 2021)

A certain breed predisposition has been recognized for each one of the abnormalities cited above, which therefore can be considered separately from an etiopathogenetic and pathophysiologic point of view, as it will be discussed further.

Male gender is frequently more represented in this condition and several Authors have interpreted this feature as a consequence of male faster rate of growth or due to the presence of a sex-linked factor. (Kirberger and Fourie, 1998) However, some authors have indicated a certain breed predisposition with regards to gender as well. In fact, in the IEWG proceedings of 2016, it is

underlined as among Labradors male dogs are affected twice as frequent as females, whereas in other breeds, with the example of Bernese Mountain dogs, it appears there is no gender predilection for CED.

Many studies have been proposed on CED prevalence in the canine population (Table 1), but results obtained by different authors for different breeds and in different countries were extremely variable and often controversial, partly due to the poorly representative data set, coming predominantly from Kennel and breeders' clubs. (Narojek et al., 2008; Hazewinkel, IEWG proceedings, 2018)

	Belgium[a] 2002-'06	Belgium[b] 2014	USA[c] 1974-2011	USA[d] 1970-2017	Netherlands[e] 2002- 2012	UK[f] 1999-2016
Bernese M.D.	20% (n=266)	19.5%	28.3% (n=11.685)	27.4% (n=16.897)	13,9% (n=1221)	36.7% (n=1922)
Labrador	13% (227)	21.4%	10.7% (59.832)	10.4% (91.188)	5.2% (3333)	13.4% (17.004)
Golden Retriever	18% (126)	26.3%	11.0% (n=28.923)	11.4% (45.948)	5.6% (1503)	21.2% (4296)
German Sh dog	12% (130)	12.1%	19.1 (32,937)	19.2% (46.055)	6.9% (480)	17.9% (3700)
Rottweiler	33% (135)	9.9%	39.7 (14172)	38.9% (19.235)	14% (314)	50.9% (1089)

a-Coopman et al Vet Rec 2008, 163, 654-658
b Coopman et al VCOT 2014,27, 395-397
c Orthop. Foundation for Animals (OFA) December 2011
d OFA August 2018
e Dutch Kennel Club 2002-2009 as in Lavrijsen et al. Vet J 2012, 193, 486-492
f Website Kennel Club August 2018

Table 1. CED prevalence in various breeds reported in different countries' clubs and veterinary journals. From Hazewinkel H.A.W. "Prevalence of elbow dysplasia, and pathogenesis of FCP in young Labradors.", IEWG Proceedings, Barcelona, 2018

A positive correlation between hip scores and elbow scores have been reported by several Authors, so that selection for one of these two features should also improve the status of the other, although using both scores would be more beneficial. (Hazewinkel, IEWG proceedings, 2018)

CED can affect only one or both elbow joints, with an estimated frequency of bilateral affected dogs from about 35% (Tobias et al., 2013) to 50% (Snaps et al., 1997).

Worldwide, CED is considered as a complex, multifactorial, hereditary, polygenic, developmental and progressive disease. (Kirberger and Fourie, 1998; Samoy et al., 2006; Vezzoni and Benjamino, 2021)

Environmental, mainly traumatic, and nutritional factors have been recognized and connected to the expression of the severity of this pathology, being able to exacerbate, but not cause by themselves, CED (Vezzoni and Benjamino, 2021).

Among the possible traumatic causes, severe trauma doesn't usually lead to elbow dysplasia expression, which is tendentially associated with repeated joint stresses caused by hyperactivity, excessive physical activity during the growth phase, or excessive body weight (Nap R.C., IEWG proceedings, 1995; Kirberger and Fourie, 1998)

Slater et al. (1992) also hypothesized that intense physical activity and high dietary calcium could result in the development of osteochondrosis (OC) and osteochondritis dissecans (OCD), one of CED entities, in dogs.

Overnutrition and consequent overweight, often accompanied by excessive energetic supplies and calcium over-nutrition, are important nutritional factor in CED development (Nap R.C., IEWG proceedings, 1995; Kirberger and Fourie, 1998; Kealy et al., 2000), and represent a significative risk factor in this pathology, together with high fat, high calories, high protein and high vitamin diets, which, promoting a rapid growth, have been given a role by several authors in the rise of OC. (Slater et al., 1992; Kirberger and Fourie, 1998; Sallander et al., 2006; Martini, 2006) It was also suggested that hypercalcemia could cause calcitonin release, which would induce a delay in bone resorption and cartilage maturation. (Martini, 2006)

Moreover, recent studies on Labrador Retrievers have found significantly higher plasmatic levels of GH and IGF-1 in obese subjects. (Martini, 2006)

On the other side, according to some Authors, low calories diets have been linked to a slower progression of OC (Kealy et al., 2000), while several researchers have suggested and demonstrated the protective effects on osteoarthrosis development of the use of food additives like nutraceuticals, such as chondroitin sulfate and omega-3 fatty acids, because of their chondroprotective, anti-inflammatory and antioxidative properties. (Vandeweerd et al., 2012; Roush et al., 2010; Manfredi et al., 2018)

CED is also known worldwide as a hereditary, genetic, but non-congenital disease of the elbow joint.

Since it is inherited as multifactorial polygenic traits, it requires more than one gene to cause the phenotype to be expressed in an individual, which means this complex disease is not expressed in all genetically predisposed subjects, as phenotypic expression is believed to be modified by all the previously described environmental factors. (Padgett et al., 1995; Vezzoni and Benjamino, 2021)

Nevertheless, further studies are still required to determine all the involved genes, as each developmental abnormality mentioned before appears to be inherited independently from the others and, in addition, seems to be inherited differently among breeds. (Michelsen et al., 2013)

In general, it is well known that selective breeding could reduce the incidence of this pathology. (Kirberger and Fourie, 1998)

As being progressive, any treatment may cause an improvement of the elbow condition, but not a complete reversion to normality.

Nonetheless, the etiopathogenesis remains still unclear and certainly requires further studies.

The flowchart 1 below illustrates the interrelations between elbow dysplasia manifestations and elbow osteoarthrosis.

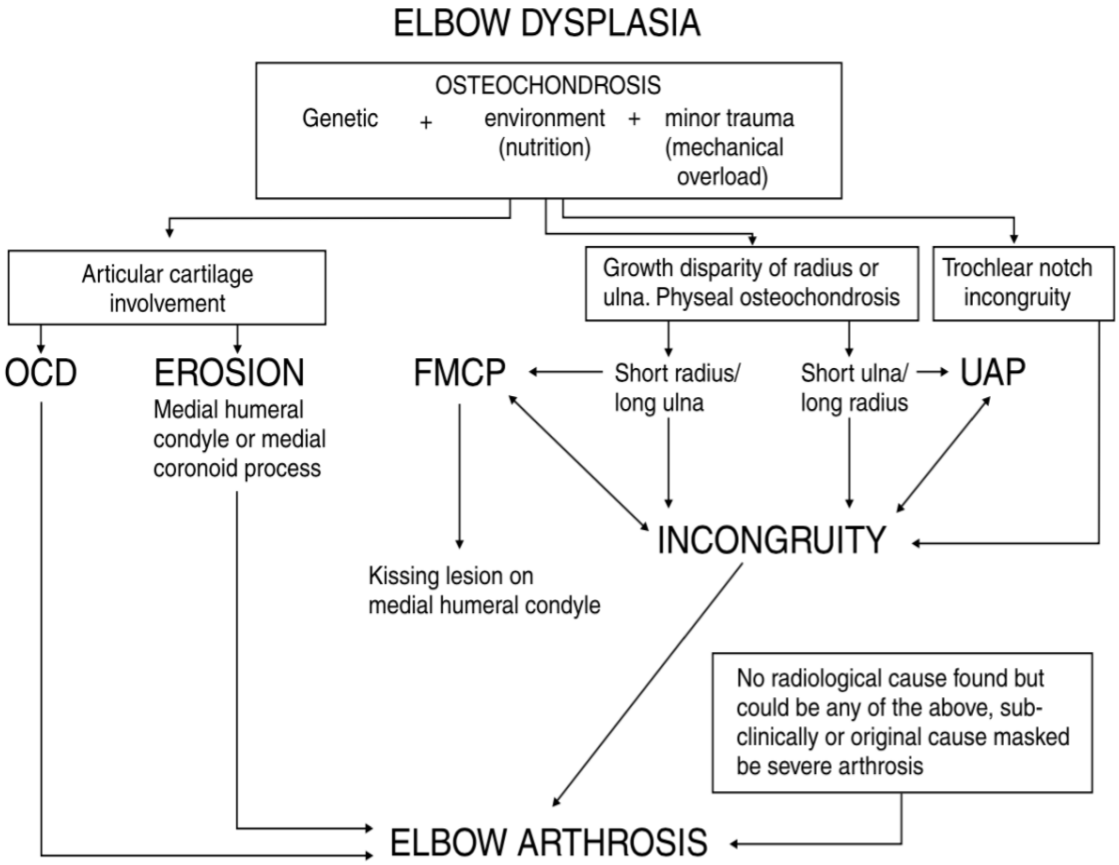

Flowchart 1. Correlations and connections between elbow dysplasia and osteoarthrosis. From Kirberger RM et al. Elbow dysplasia in the dog: pathophysiology, diagnosis and control, 1998.

3.2. FRAGMENTED CORONOID PROCESS (FCP) AND MEDIAL COMPARTMENT DISEASE (MCD)

The most common dysplastic lesion and cause of elbow osteoarthrosis is the fragmentation of the medial coronoid process (Kirberger and Fourie, 1998; Burton and Owen, 2008), which generally refers to the formation of an either fissured or separated osteocartilaginous fragment on the apical and lateral portion of the medial coronoid process of the ulna. (Lusetti, 2014)

In 2009, Fitzpatrick and Yeadon introduced the term Medial Compartment Disease (MCD) as more representative than FCP, due to the frequent findings of pathological lesions of cartilage and subchondral bone of the whole medial compartment of the elbow.

MCD is characterized by cartilage erosion, from moderated to severe, commonly found on the medial portion of the coronoid process, the medio-distal surface of the humeral condyle and the medial portion of the head of the radius, but it can be detected even without concomitant and clear FCP lesions. (Schulz, 2013)

The medial coronoid process ossifies completely at 20–22 weeks, from its base to the tip, without a separate ossification centre. (Olsson, 1983)

Regarding the etiopathogenesis of this disease, many theories have been proposed, without reaching a clear explanation yet.

Many studies support the theory of an underlying condition of osteochondrosis (OC), which leads to chondromalacia, necrosis and delay or alteration of the endochondral ossification, followed by eventual fissuring of the cartilage and consequent fragmentation. (Lewis et al., 1989; Kirberger and Fourie, 1998; Vezzoni and Benjamino, 2021) In the study by Lau and colleagues in 2013 on a cohort of MCD-prone, purpose-bred young Labrador retrievers, it was noted how a delay in endochondral ossification, thus MCD, started developing in the deeper layer of the articular cartilage, involving only the subchondral bone, whereas it did not affect the outer joint cartilage in dogs younger than 18 weeks of age. In the IEWG meeting proceedings of 2018, Theyse et al. postulated that a coronoid

dysplasia (CD) could originate from vascular compromise and subsequent osteonecrosis of the subchondral bone, hypothesizing that also the lesions on the medial portion of the humeral condyle, thus OCD, and the development of joint incongruity could derive from the same mechanism.
Moreover, in comparison with the earlier completed ossification of the MCP in small breeds, some Authors suggested that its slow maturation in large breed dogs could be a cause of MCD. (Lau, IEWG Proceedings, 2015) Several studies have investigated the role of the shape of the MCP, trochlear notch, and the articular contact areas in the development of MCD, as it will be discussed further in this dissertation.

On the other hand, several Authors consider humerus-radio-ulnar incongruities as responsible for this disease. In particular, an asynchronous growth of the radius and ulna, resulting in overgrowth of the ulna relative to the radius, is suggested to be one of the main causes of MCD, resulting in an abnormal load on the medial humeral condyle and medial coronoid process. (Kirberger and Fourie, 1998; Tobias et al., 2013; Vezzoni and Benjamino, 2021)
In 1982 Wind suggested that an underdeveloped ulnar trochlear notch could also cause or contribute to the disease, although this theory was opposed in 1998 by Kirberger et al.
Another possible cause indicated for MCD are mechanical stresses, along with microcracks and fatigue-induced microdamage of the subchondral bone. (Olsson, 1983; Fitzpatrick and Yeadon, 2009; Tobias et al., 2013) Current postulated factors contributing to MCD include abnormal tensile forces originating from the annular ligament (Kirberger and Fourie, 1998) and shear forces deriving from the ulnar insertions of the biceps brachii and brachial muscles, which would determine an over friction of the coronoid process, compressed against the radial capitulum during flexion, supination and pronation. (Hulse et al, 2010; Lusetti, 2013; Hazewinkel, IEWG proceedings, 2018)
MCD is also thought to occur secondary to a trauma of modest intensity, so environmental factors should also be considered in the etiopathogenesis. (Schulz, 2013)

Alongside all these proposed theories, for which no direct causative and univocal relationship has been found yet, the genetic and hereditary etiology must be taken into consideration.

The most affected breeds reported in literature are Labrador Retrievers, Rottweilers, Bernese Mountain Dogs, Newfoundlands, Golden Retrievers, German Shepherds and Chow Chows. (Schulz, 2013)

FCP was the most frequently diagnosed developmental disease (58.0% out of 150 affected specimens) in a study by Narojek et al in 2007. In this study, the highest incidence of FCP s was reported in Dogues de Bordeaux (87.5%), Rottweilers (84.0%), and Giant Schnauzers (75.0%), but it was also the most frequent disorder diagnosed in Labrador Retrievers, although with a lower prevalence.

Although well-known for the UAP high incidence, the frequency of MCD in the German shepherd dog has been evaluated in France by Remy et al. in 2004 in 520 dogs, resulting to be as high as of 11,3%.

Although little is still known about the differences in MCD among breeds, some hypothesis could be inferred from literature; for example, in 1986 Wind and Packard noticed how in Bernese mountain dogs an FCP often occurred with a short radius, while in German shepherd dogs with an elliptical ulnar incisure, and in 1981 Groendalen & Groendalen in their study observed a lateral fragmentation of the medial coronoid process mostly in Rottweilers and Retrievers. Conversely, Labrador retrievers have showed rarely a radio-ulnar incongruity concomitant to MCD, therefore this breed is generally believed to not manifest MCD with a significant incongruence. (Lau, IEWG Proceedings, 2015) In fact, Kirberger et al (1998) stated that the Labrador Retriever is most likely to have combined OCD and FCP.

In general, aside from its frequent correlation to the presence of IC, a fragmented medial coronoid process can be found together with OCD or erosive lesions and rarely with UAP. (Kirberger et al., 1998)

3.3. UNUNITED ANCONEAL PROCESS (UAP)

The term Ununited Anconeal Process (UAP) refers to a pathological condition in which the secondary ossification centre of the anconeal process fails to ossificate and get united with the ulnar proximal epiphysis by approximately 24 weeks of age, resulting in joint instability, eventual displacement of the process and subsequent osteoarthrosis. (Gasch et al., 2012)

Depending on breed, the separate ossification centre of the anconeal process, only present in larger breeds, appears at 11–14 weeks, mineralizes between 10 and 16 weeks of age, hence the anconeal process is united with the olecranon at 20–22 weeks (Greyhound 14–15 weeks, German shepherd dog 16–20 weeks). (Vezzoni and Benjamino, 2021; Kirberger and McEvoy, 2016; Gasch et al., 2012)

Small breeds are thought to not have this separate ossification centre, or the anconeal process may unite earlier with the ulna. (Martini, 2006)
In some cases, a fibrous or fibrocartilagenous bridge could still link the ununited process to the olecranon, therefore the separation line could be either complete, as in most cases, or incomplete. (Kirberger et al., 1998; Kirberger and McEvoy, 2016)

This condition is reported with a high incidence in the German shepherd dog, but can occur in various breeds, such as Great Dane, Newfoundland, Black Russian Terrier (Tchorny Terrier), Saint Bernard, Basset hound, Greyhound, Italian Spinone, Italian Cane Corso, Chow Chow, Bullmastiff and Irish Wolfhound. (Vezzoni and Benjamino, 2021; Kirberger and McEvoy, 2016)

Despite the well-known high prevalence of UAP in German shepherds, as high as 11,5% in a Turkish research by Gulanber (2000), other recent studies have reported a much lower incidence of the pathology in this breed: Tellhelm et al. (2000) found a 3,3% prevalence of UAP in a group of 363 dogs, while in the study of Remy et al. (2004) it was 1,1% over 520 German shepherd dogs. This may be a result of the pre-screening, considering how the radiological diagnosis, as it will be illustrated in the next chapter, is quite easily achieved, but hopefully of selective breeding as well.

Males are affected twice as much as compared to females. UAP is bilateral in 20-35% of cases (Guthrie, 1989) and is often associated to a severe ectasia of the caudo-lateral synovial recess, and subsequent lameness. (Schulz, 2013)

Traumatic, metabolic (such as hormonal influences), nutritional, genetic and hereditary factors have been proposed alongside several other hypothesis for UAP pathogenesis, which still remains unclear. (Gasch et al., 2012; Schulz, 2013)

Olsson suggested that UAP could be a manifestation of osteochondrosis, in which the alteration of the subchondral ossification, during the period of the connection between the anconeal process and the ulna, leads to cartilage thickening, necrosis and fissuring. The loading stress on this part of the joint could then result in a separated anconeal process. (Olsson et al, 1993; Gasch et al., 2012; Schulz, 2013)

Currently, an overgrowth of the radius asynchronously to a relatively shorter ulna as cause of UAP is the most accepted theory. In the growing period, a longer radius causes a proximal displacement of the humeral trochlea leading to an abnormal pressure on the anconeal process, whose ossification centre ends up being damaged (more easily if osteochondrosis is already present). (Sjostrom et al., 1995; Kirberger and McEvoy, 2016; Vezzoni and Benjamino, 2021)

Before this hypothesis, Weis (1982) and Wind (1983), followed by Morgan et al. in 2000, postulated that an underdeveloped elliptical trochlear notch, when present as a form of primary incongruity, could lead to similar pressures on the anconeal secondary ossification centre (Kirberger et al., 1998; Gasch et al., 2012).

The state of the art until now suggest a synergic action of both osteochondrosis and elbow incongruity, but even so a univocal etiopathogenesis has not been reached yet.

3.4. OSTEOCHONDROSIS (OC) AND OSTEOCHONDRITIS DISSECANS (OCD)

Osteochondrosis is an alteration, a delay or a failure of the endochondral ossification of the physeal and epiphyseal growth plates, that results in a cartilage retention. Consequently, a focal thickening of the growing epiphyseal cartilage develops, progressively causing a detachment of the cartilage layer and lack of vascular supply, therefore an alteration in the metabolism of the chondrocytes, failing the normal calcification process, and finally necrosis. Osteochondritis Dissecans (OCD) occurs when this abnormal chondromalacic cartilage starts to get fissured and may form a detached cartilaginous or osteochondral flap, partially or completely separated from the underlying bone. (Schulz, 2013; Lusetti, 2014; Vezzoni and Benjamino, 2021)

The separated flap, called "joint mouse", can either remain cartilaginous or, rarely, mineralize, and, once free in the joint space, is generally responsible for the clinical signs. (Olsson, 1983; Kirberger et al., 1998; Kirberger and McEvoy, 2016)

This condition typically affects the humeral condyles, it is most frequently bilateral, more represented in males, and with a certain predisposition in growing young dogs of large breeds, like Rottweilers, Golden Retrievers, Labrador Retrievers, Dogues de Bordeaux, Newfoundlands, Mastiffs, Neapolitan Mastiffs and Bergamasco Shepherds. (Lusetti, 2014; Kirberger and McEvoy, 2016; Vezzoni and Benjamino, 2021)

As seen previously, several authors suggest osteochondrosis to have a fundamental role in the physiopathology of FCP, UAP and OCD of the elbow. The etiology is still unknown, though often assimilated to that proposed for MCD, despite the role of joint incongruity being still unclear. In general, the suggested predisposing factors are genetic, nutritional excesses (diets rich in energy, calcium and phosphorus), rapid growth or overweight at birth, trauma, intense exercise, ischemia and hormonal factors. (Kirberger et al., 1998; Schulz, 2013; Burton and Owen, 2008; Vezzoni and Benjamino, 2021)

Kissing lesions, usually found together with FCP on the opposing medial humeral condylar surface, can be confused with OCD, hence sometimes classified as “OCD-like lesion”. The kissing lesions are usually present more laterally than OCD lesions, in which conversely the cartilage appears as excessively thickened, and are thought to develop later than OCD lesions. (Tobias, 2013; Kirberger and McEvoy, 2016)

As being abrasions of the condylar cartilage caused by the FCP, these lesions cannot be detected radiologically or by computed tomography, even though, in CT examination, they have been significantly correlated to the finding of an irregular radial incisure of the ulna. Still, the lack of this lesion cannot rule out the presence of cartilage erosions. (Coppetiers et al., 2015)

3.5. ELBOW INCONGRUITY (IC)

The term Elbow Incongruity (IC) refers to a malalignment of the joint surfaces of the elbow joint, more precisely involving one or more of the three joints that constitute the elbow, the humero-ulnar, humero-radial and radio-ulnar joints (Samoy et al., 2005; Kirberger and McEvoy, 2016)

In several studies, a physiological form of incongruity was described in healthy elbows, as seen in humans, and distinguished from the pathological forms found in CED. This physiological incongruity is thought to be typical of young dogs and ensure a better stress distribution during gait and a better nutrition of the articular cartilage, apparently without implying clinical signs or development of osteoarthrosis. (Wind et al, 1986; Eckestein et al., 1994; Preston et al., 2000; Samoy et al., 2005; Alves-Pimenta et al., 2019)

On the other hand, in literature two main pathological forms of incongruity were acknowledged to take an important role in the etiopathogenesis of elbow dysplasia: the asynchronous growth of radius and ulna and the elliptical shape of the trochlear notch. Samoy et al. (2005) also suggested that an altered growth of the humerus as well could result in abnormal pressure and loading of the joint, thus leading to a pathologic condition.

The asynchronous growth of radius and ulna can determine either a shorter ulna or a shorter radius and is generally referred to as radio-ulnar incongruency (RUI). Some Authors proposed, as possible causes of these conditions, trauma or a persistent cartilaginous core within the growth plate, or hypertrophic osteodystrophy. (Olsson, 1993; Samoy et al., 2005)

As previously explained, a shorter ulna is commonly linked to the development of UAP, since it causes a displacement of the humeral condyle proximally towards the anconeal process, leading to an increased pressure on the latter (as verified by Sjöström and colleagues in 1995).

On the contrary, a shorter radius is usually associated mainly to FCP disease, and subsequently to MCD, as it leads to an increased pressure on the medial part of the humeral condyle and the medial coronoid process. (Samoy et al., 2005; Fitzpatrick and Yeadon, 2009)

In particular, Fitzpatrick and Yeadon in 2009 introduced the concept of dynamic incongruity, in which a relative distal displacement of the radius is observed when compared to the ulna during stance. Although weight-bearing and biomechanical forces during motion must be surely taken into consideration when evaluating joint congruity, this theory seemed less probable, as it would imply a certain degree of laxity of the elbow joint. (Tobias, 2013; Kirberger and McEvoy, 2016)

In this context, Gemmill et al. had earlier described a form of RUI related to the apex, but not to the base, of the medial coronoid process in a sample of FCP affected dogs.

Some Authors have proposed a type of rotational incongruity related to shear forces and mismatched development of musculotendinous components in relation to the joint surfaces, possibly implicated in the MCD pathophysiology as well. (Tobias, 2013)

The second form of pathological incongruity is the elliptical trochlear notch, in which the humeral condyle is not properly embraced by a smaller or altered diameter of the notch. (Samoy et al., 2005)

In some authors opinion, this type of incongruity would lead to osteoarthrosis when presenting after 6 months of age, while before, increasing the pressure on either the medial coronoid or the anconeal process, it may predispose the elbow to FMCP, OCD and UAP. (Kirberger and McEvoy, 2016)

In 1986, Wind and Packard observed that larger breeds were more prone to have a longer proximal ulna relative to the radius, which could be due to the anatomical need of encompassing a wider trochlea, so that this form of incongruity would be most likely to happen in these dogs. In fact, Bernese mountain dogs are predisposed to this kind of disease. (Kirberger et al., 1998)

Several Authors stated that incongruity may not always be evident at the radiographic examination, suggesting it could manifest as a transient condition of the growing period. (Kramer et al., 2006; Kirberger and McEvoy, 2016)

3.6. TREATMENT

Achieving a precise diagnosis is fundamental to establish the correct treatment plan, whether a medical conservative treatment or a surgical one, that will be tailored in relation to the patient age, pathologic condition and grade of dysplasia. (Kirberger & Fourie, 1998)

Conservative treatment is the same for all the forms of CED, often recommended for adult, older dogs, and its cornerstones consist in weight management, limited or controlled physical activity, nonsteroidal antinflammatory therapy (for their analgesic effect too), and chondroprotectors administration. (Todd Trostel et al., 2003; Vezzoni and Benjamino, 2021) In the recent years, other non-surgical therapies have been proposed, with the aim of improving the joint function and delaying but not interrupting the progression of the disease, and often used in combination also for the long-term management of the patient after surgery: acupuncture, laser-therapy, physiotherapy, intra-articular injection of hyaluronic acid, steroids, platelet-rich plasma (PRP) or mesenchymal stem cells. (Todd Trostel et al., 2003) In addition, palliative surgical treatment could be considered. (Vannini, IEWG Proceedings, 2015)

Surgical treatment will be chosen depending on the primary causes of elbow dysplasia, and should follow a preventive approach, therefore be performed as early as possible; however, diagnosis is often controversial, CED appearance is frequently complex and not univocal, and literature lacks sufficient evidence, making treatment decisions often empirical and subjective. (Vannini, IEWG Proceedings, 2015)

With regards to its pathophysiology, FCP treatment has the purpose of removing altered cartilage and/or free bony fragments, restoring joint congruency when needed, and diminishing articular pain. (Lewis et al., 1989) Consequently, arthrotomy and above all arthroscopy have been used largely, and in particular have been advised to remove the fragments in dogs younger than 12 months old, with clinical or radiographic signs, before the development of severe arthrosis, or even in dogs until 24

months of age with an evident severe course of the disease. This technique could be beneficial also in older dogs with extensive osteoarthrosis. (Kirberger and Fourie, 1998; Todd Trostel et al., 2003)

A similar procedure is indicated for the treatment of medial humeral condyle OC/OCD as well, ensuring removal of cartilage fragments, curettage, and inspection of the medial coronoid process. (Kirberger and Fourie, 1998) Few publications about the use of osteochondral autograft transfer (OATS) in this pathology are currently available. (Michelsen, 2013)

When technically challenging, arthroscopy can be converted rapidly in a medial mini-arthrotomy procedure, while in some cases, with an extended MCD, a subtotal coronoid ostectomy (SCO), with removal of the majority of the medial coronoid process, may be needed. (Palmer, IEWG Proceedings, 2015)

Among the multifactorial etiologic theories of MCD and FCP, a shear tearing force originating from the biceps brachii muscle tendon had been suggested, which some surgeons have hypothesized to treat through a tenotomy of its ulnar insertion, called the Biceps Ulnar Release Procedure (BURP), whose efficacy has yet to be assessed. (Palmer, IEWG Proceedings, 2015)

However, in several Authors opinion, treating the underlying elbow incongruity would be more advantageous. (Kirberger and Fourie, 1998)

Dynamic Proximal Ulnar Osteotomy (PUO) and Distal Ulnar Osteotomy (DUO) are reported in the treatment of radio-ulnar incongruities (RUI), the latter both in case of subsequent FCP or UAP. (Michelsen, 2013; Palmer, IEWG Proceedings, 2018)

On the other hand, in cases of severe or end-stage MCD, other procedures are often preferred, with the aim of unloading the medial compartment of the elbow joint: sliding humeral osteotomy (SHO), canine uni-compartmental elbow (CUE) and proximal abducting ulnar osteotomy (PAUL). (Palmer, IEWG Proceedings, 2018)

As for UAP affected elbows, three main strategies have been proposed: (1) anconeal process removal, especially recommended in older, severely arthrosic dogs; (2) Proximal Ulnar Osteotomy (PUO), preferably with concomitant RUI; and (3) anconeal process reattachment, not anymore suggested

alone, but in combination with PUO. However, there is still scarce evidence on the clinical effectiveness of these techniques, therefore further studies are needed. (Michelsen, 2013; Palmer, IEWG Proceedings, 2018) Moreover, according to some authors, in some patients the anconeal process can spontaneously undergo union to the ulnar physis, without any treatment. (Sjöström et al., 1995)

In most severe cases, a Total Elbow Replacement (TER) with prosthesis has been suggested, but few experiences have been reported to date, though with high costs and a challenging procedure. (Vannini, IEWG Proceedings, 2015)

Ultimately, current treatment recommendations are dependent not only on the patient's age at the time of diagnosis, but also (if present) on the type and severity of IC, on the condition of the cartilage and the severity of present OA. Several authors have postulated decision process algorithms to proceed with different approaches, as it is exemplified in the flowchart 2.

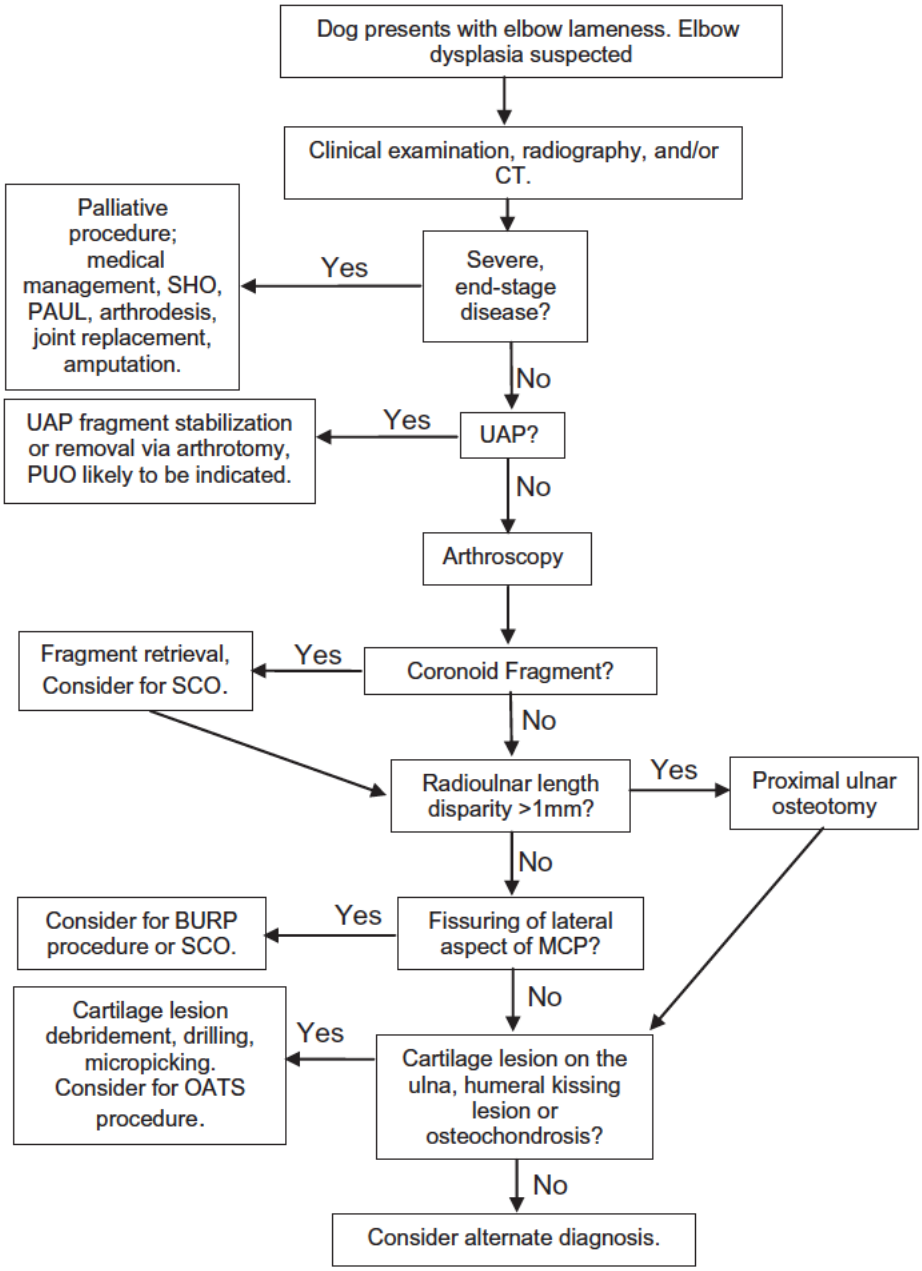

Flowchart 2. Proposed algorithm for the treatment of elbow dysplasia. From "Canine elbow dysplasia: Aetiopathogenesis and current treatment recommendations.", by Michelsen J., *Veterinary Journal*, *196*(1), 12–19

4. DIAGNOSTIC METHODS

After the first publication about FCP by Tirgari in 1974, an increasing interest rose over elbow dysplasia, until, in 1989, a group of researchers founded the International Elbow Working Group (IEWG) with the aim of raising awareness and achieving a better understanding of this disease, above all on its etiological, genetic, clinical and diagnostical point of view.

The IEWG, affiliated to the WSAVA (World Small Animal Veterinary Association), works together with FCI (Federation Cynologique International) to gather and exchange knowledge and experiences about elbow diseases and to develop a protocol for screening that would be acceptable and accessible to the international scientific community and breeders.

In Italy, ENCI (Ente Nazionale Cinofilia Italiana) has followed FCI-IEWG protocols and established that official screening for elbow dysplasia should be done at the minimum age of 12 months in all breeds, when the animals are supposed to have reached complete skeletal maturity.

Sensibly decreasing the incidence of elbow dysplasia, according to its hereditary and genetic characteristics, is the main purpose of this screening protocol. In fact, with reference to the knowledge that genetic transmission of this pathology has proved to be linked to multiple genes far from being identified yet, the breeding selection is essentially based on phenotype, with the hope to affect genotype as a consequence.

Nevertheless, diagnosis could be reached in other occasions too, and, according to Martini (2006), three different diagnostic levels can be distinguished:

- Early diagnosis in asymptomatic dogs
- Official diagnosis following FCI-IEWG protocols
- Diagnosis in symptomatic dogs, independently of the age

An early diagnosis represents the best approach to this pathology and the main purpose of clinicians, since it is fundamental to start treatment in order to delay the dysplastic development and to prevent the onset of secondary degenerative joint disease. (Martini, 2006; Lusetti, 2014)

As said before, treatment of CED is aimed to improve the joint function and slow down the progression of the disease, which will inevitably lead to the development of osteoarthrosis, therefore a complete reversion to normality cannot be expected.

When present, clinical signs are common to all of the previously described forms of elbow dysplasia, so that clearly differentiating between the lesions based only on symptoms is not possible. (Michelsen, 2013)

Overall, breed, gender, age of onset, and moment of lameness should be taken under consideration when collecting the anamnesis. In general, dogs manifest limping from 5-7 months of age, but the reference period is wider, from 4 to 12 months of age. (How, IEWG Proceedings, 2016; Michelsen, 2013) According to literature, subjects affected by UAP usually don't show any symptom before 7 - 8 months old, while in case of FCP or OCD clinical signs manifest generally around 4 - 7 months of age. (Martini, 2006)

Lameness can be intermittent and appear as inactivity stiffness, mostly in the morning or after resting. When CED is bilateral, the patient will tend to shift the weight to the hindlimbs, so that the lameness is more difficult to identify or can migrate from one leg to the other. (Martini, 2006)

Pain can be detected during passive motion, in which the normal range could result decreased and crepitation could be felt in advanced cases of arthrosis, and palpation of the elbow joint, that could unveil periarticular swelling, muscle atrophy, and thickening of the capsule. (How, IEWG Proceedings, 2016 Martini, 2006)

The posture assumed by affected dogs while sitting or standing, with the paw externally rotated, is considered a manifestation typical of CED. (How, IEWG Proceedings, 2016) Subjects with UAP generally show abducted elbows and supination of the carpus, while the fingers appear to be divaricated. On the other hand, in case of FCP and OCD, the elbow is adducted, with the paw externally rotated and 'pseudo valgism' of the carpus. (Martini, 2006)

After a through clinical examination, in addition to the recommended radiographic evaluation, many other diagnostic techniques, with both strengths and limitations, have been proposed to obtain the

most accurate evaluation of the elbow joint: computed tomography (CT), arthroscopy, magnetic resonance imaging (MRI), ultrasonography and scintigraphy. (Gielen et al., IEWG Proceedings, 2017)

4.1. RADIOGRAPHIC STUDY

Radiography is worldwide the most frequently used imaging technique for the diagnosis of elbow dysplasia, due to its availability and as it is the most effective-cost method, even in daily practice. Narrow and precise collimation, exposure without grid, high mAs and low MHz values are required in order to obtain an optimal radiograph, and, as in every proper radiographic study, a minimum of 2 orthogonal projections should be necessary. (Boroffka, IEWG Proceedings, 2015; Heng, IEWG Proceedings, 2015)

Even so, only one projection is required for the official screening by FCI, under approval of the IEWG, that is a 45° flexed mediolateral (ML flex) projection of each elbow at a minimum age of 12 months old. A craniolateral-caudomedial oblique (Cr15°LCdMO) view with the limb pronated by 15° is recommended but not mandatory. These views are usually taken respectively in lateral and sternal recumbency, with the patient under anesthesia.

Performing only one flexed ML projection has the purpose of solely evaluating signs of secondary arthrosis, but to clearly identify the primary underlying cause, hence, to differentiate between the types of CED, additional views are needed (as can be seen in Table 2), and so it is established in some countries. (Heng, IEWG Proceedings, 2015)

The ML flex projection gives a clear visualization of the anconeal process, but not directly of the medial coronoid process, therefore the Cr15°LCdMO view is advised to determine medial humeral condyle OC lesions and eventual coronoid fragments. In the latest reports, though, it is said that a ML flex (40-45°) and a neutral mediolateral (100° - 120°) projections should provide the best information regarding the medial coronoid process, incongruity, and presence of osteophytes. (Ondreka and Tellhelm, IEWG Proceedings, 2017)

Nonetheless, in the latest available IEWG proceedings different radiographic projections are suggested, underlying their pros and cons, for an optimal radiographic evaluation of the elbow joint: neutral craniocaudal (CrCd), pronated craniolateral-caudomedial 15° oblique (CrLCdM15°O), 45°

flexed mediolateral (ML flex) and neutral mediolateral (ML). In some cases, also the 90° flexed mediolateral view (ML 90° flexed) is taken into consideration.

Finally, several authors in the recent years have proposed digital analysis on radiography in order to quantitatively assess subtrochlear and ulnar trochlear notch sclerosis, with controversial results, mostly in terms of repeatability of the exams. (Burton et al., 2007; Válega et al., 2021) Additionally, an attempt to evaluate bone density of the medial coronoid process through dual energy x-ray absorptiometry has been made by Burton et al. in 2009, finding lower values on the axial portion of the MCP, especially in affected joints, hence suggesting a predisposition to osteochondral failure and microcracks in this region.

Condition	Breeds most susceptible	Age first seen from	Best views	Primary radiological changes	Interpretation pitfalls
Fragmented medial coronoid process	Rottweiler, Labrador and Golden Retrievers, Bernese Mountain Dog, Newfoundland, German Shepherd Dog	7 months or older	Cd75°MCrLO Cr15°LCdMO Di35°MPrLO ML extended	Separate fragment(s) Blunted, irregular, osteopenic or absent medial coronoid process Distal trochlear notch sclerosis Joint incongruity may be present (see below) Often only diagnosed based on secondary arthritic changes	Laterally located sesamoid in the supinator muscle Medial coronoid osteophytes mimicking a fragment especially on the Cd75°MCrLO view
Ununited anconeal process	German Shepherd Dog, Great Dane, Irish Wolfhound, St. Bernard, Chow Chow, Basset Hound, Bullmastiff, Boerboel	5 months	ML flexed	Irregular vertical radiolucent line through caudal anconeal process Joint incongruity may be present (see below)	Open physis of anconeal process <22 weeks of age On ML extended views the separate physis of the medial epicondyle mimics the pathology (closed by 5 months)
Osteochondritis dissecans	Labrador and Golden Retrievers, Rottweiler	4–5 months	CrCd Cr15°LCdMO ML extended ML flexed	Radiolucent area on medial humeral condyle with possible sclerotic rim Subchondral saucer defect Mineralized flap (rare) Flattening of the cranioventral aspect of the medial condyle	May have minimal secondary osteoarthrosis
Joint incongruity	Bernese and Swiss Mountain Dogs	4 months or older	ML extended	Step formation between lateral coronoid process and adjacent radial head Medial coronoid process located more proximally Asymmetrical widening of humeroulnar joint Widened humeroradial joint Indistinct outline of trochlear notch Cranial displacement of the humerus towards the cranial radial head margin	Poorly positioned and centred views

Table 2. Breed incidence, best radiographic views and primary radiological signs of elbow dysplasia. From Kirberger et al BSAVA manual of canine and feline musculoskeletal imaging, 2006, p.112

a) neutral craniocaudal view (CrCd)

For a neutral craniocaudal view (CrCd), the patient is positioned in sternal recumbency, the forelimbs are extended in a straight line and lying on the radiographic cassette, the head is retracted caudally, and the beam is centred on the joint space.

This projection allows to evaluate the medial compartment, in particular the medial humeral condyle and epicondyle and the medial coronoid process, therefore could unveil the presence of eventual osteophytes or the suspect of kissing lesions and give a good view on the transverse profiles of the articular surfaces. (Martini, 2006; Boroffka, IEWG Proceedings, 2015)

It can also help to differentiate between a coronoid fragment and the presence of a supinator long tendon sesamoid. (Boroffka, IEWG Proceedings, 2015)

b) craniolateral-caudomedial oblique view (Cr15°LCdMO)

In the craniolateral-caudomedial oblique (Cr15°LCdMO) view the patient is positioned in sternal recumbency extending straightly the forelimbs, and the affected limb is pronated 15 degrees (until 50° is accepted by experts). The beam is centred on the joint. (Kirberger et., 2006; Boroffka, IEWG Proceedings, 2015) Ideally, in this view the superimposed tip of the olecranon should not overlap the lateral margin of the humerus.

This projection is generally used as a skyline to enlighten the medial coronoid process and the medial humeral condyle, to expose coronoid alteration and FCP in the former and OCD lesions in the latter, and eventually to evaluate osteophytic reactions of these structures. (Martini, 2006)

According to some authors, the Cr15°LCdMO view could also give some information in joint incongruity, but remains unreliable when compared to the ML view.

c) 45° flexed mediolateral view (ML flex)

In this view, the patient is positioned in lateral recumbency lying on the affected limb and with the upper limb retracted caudally. The angle between the humerus and radius and ulna has to be about 45 degrees, so the carpus is pulled towards the neck, but should not be elevated to avoid supination. The beam should be centred on the medial epicondyle. (Boroffka, IEWG Proceedings, 2015)

This projection is the most useful for UAP diagnosis, avoiding the superimposition of the humeral epitrochlea on the anconeal process. An irregular radiolucent line between anconeal process and ulnar metaphysis has a diagnostic value only if seen in subjects older than 16-20 weeks. (Martini, 2006)

Performing an ML flex projection allows to identify osteophytes on the anconeal process and could also help in diagnosing a flexor enthesiopathy. (Boroffka, IEWG Proceedings, 2015)

d) neutral mediolateral view (ML)

The neutral mediolateral view (ML) obtained with an angle between humerus, radius and ulna of about 110°, is a routinely performed projection, again with the patient in lateral recumbency, lying on the affected limb, while the upper is retracted caudally. In this view as well a true lateral position is fundamental. (Kirberger and Fourie, 1998; Boroffka, IEWG Proceedings, 2015)

This projection enlightens the structure and conformation of the articular epiphysis and gives a better view to evaluate the joint incongruity and the initial subtrochlear sclerosis. (Martini, 2006) OCD could be spotted on the humeral condyle, but this is not the optimal view for its diagnosis. (Kirberger and Fourie, 1998)

Nevertheless, the medial coronoid process results overlapping the proximal radius, and similarly the dorsal part of the anconeal process can be hidden by the medial humeral condyle. (Kirberger and Fourie, 1998; Martini, 2006)

e) 90° flexed mediolateral view (ML 90° flexed)

For this view, the patient is positioned in lateral recumbency, lying on the affected limb, with the upper pulled caudally; the angle between humerus and radio/ulna is about 90°. It is overall quite similar to the previously explained ML view, only with a slightly tighter angle.

Some authors advise this projection for the detection of elbow incongruity, as it enlightens the presence of a radio-ulnar step and increases the humero-ulnar joint space. (Heng, IEWG Proceedings, 2015) In a recent research by Lappalainen et al. (2015) on the Skye terrier, a chondrodystrophic breed, the ML 90° flexed projection was purposely chosen for its reliability in the detection of IC, resulting beneficial in their screening, over the standard ML flex view, in which the humero-ulnar joint space could be modified by an eventual rotation of the elbow, as suggested by Murphy et al. (1998) It could also give a good visualization of the medial coronoid process and medial compartment, but the anconeal process would be superimposed. (Heng, IEWG Proceedings, 2015)

Nevertheless, there is still a consistent lack of agreement among authors. Samoy et al., in 2012, affirmed that, basing on their results, a 90° ML view did not appear as necessary to detect elbow incongruity, for which a neutral ML and a Cr15°LCdMO were sufficient.

4.2. COMPUTED TOMOGRAPHIC STUDY

In the recent years, Computed Tomographic (CT) imaging has gained growing interest and importance in the study and identification of elbow pathologies, and, although not routinely used, it's been increasingly suggested to verify suspected diagnosis based on signalment, physical examination, radiography or the diagnostic methods. Being significantly more accurate and with a higher sensitivity and specificity when compared to radiography, CT is considered to be considerably of help, whenever radiographs result unclear or questionable, as is often the case with MCD. (Reichle and Snaps, 1999; von Pückler, IEWG Proceedings, 2016)

The procedure for CT is performed with the patient under general anaesthesia and positioned in dorsal or sternal recumbency. A lateral positioning has been proposed and compared to the sternal recumbency method (Rycke et al., 2002; Murino, 2017), demonstrating a higher imaging quality and less artifacts, as well as an easier procedure. The most symmetric positioning should be obtained, with both forelimbs extended forward and parallel, and the head should be retracted caudally, to avoid streak or beam hardening artifacts and have a better-quality imaging. (Gielen and Villamonte-Chevalier, IEWG Proceedings, 2018)

No standard protocol has been clearly proposed for CT studies until now, but the scanning slice thickness has been the object of several studies. CT images should be acquired using contiguous 1 mm slices, since it has been demonstrated how slices thicker than 2mm could considerably reduce the detection of FCP. (Zweifel et al., 2020)

Other matters of concern are the field of view, which should preferably comprehend both elbows simultaneously, and the use of an appropriate bone reconstruction algorithm, generally recommended with a window width between 1500 and 3500 HU (the latter is thought to assess more reliably the changes of the subchondral bone) and a window level of 500 HU. (Cook and Cook, 2009; von Pückler et al., IEWG proceedings, 2016)

The main benefit of CT imaging when compared to conventional radiography is certainly the possibility of achieving a complete overview of the elbow joint, gaining a multiplanar reconstruction without any superimposition. (Rycke et al., 2002)

Furthermore, CT mean HU values in specific areas and CT osteoabsorptiometry assessment of bone density (BD) have been proposed in several publications as objective measurements for subchondral bone sclerosis. In particular, Villamonte-Chevalier et al. in 2016 evaluated these features in both healthy and MCD affected joints of dogs of 2 different breeds, Labrador retriever and Golden retriever dogs, finding increased HU and BD values in MCD affected elbow in different regions of interest, when compared to the sound group. In addition, Labrador retrievers showed higher values in comparison to the Golden retriever group, suggesting a certain degree of difference between breeds.

However, similarly to radiography, the disadvantages of CT is that it cannot distinguish cartilage from soft tissue, resulting in a lack of identification of cartilage erosion. (Moores et al., 2008) Arthro-CT has been proposed in addition to the plain CT scan as it could allow to assess cartilage conditions and eventual lesions. (Gielen and Villamonte-Chevalier, IEWG Proceedings, 2018)

Moreover, the patient must undergo general anesthesia, and cannot be put in a weight-bearing position, possibly altering measurements of the joint space, and perhaps concealing the presence of IC. (Lau and Voorhout, IEWH Proceedings, 2015)

4.3. ARTHROSCOPY

Arthroscopy of the canine elbow is currently considered the gold standard for the inspection of this joint, especially with regards to cartilage evaluation and as it allows the clear identification of primary elbow dysplasia lesions and direct visualization of the articular surfaces. (Moores et al., 2008)

Arthroscopy is often performed to confirm a diagnosis made through other diagnostic methods and, at the same time, to treat the pathology (usually MCD) with removal of the fragmented or detached fragment and the damaged cartilage. It is therefore both a diagnostic and a therapeutic technique.

Moores et al. (2008) observed, in a sample of dogs that underwent both arthroscopy and computed tomography, that in some cases arthroscopy could detect MCD in spite of CT, and vice versa. A similar inference is made by the Authors with regards to elbow incongruity. According to these findings, the two procedures could be considered as complementary.

The technique is performed with the patient under general anesthesia, placed in dorsal recumbency, and through medial portals. Compared to the other diagnostic techniques, though, arthroscopy is certainly more invasive, although minimally, and operator-dependent.

4.4. MAGNETIC RESONANCE STUDY

Magnetic resonance imaging (MRI) is rarely considered in CED diagnosis for several reasons, although further studies would be needed to better assess its potentiality.

In comparison with CT imaging, MRI has considerably higher costs and is more time-consuming, while requiring general anesthesia as well. (Kirberger and Fourie, 1998) Even so, MRI is considered more sensitive especially in the detection of OCD and MCD lesions due to its capability of differentiating cartilage and soft tissues, whereas CT is well-known to have a better bone resolution. ((Kirberger and Fourie, 1998; Cook and Cook, 2009) Nonetheless, MR arthrography, using a contrast agent like gadolinium-DTPA or gadopentate dimeglumine, has been advised to better identify cartilage lesions, because of the limitations of the relatively small and complex elbow joint and thin cartilaginous surfaces. (Cook and Cook, 2009) However, in the study by Franklin et al. (2017), MRI and arthro-MRI did not prove to be a valid alternative to arthroscopy in assessing articular cartilage diseases. MRI has also been suggested in the evaluation of elbow incongruity, but few studies have been performed until now. (Cook and Cook, 2009)

The proposed positioning for MRI examinations in literature are similar to that of CT, with the patient in sternal recumbency and the forelimbs straightly extended cranially and parallel. (Franklin et al., 2017)

4.5. ULTRASONOGRAPHIC STUDY

Ultrasonography (US) is generally recommended for the evaluation of musculoskeletal soft tissues as a valid and accessible imaging technique, usually not requiring general anesthesia, although quite operator-dependent. (Cook and Cook, 2009; Gielen et al., IEWG Proceedings, 2017)

With regards to the elbow joint evaluation, US has been investigated using high frequency linear transducer with some difficulty due to the reduced approachable area when compared to larger joints as the shoulder, but several studies were made from an anatomical point of view. (Cook and Cook, 2009)

The use of US imaging has proved to be suitable for the diagnosis of flexor tendon pathologies and intratendinous calcifications, but limited in elbow dysplasia diagnosis, being able to detect with certainty only clearly displaced coronoid fragments. (Gielen et al., IEWG Proceedings, 2017) It could also perceive the presence of UAP by identifying the discontinuity on the surface of the subchondral bone, while OC lesions and elbow incongruity might be unlikely identified by this technique, although these features have not been thoroughly evaluated yet. (Cook and Cook, 2009)

4.6. NUCLEAR SCINTIGRAPHY STUDY

Nuclear Scintigraphy can be used to localize the cause of lameness when clinical examination is unclear, as it is very sensitive bone metabolism changes, although it is not a very specific technique. (Debruyn et al., 2013; Gielen et al., IEWG Proceedings, 2017)

The localization is possible by the increasing uptake of radiopharmaceuticals by the elbow bones, and particularly in specific regions attributable to the various forms of CED. (Cook and Cook, 2009) For this purpose, a micro-single photon emission tomography (μ-SPECT) has been described, as it provides better anatomical resolution; for example, it proved to be reliable in identifying flexor enthesopathy. (Gielen et al., IEWG Proceedings, 2017)

In a study by Debruyn et al. (2013), semi-quantitative bone scintigraphy was valuable in detecting simple MCP lesions and flexor enthesopathy but resulted less reliable with complex lesions.

Owing to costs and scarce availability, due to the strict requirements in licences, facilities, equipment and trained personnel for radiation handling and safety, currently the use of nuclear scintigraphy is largely limited in this field. (Cook and Cook, 2009)

4.7. OFFICIAL CLASSIFICATION FOR CANINE ELBOW DYSPLASIA

The IEWG has established guidelines for elbow screening and these have been adopted by the FCI and WSAVA as the official standard, spread worldwide with the purpose of selective breeding.

The current IEWG elbow screening protocol includes submission of permanently identified good quality ML flex radiographs of both elbows from 12 months onwards.

The system of radiographic classification of elbow disease is based on severity of arthrosis and/or the presence of a primary lesions, or indirect signs of it. Therefore, signs of arthrosis should be considered as supportive of a diagnosis of elbow dysplasia in the young dog. The grade of arthrosis should be determined for owners, breeders and veterinarians in the determination of heritability of the degree of the disease. The report of the elbow joint status should include the present grade of arthrosis and, if possible, the diagnosis of a primary lesion attributable to elbow dysplasia.

Dogs operated for elbow dysplasia are included in this classification, independently from the grade of the joint alterations, if signs of the surgery are radiographically demonstrable.

In some countries, like Italy, France and Germany, a Border Line (BL) score is admitted and assigned between ED 0 and ED 1 scores, when there is minimal modelling of the anconeal process.

In the Figure 7 below, scorings locations according to the IEWG scoring system (Table 3) are shown. New bone formation and presence of osteophytes are to be looked for at the dorsal edge of and laterally the anconeal process (**a**), at the cranial edge of the radius (**b**) and at the medial condylar ridge of the humeral condyle (**d**) on the ML projection, whereas at the medial humeral epicondyle and medial coronoid process (**f** and **g**) on the CrCd projection. On the ML view, the contour of the medial coronoid process can be assessed superimposed by the radial head (**c**), while an increased subchondral bony opacity and loss of trabecular pattern, therefore sclerosis, can be seen in distal part of semilunar

notch (**e**). On the CrCd view, the medial aspect of the humeral condyle (**h**) can be inspected for the presence of OC/OCD lesions.

Elbow Dysplasia Scoring		**Radiographic Findings**
0	Normal elbow joint	Normal elbow joint, No evidence of incongruity, sclerosis or arthrosis
1	Mild arthrosis	Presence of osteophytes < 2 mm, sclerosis of the base of the coronoid processes - trabecular pattern still visible
2	Moderate arthrosis or suspect primary lesion	Presence of osteophytes 2 - 5 mm Obvious sclerosis (no trabecular pattern) of the base of the coronoid processes Step of 3-5 mm between radius and ulna (INCONGRUITY) Indirect signs for other primary lesion (UAP, FCP/Coronoid disease, OCD)
3	Severe arthrosis or evident primary lesion	Presence of osteophytes > 5 mm Step of > 5 mm between radius and ulna (obvious INCONGRUITY) Obvious presence of a primary lesion (UAP, FCP, OCD)

Table 3. Elbow Dysplasia Scoring last updated in 2010. From "Explanation of grading according to IEWG and discussion of cases", by Ondreka N. & Tellhelm B., IEWG Proceedings, Verona, 2017

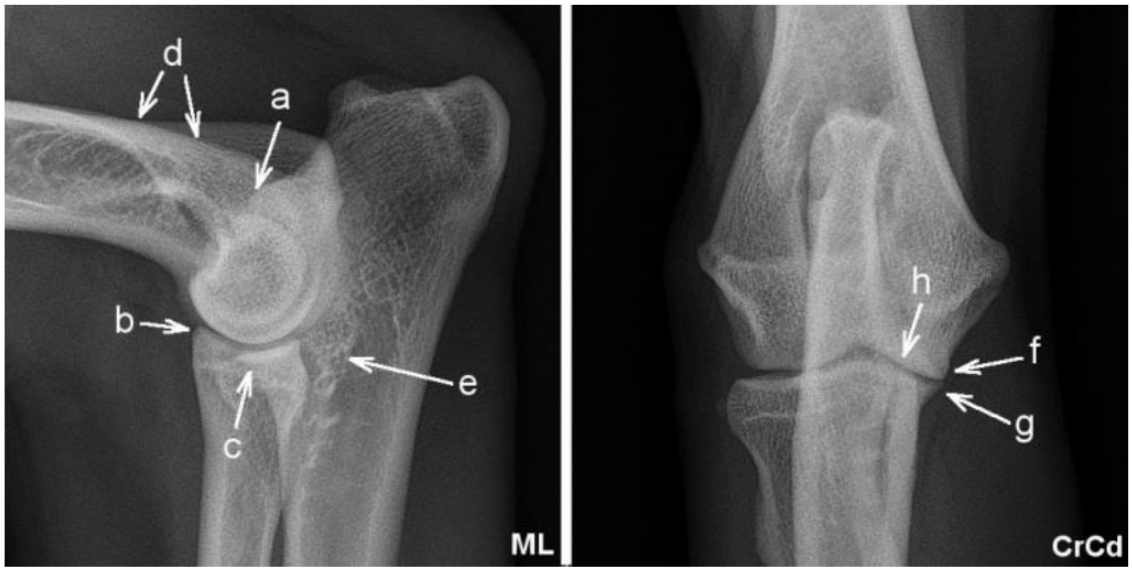

Figure 7. The scorings locations according to IEWG scorings system, indicated on the mediolateral (ML) and the craniocaudal (CrCd) view. From "Screening for elbow dysplasia, grading according to the IWEG.", by Hazelwinkel, H., *33rd Annual Meeting of the International Elbow Working Group. Singapore*, 2018

CLINICAL STUDY

5. INTRODUCTION

Diagnostic imaging is essential to identify elbow diseases in dogs. Lesions of the elbow joints are traditionally evaluated first with radiography.

Although it is known that radiographic diagnosis of elbow dysplasia may be difficult, especially regarding MCD (Medial Compartment Disease) and FCP (Fragmented Coronoid Process), with poor sensitivity compared to advanced imaging modalities, such as computed tomography (CT) and magnetic resonance imaging (MRI), radiology still remains the primary imaging technique in general practice.

Several studies confirmed CT higher accuracy, sensitivity and specificity in achieving a precise diagnosis, when compared to radiology, a technique that often tends to make presumptive diagnosis based solely on the detection of secondary arthrosis, identifying osteophytes and sclerosis rather than the primary cause. (Moores et al., 2008; Heng, IEWG Proceedings, 2015)

In veterinary medicine, arthroscopy is considered the gold standard to detect MCD. (Moores et al., 2008; Gielen & Villamonte_Chevalier, IEWG Proceedings, 2018) However, CT could be the preferred non-invasive and less operator-dependent technique to assess elbow lesions, assuring a full anatomic detail of the bony structures of the elbow joint, without any superimposition, as well as the possibility of computer reconstruction of multiplanar images.

To our knowledge, there are no studies on computed tomography made on a growing population of dogs of different breeds, followed from 6 months of age until 12 months, until the full development of the skeleton; in particular there are not breed specific studies throughout growth, that could allow to better characterize the breed dependent manifestations of this condition, comparing and studying

the same characters in different breeds throughout their growth, showing differences and common features in the elbow joints. Particularly at an early stage, the screening of elbow and hip dysplasia in puppies through objective digital measurement is very likely to require calibrations for each breed, owing to the morphological differences in various breeds.

Moreover, there are several reports on computed tomographic evaluation of elbow joints in dogs, but there is no standard protocol describing patient positioning, slice thickness and slice selection, and above all there are no standard or quantitative parameters that could be used for elbow dysplasia classification as reliable and objective as in radiography.

In our study, two groups of growing dogs of different breeds were enrolled: a group of 34 German shepherd dogs (GSDs) and a group of 20 Labrador retriever dogs (LRDs) underwent CT examination of the elbow joints at about 6 months of age and again at about 12 months of age and were evaluated for the presence of early signs of elbow dysplasia.

In particular, the purposes of the study were:

- ⇒ To describe the computed tomographic appearance of healthy canine elbow joints in German shepherd and Labrador retriever dogs throughout growth, making comparisons between the two breeds
- ⇒ To describe the computed tomographic appearance of lesions attributable to canine elbow dysplasia (MCD/FCP, UAP, IC, OC/OCD) in German shepherd and Labrador retriever dogs throughout growth, making comparisons between the two breeds
- ⇒ To compare lesions as seen at 6 and 12 months old, in order to observe the progression of this pathology during growth
- ⇒ To evaluate specific features and measurements with a hypothetic predictive value for the development of canine elbow dysplasia, assessing their reproducibility and repeatability in different breeds and by different operators of various levels of experience

6. MATERIAL AND METHODS

6.1. CASE ENROLMENTS

Thirty-four German shepherd dogs were considered in this research, including 15 male and 19 females, all from the same breeder.

Additionally, twenty Labrador Retriever dogs were included. Among these, 11 were males and 9 were females; 16 came from different litters of the same breeder, while the other 4 puppies came from another breeder.

All dogs were raised on a homogeneous diet of commercial dog food, lived half of the time indoor and half outdoor and were subjected to controlled, not excessive physical exercise.

Dogs with acute trauma or major surgery of the elbow joints were excluded.

All veterinarians followed guidelines established for good clinical practice and the owners gave informed consent to participate in the study.

Body weight was monitored throughout the study (at about 6 and 12 months old).

None of patients were neutered during the study period.

The dogs underwent two computed tomographic examinations at 6 and 12 months at the Department of Veterinary Science, University of Parma, Italy.

The presence or absence of lameness on the forelimbs was reported after a clinical examination performed by the veterinarian in charge of the patient.

6.2. DATA RECORDS

To perform computed tomographic examinations, in the same session with the standard radiographic screening, the animals were sedated with a standard protocol, consisting in:

* Butorphanol (0.25 µg/kg, IM)
* Dexmedetomidine (0.05 mg/kg, IM)

Anaesthesia was then induced and maintained by Propofol administration (1-4 mg/kg, IV).

Computed Tomographic studies were obtained mostly using a single-slice helical scanner (Somatom Emotion, Siemens Healthcare, Milan, Italy); only 8 German shepherd dogs underwent CT scanning using a 20-slices helical scanner (Somatom Sensation Open, Siemens Healthcare, Milan, Italy).

The dogs were positioned in sternal recumbency on the CT scanning table, head first, with the aid of tapes and/or bandages and foam wedges for a better positioning and to extend the forelimbs in the most symmetric way. The head was retracted caudally to avoid artefacts. (Figures 8 – 9)

Figure 8. Patient positioning in the tomographic scanner. From the Veterinary Science Department of the University of Parma

Figure 9. patient positioning in the tomographic scanner. From the Veterinary Science Department of the University of Parma

Each scan of single-slice scanner was made using 130 kVp and 60 mA, slice thickness of 1 mm, a pitch 1.0, tube rotation time of 1 s, matrix of 512 x 512. Scans from the multi-slice scanner were made using 140 kVp and 150 mA, slice thickness of 1 mm, a pitch 0.55, tube rotation time of 1 s, matrix of 512 x 512. All images were reconstructed both with bone and soft tissue algorithms and viewed with standard soft tissue (WW 400, WL 40) and bone (WW 4000, WL 400) windows.

All the computed tomographic studies were evaluated independently, through multiplanar reconstructions, scoring right and left joints of each dog on the basis of specific alterations.

At 6 and 12 months, the following CT parameters were considered:

* Medial coronoid disease grade
* Medial coronoid process conformation
* Irregular or cystic radial incisure of the ulna
* Elbow osteophyte grade
* Ulnar subtrochlear sclerosis grade
* Evaluation of ulnar subtrochlear sclerosis quantitatively in specific ROIs (Regions of Interest)
* Joint incongruity grade
* Presence or absence of an elliptical trochlear notch
* Presence or absence of an ununited anconeal process
* Elbow Dysplasia Score

6.3. CT DATA EVALUATION

Each elbow was evaluated at about 6 and 12 months of age including the following features:

- **Medial coronoid disease grade**

  As described by Draffan et al. (2008), the medial coronoid process was evaluated mainly in the transverse and sagittal views, and with the aid of 3D MPR function. (Figure 10)

  When clearly visible, the presence of hypodense areas on the apex of the MCP were noted.

  Grades were assigned following the rating below:

  - 0 normal coronoid
  - 1 mild change in coronoid shape
  - 2 fissured coronoid
  - 3 fragmented coronoid

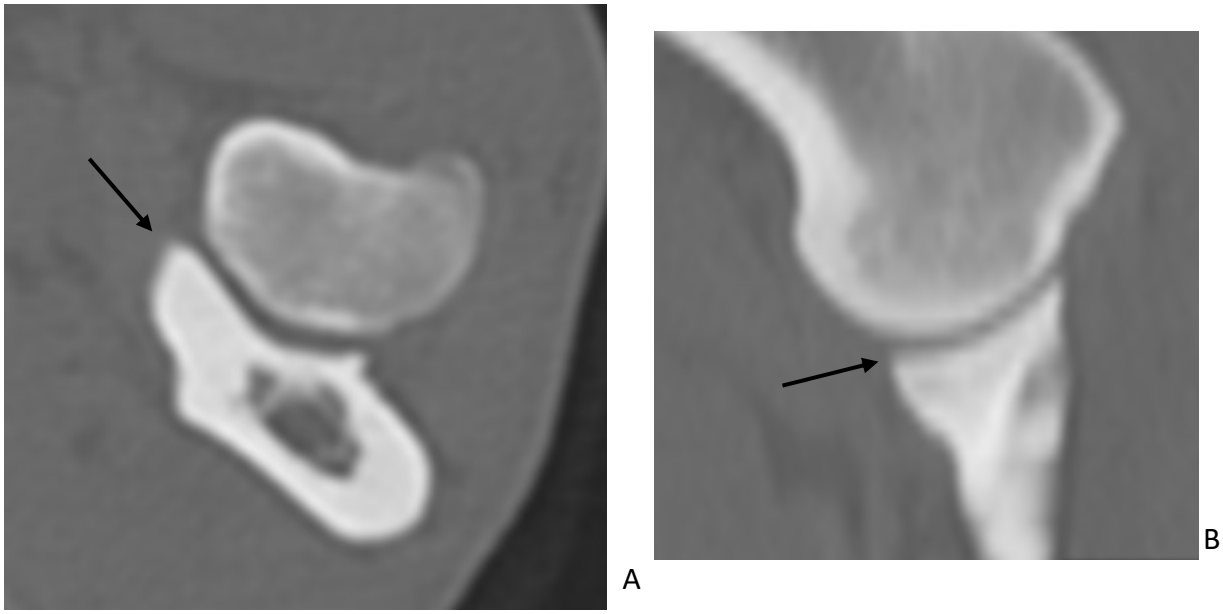

Figure 10. CT scan, transverse view (A) and sagittal view (B) of the left elbow of a 12 months old dog. The black arrows indicate the medial coronoid process. From the Veterinary Science Department of the University of Parma

- **Medial coronoid process conformation**

  Basing on the work by Klumpp et al. (2013), and as later resumed in 2016 IEWG meeting by Ondreka et al. (Figure 11), the shape of the medial coronoid process of each elbow was evaluated in the transverse view and ascribed to the following possible conformations:

  - round

  - pointy

  - flattened

  - irregular

  When irregular, the medial coronoid grade was considered 1.

  Once fissured or fragmented, coronoid processes were not evaluated for their shapes.

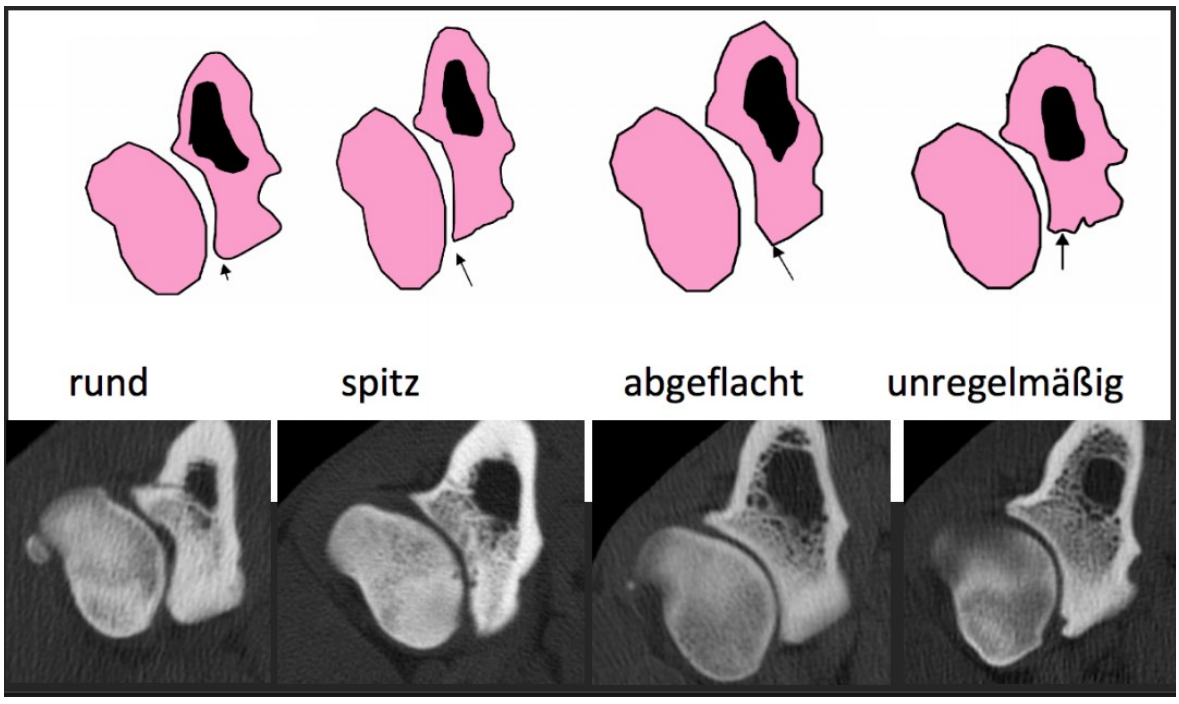

Figure 11. MCP conformations as proposed by Klumpp et al. (2013) and their appearance in CT scans, transverse views. Rund = round, spitz = pointy, abgeflacht = flattened, unregelmäßig = irregular. From Proceedings of the 30th International Elbow Working Group Meeting, Vienna, 2016, by Ondreka et al.

- **Irregular or cystic radial incisure of the ulna**

  According to the studies by Reichle et al. (2000) and Moores et al. (2008), it was evaluated on the trasverse view, considering both the presence of an irregularity in the incisure profile or subchondral lucencies and/or cystic lesions:

  - 0 normal incisure (Figure 12 A)

  - 1 irregular contour of the incisure (Figure 12 B)

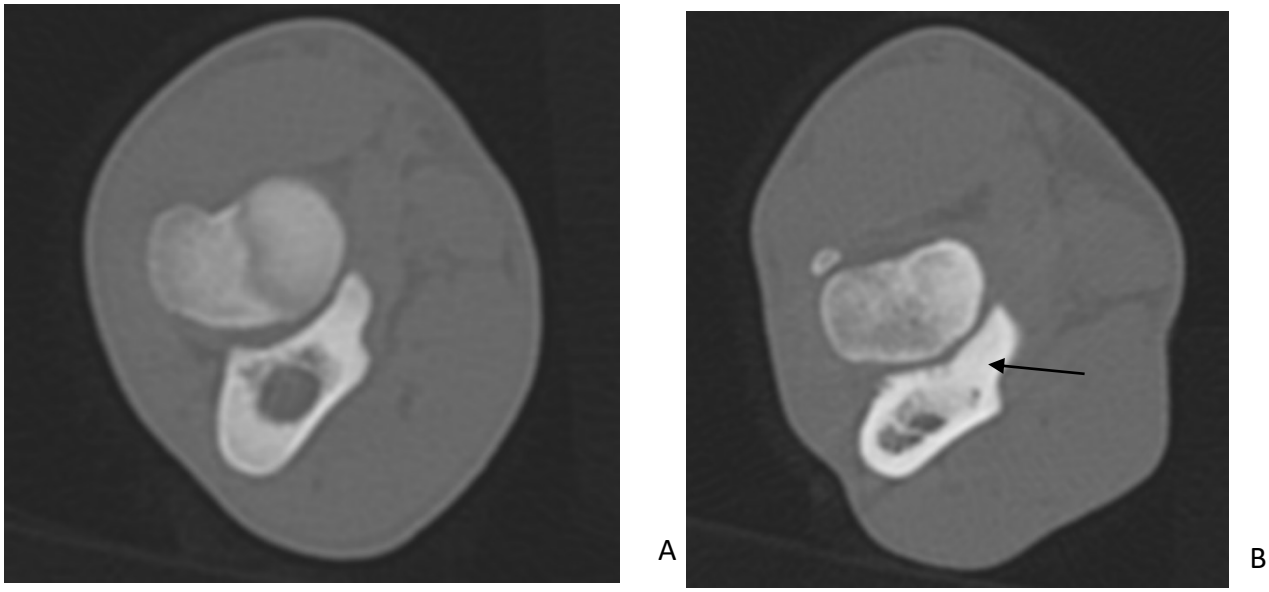

Figure 12. A: CT scan, transverse view of the right elbow of a 4 months old puppy. Regular radial incisure of the ulna. B: CT scan, transverse view, left elbow of a 15 months old dog. The radial incisure is irregular and with lucencies in the cortex (black arrow). From the Veterinary Science Department of the University of Parma

- **CT osteophyte score**

  Osteophytes were evaluated in all views with the aid of 3D MPR function, located and measured to be classified as described by Moores et al. (2008):

  - 0 no osteophytes present

  - 1 osteophytes < 2 mm present

  - 2 osteophytes between 2- and 5-mm present

  - 3 osteophytes > 5 mm present

- **Ulnar subtrochlear sclerosis grade**

  The TNS (Trochlear Notch Sclerosis) grade was assessed subjectively on the sagittal view, obtained on MPR as it will be described below, observing intensity and extent of the sclerosis, on the basis of a radiographic descriptive, categorical scale by Draffan et al., 2009:

  - 0 no sclerosis
  - 1 mild sclerosis, trabecular pattern still easily seen
  - 2 moderate sclerosis, trabecular pattern slightly unclear
  - 3 severe sclerosis, trabecular pattern cannot be seen

- **Evaluation of ulnar subtrochlear sclerosis quantitatively in specific ROIs**

  An objective, quantitative evaluation of the TNS has been attempted using determinate ROIs (Regions of Interest), operating on the medical viewer *Horos (The Horos Project and OsiriX Team, 2020)*, with the aim of evaluating the mean HU (Hounsfield Unit) values, interpreted as bone density, hence grade of sclerosis.

  Three different, specific areas of the ulnar trochlear notch were chosen in the sagittal view, obtained in a standardized procedure.

  UAP positive elbow joints were excluded from this examination.

  CT studies were evaluated for ROIs assessment in consensus by a senior radiologist and a Phd student, independently from the subjective TNS grade.

  A pilot study on 19 of the German shepherd dogs included in this study was made, adding the evaluation of a fifth-year student of Veterinary Medicine as a third operator.

  All the ROIs (Figure 13) were positioned avoiding the cortex and in the most homogeneous point, maintaining a standard deviation lower than 50.

  - Proximal ROI (area 0,015 cm^2), caudally to the anconeal process
  - Central ROI (area 0,015 cm^2), located at the mean point of the ulnar notch

- Distal ROI (area 0,010 cm^2), close to the medial coronoid process

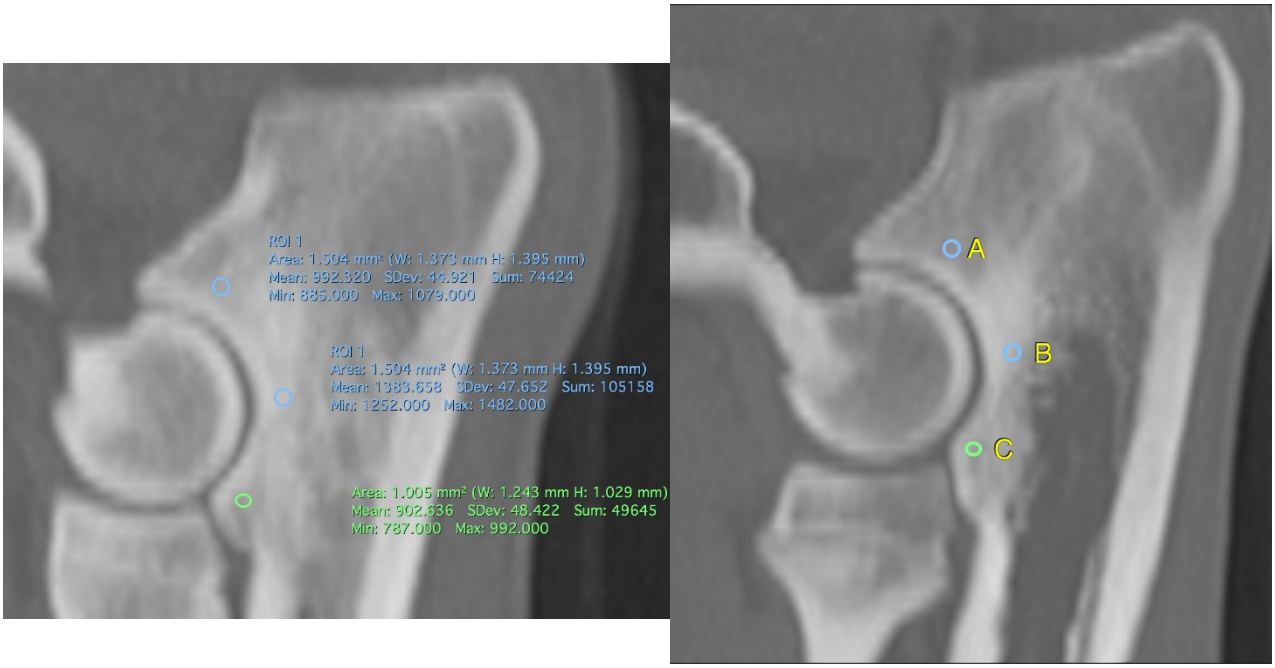

Figure 13. CT scan, transverse view, right elbows of 12- and 6-months old GSDs. A: Proximal ROI. B: Central ROI. C: Distal ROI. From the Veterinary Science Department of the University of Parma

The standard positioning of the sagittal view was obtained starting from the transverse view, in which the MPR was centred on the ulna with an axis passing between the humeral condyles, and then centring the axis in the middle of the ulna on the dorsal view (Figure 14).

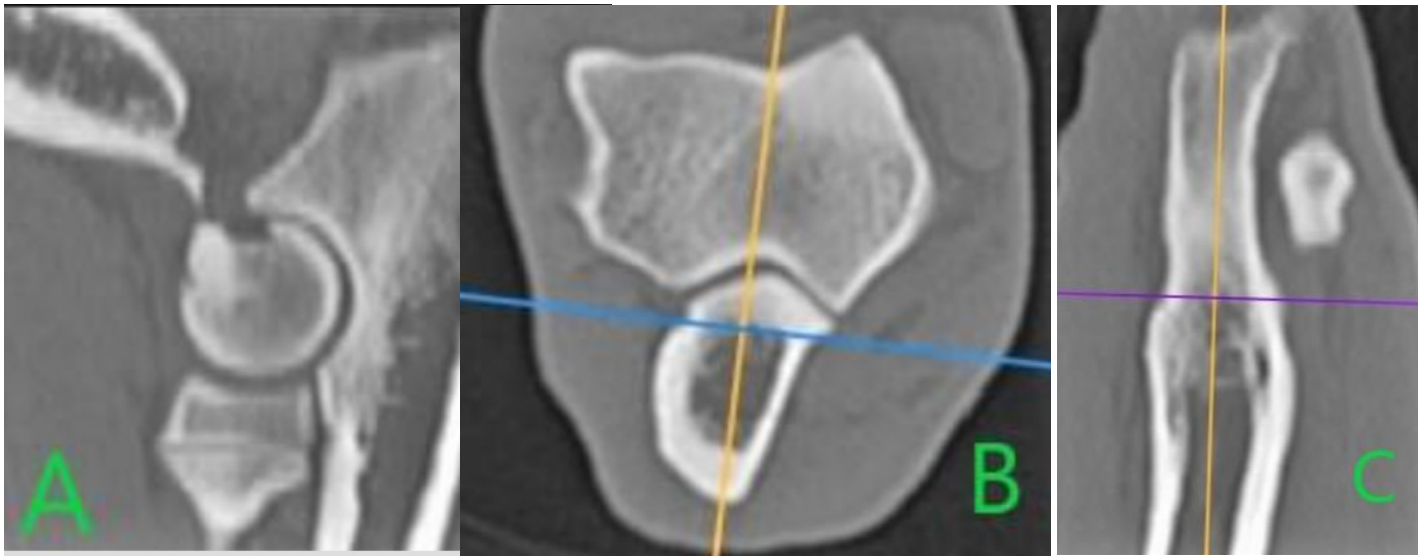

Figure 14. CT scan of a 12 months old canine elbow, standardized multiplanar reconstruction for collecting ROI values; sagittal view (A), transverse view (B) and dorsal view (C). From the Veterinary Science Department of the University of Parma

- **Joint incongruity grade**

  Elbow incongruity was evaluated subjectively and then quantitatively measuring the radio-ulnar joint space in the sagittal view of each elbow joint (Figure 15). In particular, we considered the presence and the extent of a radio-ulnar step at the base of the coronoid process. (Kramer et al., 2006; Hebel et al., 2021) However, we modified the method described by Kramer and colleagues (2006), as the measures were taken in the sagittal view obtained by the standard positioning used to collect the ROIs values, therefore centring the midline of the ulna.

  The score was made on the basis of the one used for the same parameter in radiography:

  - 0 no incongruity (< 1 mm)

  - 1 mild incongruity (> 1 < 2 mm)

  - 2 moderate incongruity (2 – 3 mm)

  - 3 severe incongruity (> 3 mm)

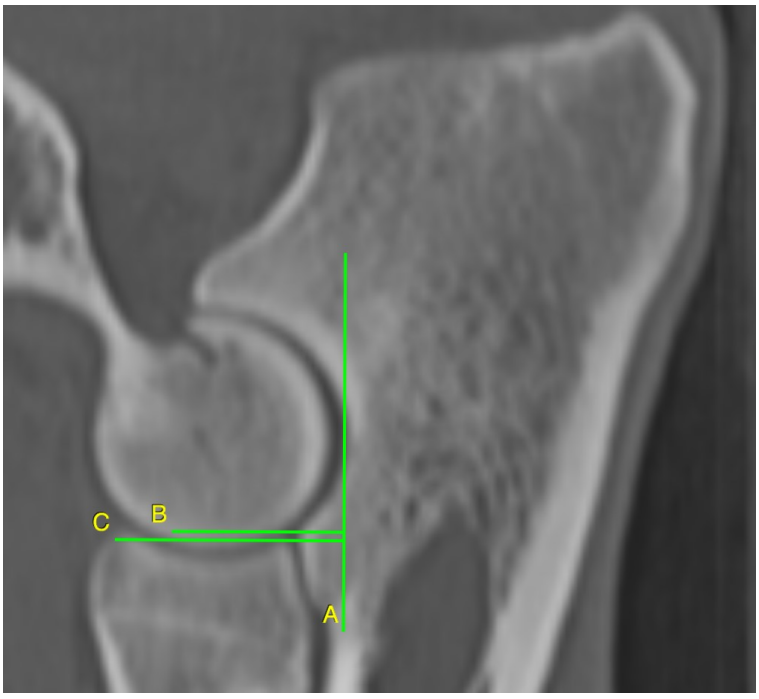

Figure 15. CT scans, sagittal view of the right elbow of a 12 months old female German shepherd dog, measurement of the radio-ulnar joint space (green line). A: line tangent to the trochlear notch. B: line crossing the MCP. C: line tangent to the radial head, parallel to B. From the Veterinary Science Department of the University of Parma

- **Presence or absence of an elliptical trochlear notch**

  The curvature degree of the ulnar trochlear notch was evaluated in relation to the humeral trochlea, to underline the presence of a smaller and/or altered shape in comparison to the round condyles' profile (Figure 16).

  This assessment was made in the sagittal view, acquired in a standard way as described previously.

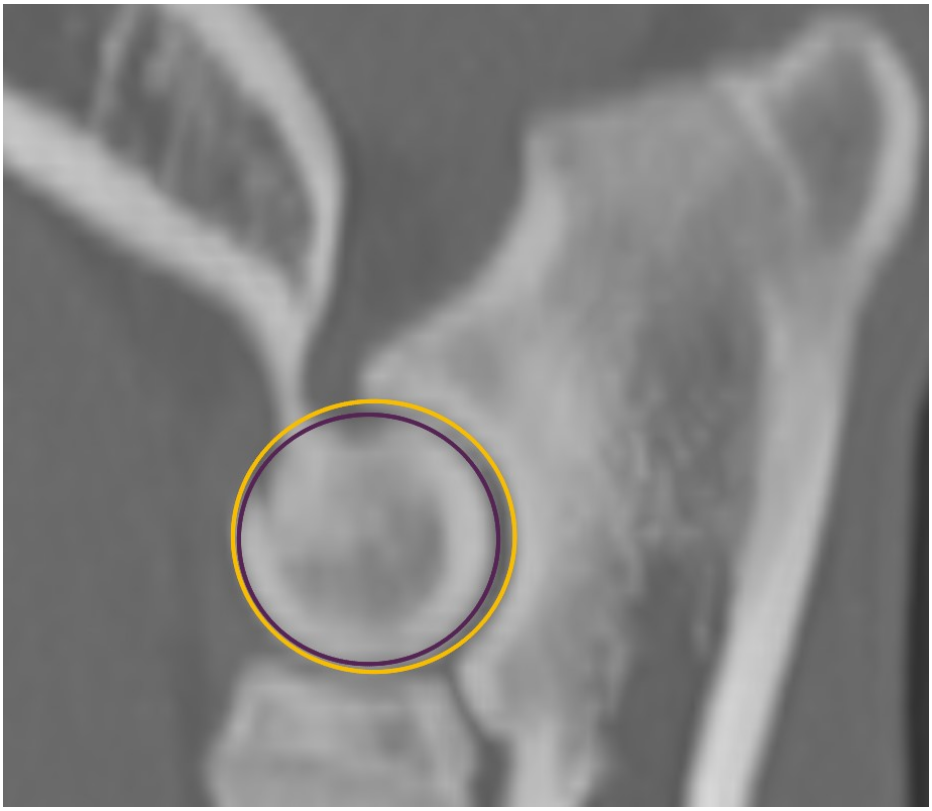

Figure 16. CT scans, sagittal view of the left elbow of a 7 months old female Labrador retriever dog, evaluation of the curvature and shape of the ulnar trochlear notch. From the Veterinary Science Department of the University of Parma

- **Presence or absence of an ununited anconeal process**

  Each elbow has been evaluated for the presence of this pathologic condition as it follows:

  - 0 UAP absent

  - 3 UAP present

- **Elbow Dysplasia Score**

Each elbow was given a final ED score, at both 6 and 12 months old, on the basis of the highest score given on the single examined features (in particular the medial coronoid disease grade, the elbow osteophyte grade, the ulnar subtrochlear sclerosis grade, the joint incongruity grade, and the presence or absence of an ununited anconeal process).

The adopted scoring chart, as shown in Table 4, was similar to that used for radiographic findings.

Elbow Dysplasia Scoring		**Computed tomography**
Grade 0	Normal elbow joint	- Normal elbow joint - No evidence of incongruity, sclerosis or arthrosis
Grade 1	Mild arthrosis	- Osteophytes < 2 mm high - Radioulnar step of 1,5- 2 mm - Mild sclerosis, trabecular pattern still easily seen
Grade 2	Moderate arthrosis	- Osteophytes between 2-5 mm high - Radioulnar step between 2-5 mm (suspect IC) - Moderate sclerosis, trabecular pattern slightly unclear
Grade 3	Severe arthrosis	- Osteophytes of > 5 mm high - Radioulnar step > 5 mm (obvious IC) - Severe sclerosis, trabecular pattern cannot be seen - Presence of UAP, FCP, OCD

Table 4. Assumed Elbow Dysplasia Grading Score in Computed Tomographic evaluation.

6.4. STATISTICAL ANALYSIS

A statistical software (SPSS 16.0 for Windows, SPSS, Inc., Chicago, IL) was used for the statistical analysis.

The main goal was to evaluate a hypothetical predictive value of the taken measurements (proximal, central, distal ROIs, and radio-ulnar step) on the development of elbow dysplasia.

First, in order to assess reproducibility of the ROIs evaluation between different operators of different experience and repeatability of these measures by the same operator, the ICC (Inter-Class Correlation) was calculated to measure inter-rater agreement, considering:

- > 0,75 excellent correlation
- 0,60 - 0,74 good correlation
- 0,40 - 0,59 fair correlation
- < 0,40 poor correlation

Consequently, for each parameter at 6 months of age a ROC (Receiver Operating Characteristic) curve was outlined, to evaluate its accuracy as a diagnostic test and identify the cut-off between true positives and false positives, in relation to the final ED score at 12 months of age (considering grade 0 as negative and grade 1-2-3 as positive). According to Hosmer & Lemeshow (2000), the AUC (Area Under the Curve) values were evaluated in this way:

- < 0.5 no discrimination (i.e., ability to diagnose patients with and without the disease or condition based on the test)
- 0.7 to 0.8 acceptable
- 0.8 to 0.9 excellent
- > 0.9 outstanding

Data were tested for normality with Shapiro Wilk test and did not result normally distributed.

A comparison of the mean values of Proximal, Central and Distal ROIs in the FCP positive elbows between LRDs and GSDs were calculated for each variable through Mann-Whitney U Test. Differences were considered significant at p <0,05.

A Mann-Whitney U Test was performed in the two breeds populations to verify if the presence of a radio-ulnar step was greater among the patients that resulted positive to the ED grading than in the healthy dogs. P value <0,05 was considered significant.

To confirm our hypothesis about an eventual association between the presence of an elliptical trochlear notch and the development of elbow dysplasia in the German shepherd dog's population, a Fisher's exact test was used.

Fisher's exact test was used also to evaluate association between the presence of radio-ulnar steps and an elliptical ulnar trochlear notch. P value <0,05 was considered significant.

Pearson correlation coefficient was calculated between Proximal, Central and Distal ROIs at 6 and 12 months of age for GSDs and LRDs and radio-ulnar step at 6 and 12 months of age.

The size of correlation coefficient was interpreted according to the table 5 below.

Size of correlation	Interpretation
0.90-1.00 (−0.90 to −1.00)	Very high positive (negative) correlation
0.70-0.90 (−0.70 to −0.90)	High positive (negative) correlation
0.50-0.70 (−0.50 to −0.70)	Moderate positive (negative) correlation
0.30-0.50 (−0.30 to −0.50)	Low positive (negative) correlation
0.00-0.30 (0.00 to −0.30)	Negligible correlation

Table 5. From S. Yadav: Correlation Analysis in Biological Studies, Journal of the Practice of Cardiovascular Sciences, 2018, 4 (2),116-121.

7. RESULTS

Sixty-eight elbow joints of 34 German shepherd dogs (GSDs) and forty elbow joints of 20 Labrador retriever dogs (LRDs) at the mean age of 6 and 12 months were evaluated in this prospective study. Of the 34 evaluated GSDs, 15 (44,1%) were male and 19 (55,9%) were female, while of the 20 LRDs, 13 (65%) were male and 7 (35%) were female; none of them was neutered.

The mean weight of the GSDs at the mean age of 6 months was 25,64 kg (range 18 – 35 kg), whereas at the mean age of 12 months was about 31,53 kg (range 19 - 40 kg).

As for the LRDs, the mean weight of the population at 6 months of age was 20,82 kg (range 10 – 28,8 kg), while at 12 months of age it was 30,26 kg (range, 20 – 40 kg).

Six GSDs were reported with forelimb lameness at 6 months old, 2 bilateral and 4 unilateral, 2 males and 4 females. One male dog had bilateral lameness at 4 months of age, according to the owners, which later resolved. Eight patients, 6 females and 2 males, presented lameness at 12 months, 6 of which unilaterally; three did not show limping at 6 months of age, while one dog was lame only as a puppy.

Only one male dog in the LRDs group was reported to show lameness on one forelimb at 12 months of age. All lame dogs had a final ED score of 3.

Medial Coronoid Disease Grade (Graphs 1 – 2)

Of the 68 elbow joints of the 34 GSDs, at 6 months old, 47 (69,2%) had a normal MCP (grade 0), 13 (19,1%) MCP were irregular (grade 1), 3 (4,4%) were fissured (grade 2) and 5 (7,3%) were fragmented (grade 3).

At 12 months old, 39 (57,4%) elbows had a medial coronoid disease grade of 0, 15 (22%) MCP were considered grade 1, only 1 (1,5%) MCP was fissured (grade 2), and 13 (19,1%) MCP were clearly fragmented.

In our population of GSDs at 6 months, 23 (33,8%) elbows were reported with medial coronoid disease, increasing up to 29 (42,6%) elbows at 12 months. Ten dogs had clear FCP, 3 bilaterally.

Out of the 40 elbow joints of the LRDs group, at 6 months of age, 33 (82,5%) had a medial coronoid disease grade of 0, only 1 (2,5%) had a grade of 1, 1 (2,5%) had a fissured MCP (grade 2), and 5 (12,5%) elbows had a clear FCP (grade 3).

At 12 months of age, the same population of LRDs counted 30 elbow joints (75%) without signs of medial coronoid disease (grade 0), 3 (7,5%) had an irregular MCP (grade 1), 1 (2,5%), as at 6 months of age, had a fissured MCP (grade 2), while the FCPs (grade 3) rose up to 6 (15%).

In our population of LRDs at 6 months, 7 (17,5%) elbows were reported with medial coronoid disease, whereas 10 (25%) elbows were affected at 12 months. Five dogs had clear FCP, only 1 bilaterally.

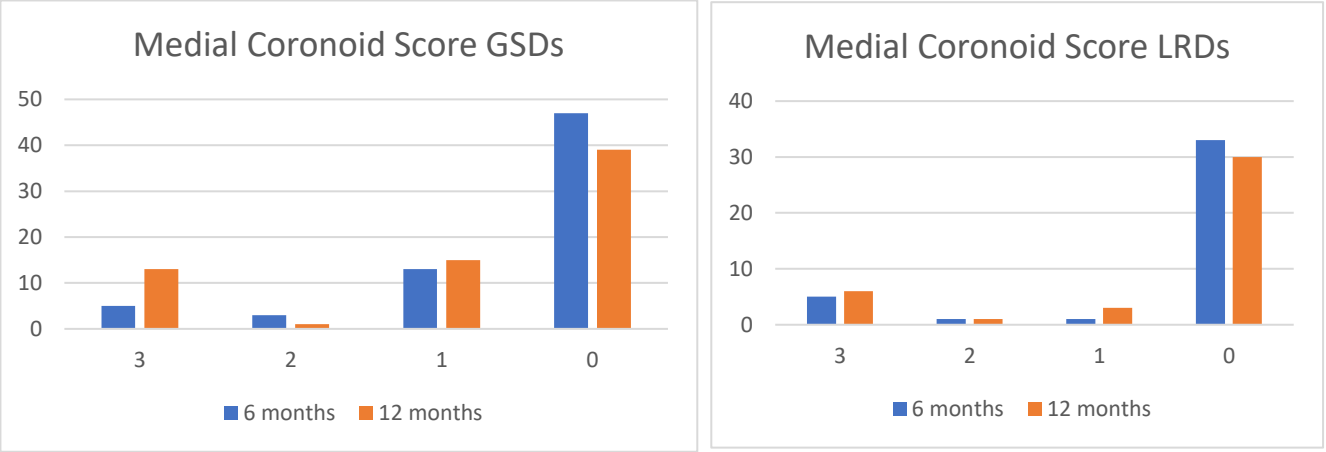

Graphs 1-2. Comparisons of the Medial Coronoid Disease scores at 6 and 12 months of age in the two study population groups of German shepherd and Labrador retriever dogs.

Medial Coronoid Process Conformation

As explained previously, in accordance with Klumpp et al. (2013), each medial coronoid process was separately evaluated for its shape and attributed to 4 different conformations (round, pointy, flattened or irregular). Fissured and fragmented coronoids were not considered in this categorisation.

In contrast to their study, MCP were observed during growth in the same subjects, at 6 and 12 months old, to identify eventual changes in shape, both in healthy and affected elbows.

The two breeds object of this study showed some differences, which will be discussed in the next chapter, both in relation to the frequency of a certain conformation, and to the appearance of the same shape between subjects of different breed.

Among the GSD population, the pointy conformation of the MCP was the most frequently observed at all ages, followed closely by a round shape at 6 months of age, while at 12 months round and irregular conformations were almost equally represented.

In particular, at 6 months old there were: 22 pointy MCP (32,3%), 20 round MCP (29,4%), 13 irregular MCP (19,1%) and 5 flattened MCP (7,3%).

At 12 months we counted: 21 pointy MCP (30,9%), 14 round MCP (20,6%), 15 irregular MCP (22%) and 4 flattened MCP (5,9%).

Conversely, in the LRDs group, a round conformation of the medial coronoid process was by far the most frequent in this breed; a flattened shape, especially at 12 months, was less rarely observed than in GSDs, as opposed to the irregular conformation, while only one pointy MCP was noted at 6 months.

To summarize, at 6 months of age 23 (57,5%) MCP were round, 9 (22,5%) flattened, 1 (2,5%) pointy and 1 (2,5%) irregular, while at 12 months of age, 18 (45%) MCP were round, 12 (30%) flattened, 0 pointy and, lastly, 3 (7,5%) appeared irregular.

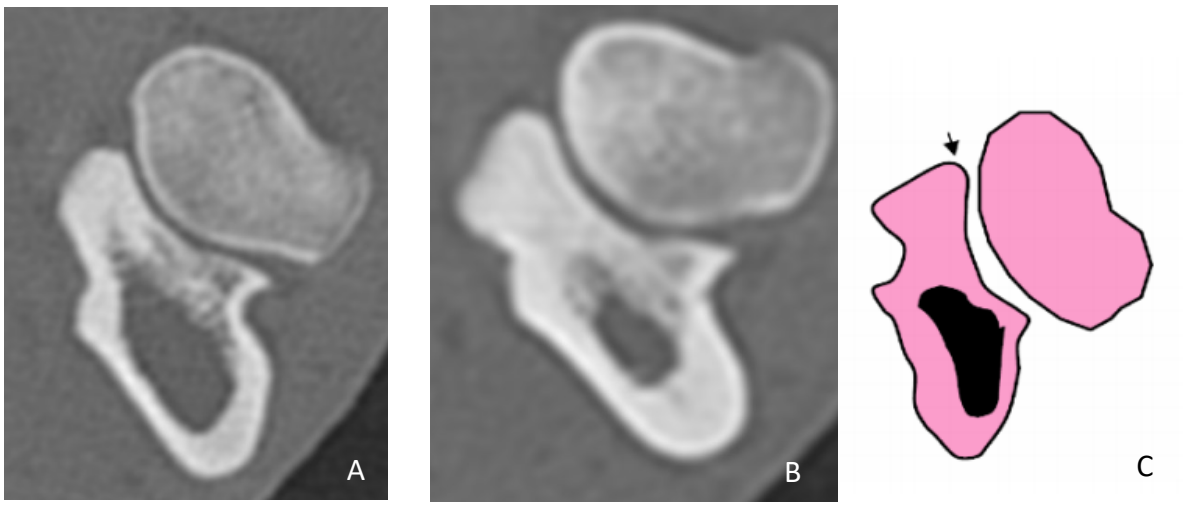

Figure 17. CT scans, transverse views. Round MCP conformations. A: left elbow joint of a 12 months male GSD. B: left elbow joint of a 12 months female LRDs. From the Veterinary Science Department of the University of Parma. C: model of round shape from Klumpp et al. (2013)

Each conformation appearance was slightly different between the two breeds, as can be noted in the Figures 17 to 20.

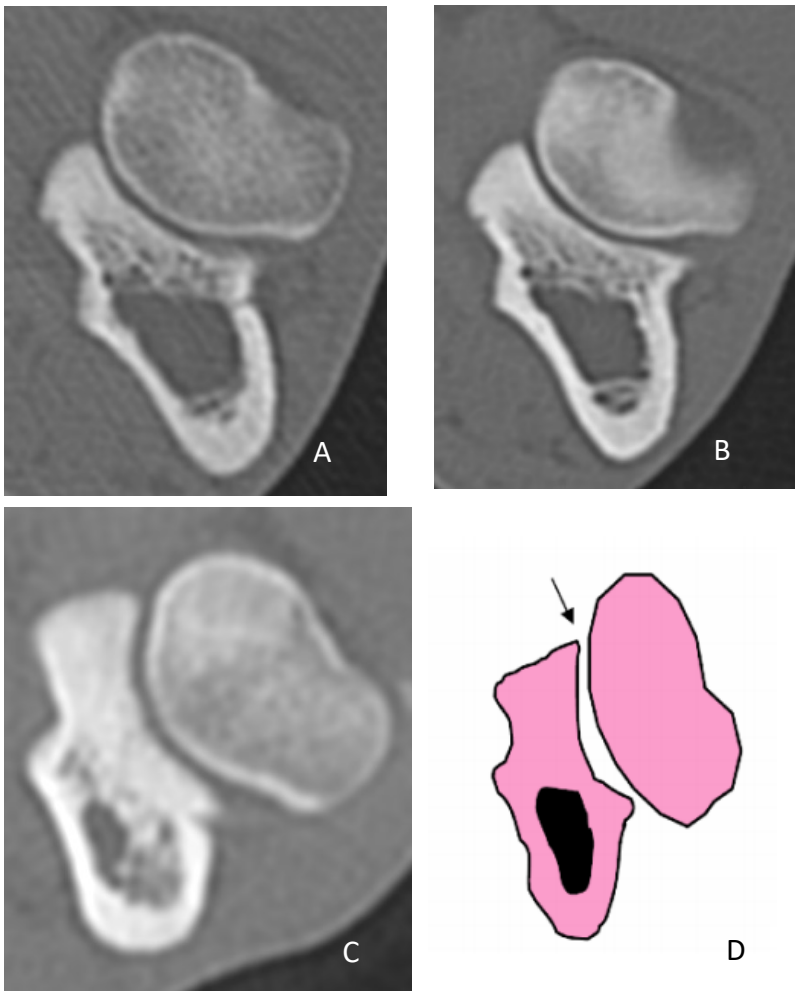

Figure 18. CT scans, transverse views. Pointy MCP conformations. A: right elbow of a 6 months female GSD. B: the same elbow at 12 months old. C: right elbow joint of a 6 months male LRDs. From the Veterinary Science Department of the University of Parma. D: model of pointy shape from Klumpp et al. (2013)

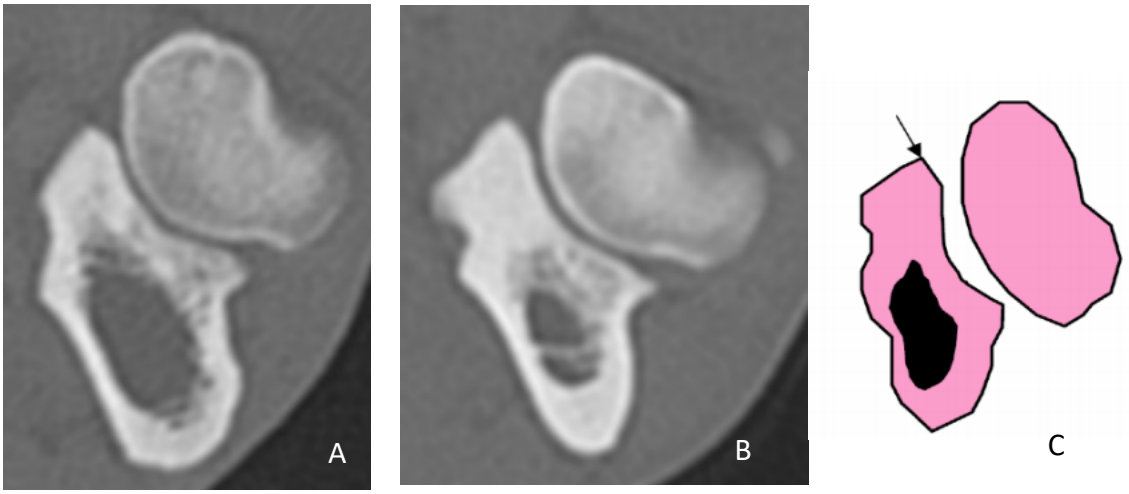

Figure 19. CT scans, transverse views. Flattened MCP conformations. A: right elbow joint of a 12 months male GSD. B: right elbow joint of a 12 months male LRD. From the Veterinary Science Department of the University of Parma. C: model of flattened shape from Klumpp et al. (2013)

A score 1 in the medial coronoid disease classification was given to all irregular shaped medial coronoid processes, although with different grades of irregularity and present signs of osteoarthrosis.

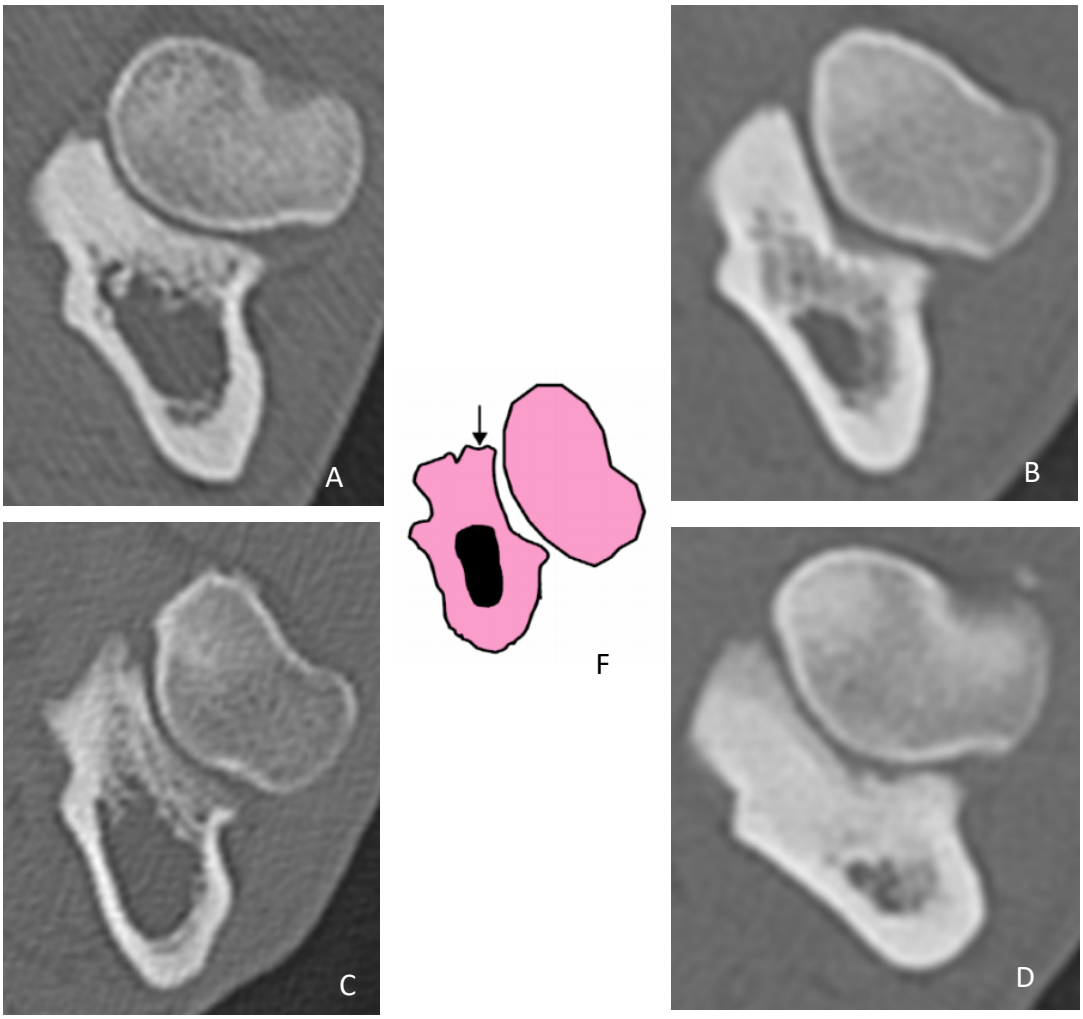

Figure 20. CT scans, transverse views. Irregular MCP conformations. A-B: mild/moderate irregular shape. A: right elbow joint of a 12 months male GSD. B: left elbow joint of a 12 months male LRD. C-D: severe irregular shape; arthrosis is present. C: left elbow joint of a 12 months female GSD. D: right elbow joint of a 12 months female LRD. From the Veterinary Science Department of the University of Parma. F: model of irregular shape from Klumpp et al. (2013)

In the growing canine population of our study, we observed some changings in the conformation of the medial coronoid process over time, with some differences between the two breeds.

In German shepherd dogs there were several changes in MCP conformations; most of them represented an increase in the medial coronoid disease grade, thus a worsening in the elbow dysplasia score, while only 2 shape shifts occurred in two grade 0 elbows of different subjects, both from a round to a pointy conformation (Figure 21).

Four irregular shaped MCPs underwent fragmentation over time; however, in one elbow graded as 1 at 6 months, with a bilateral radio-ulnar step, a round MCP became fragmented at 12 months old (Figure 22). Three pointy MCP shifted to an irregular conformation (Figure 23), while, conversely, in one elbow we observed the opposite (Figure 24). Another pointy shaped MCP underwent fissuring. Similar to the LRDs group, 3 round MCPs changed to being irregular, as happened to one of the flattened MCPs (Figure 25), rarely seen in this breed population.

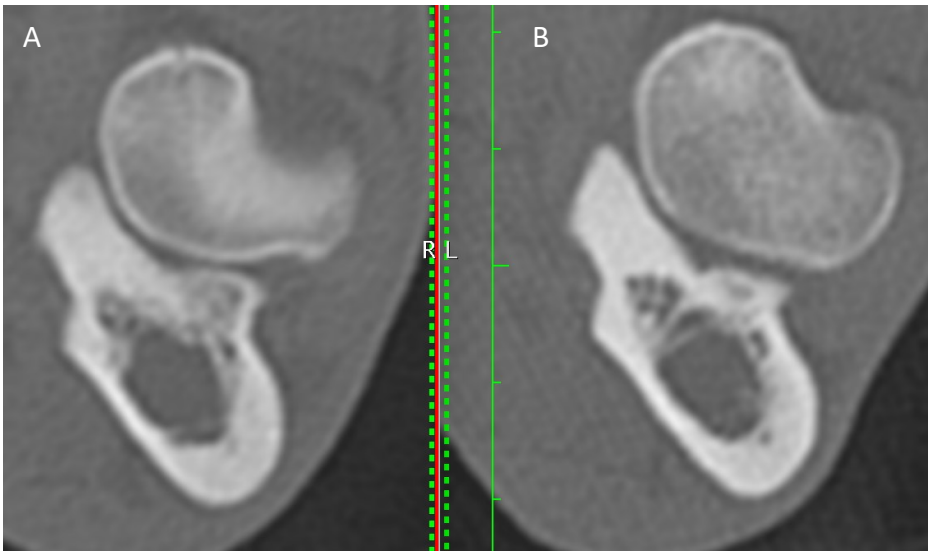

Figure 21. CT scans, transverse views. MCP conformation change from round (and hypodense) to pointy in a male GSD from 6 months (A) to 12 months (B) of age. From the Veterinary Science Department of the University of Parma

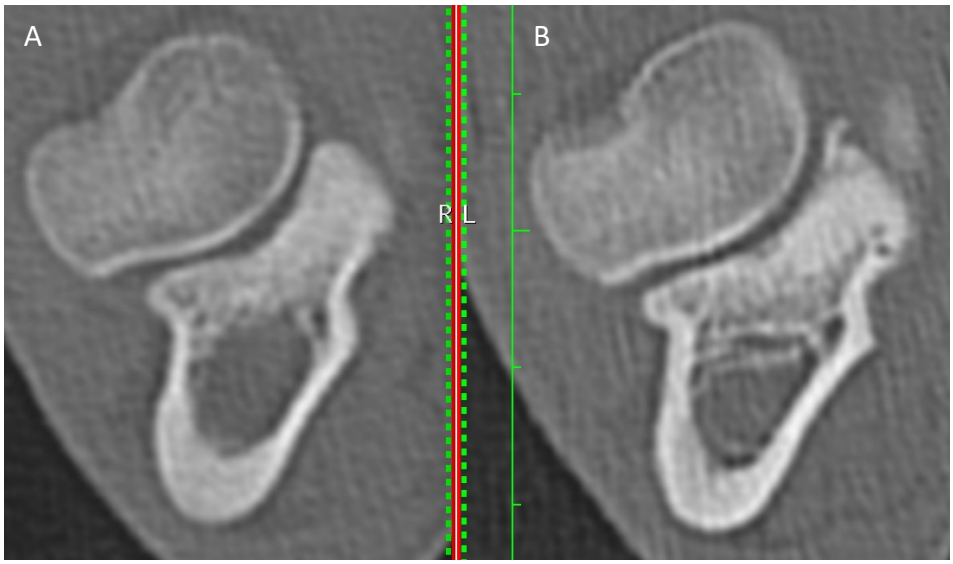

Figure 22. CT scans, transverse views. MCP conformation change from round to fragmented in a male GSD from 6 months (A) to 12 months (B) of age. From the Veterinary Science Department of the University of Parma

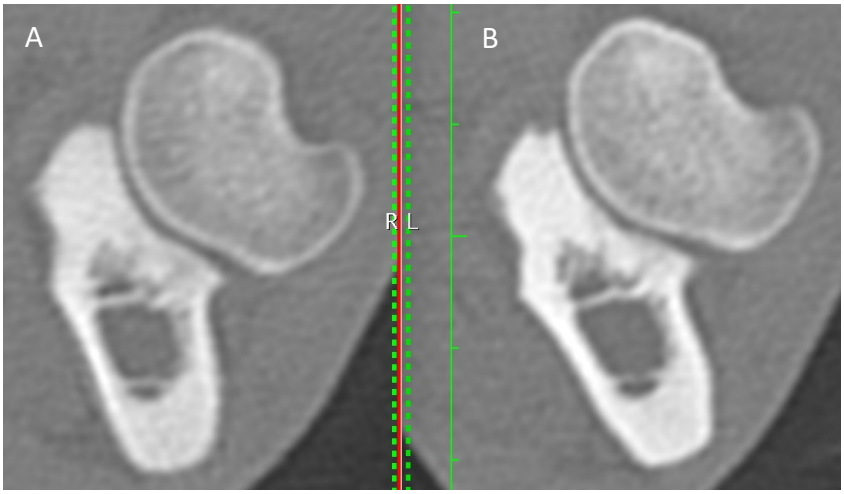

Figure 23. CT scans, transverse views. MCP conformation change from pointy to irregular in a male GSD from 6 months (A) to 12 months (B) of age. From the Veterinary Science Department of the University of Parma

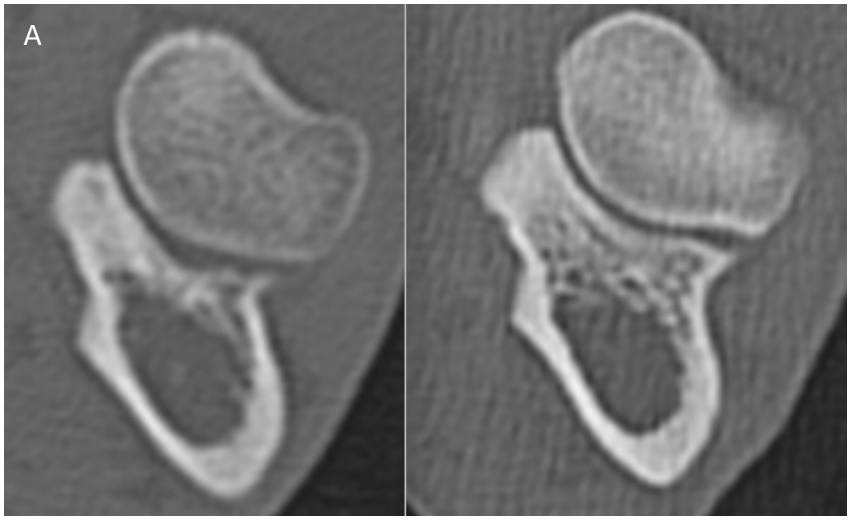

Figure 24. CT scans, transverse views. MCP conformation change from irregular (and hypodense) to pointy in a male GSD from 6 months (A) to 12 months (B) of age. From the Veterinary Science Department of the University of Parma

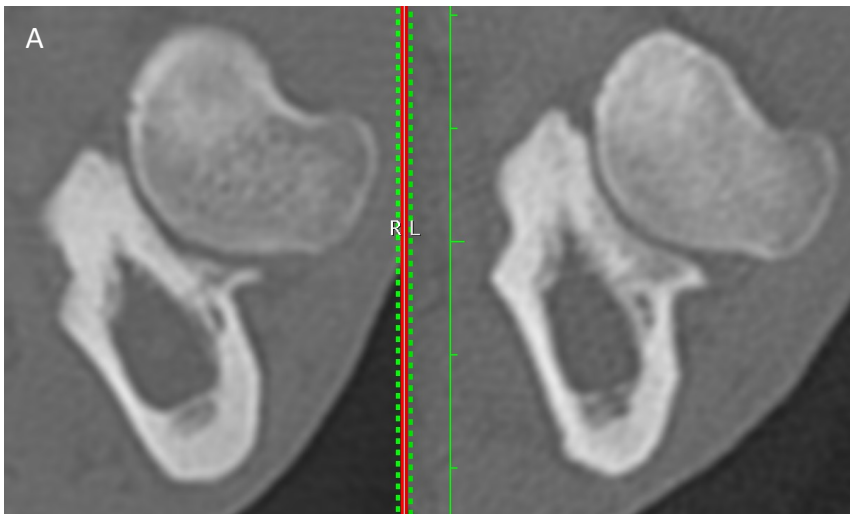

Figure 25. CT scans, transverse views. MCP conformation change from flattened to irregular in a male GSD from 6 months (A) to 12 months (B) of age. From the Veterinary Science Department of the University of Parma

In LRDs, few shape shifts were observed, when compared to the other examined breed.

In three healthy dogs, three round coronoids seen at 6 months old became flattened at 12 months of age (Figure 26). Other 2 round MCP became irregular, one of them being in the contralateral elbow to one affected by FCP. Interestingly, the only clearly pointy MCP underwent fragmentation at 12 months (Figure 27).

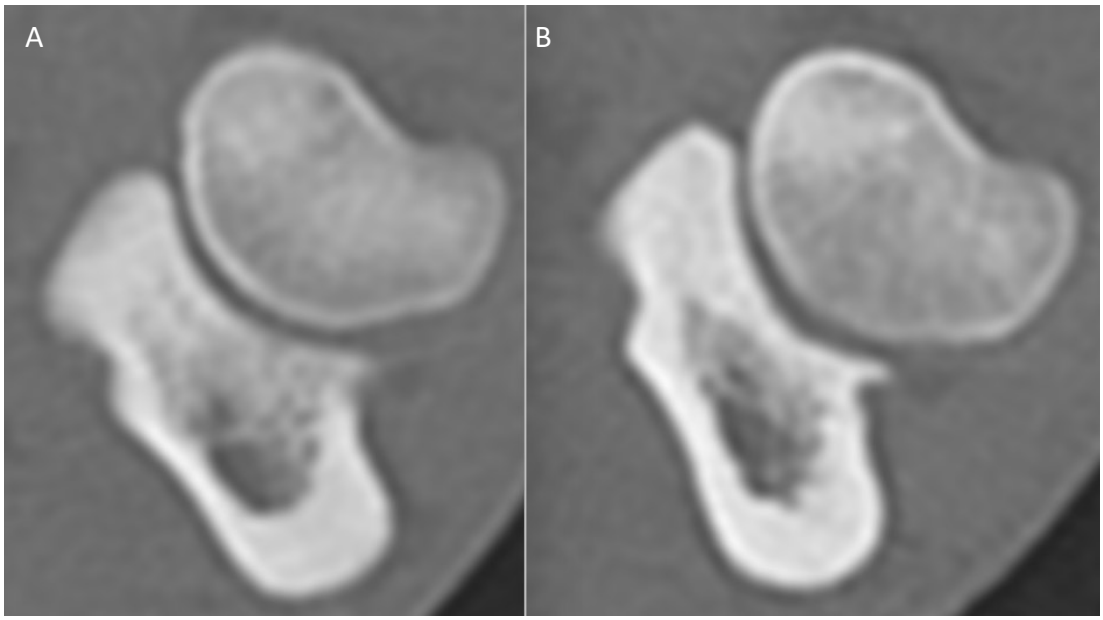

Figure 26. CT scans, transverse views. MCP conformation change from round to flattened in a male LRD from 6 months (A) to 12 months (B) of age. From the Veterinary Science Department of the University of Parma

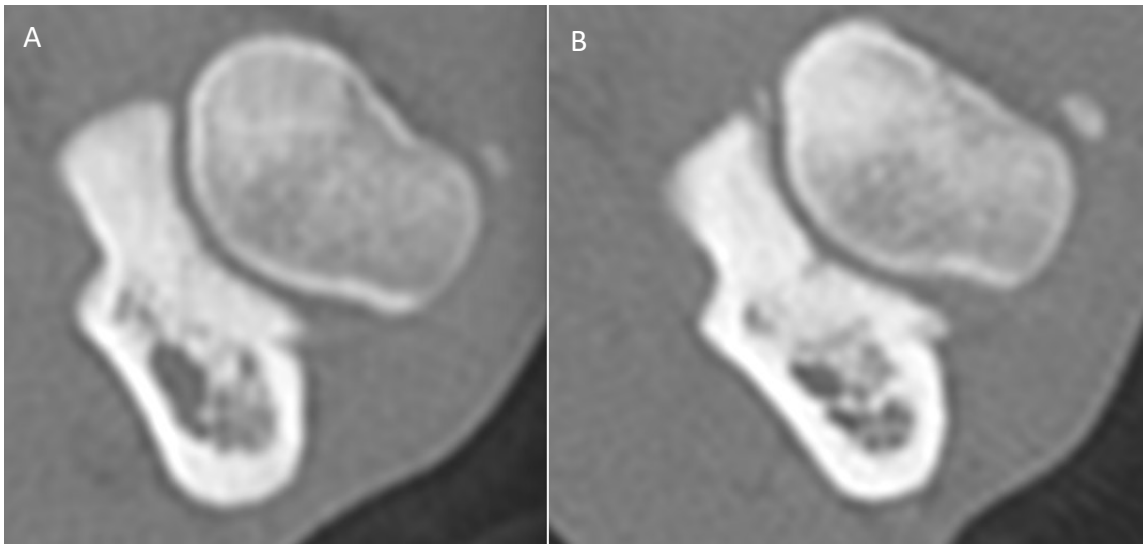

Figure 27. CT scans, transverse views. MCP conformation change from pointy to fragmented in a male LRD from 6 months (A) to 12 months (B) of age. From the Veterinary Science Department of the University of Parma

Irregular or cystic radial incisure of the ulna

In GSDs, an irregular radial incisure of the ulna without cystic lesions was found at 6 months in 4 elbows (5,9%), two of which with concomitant FCP, one with a fissured coronoid, and the last graded as 1, but developing into a fragmented coronoid at 12 months.

At 12 months, the number of elbows with an irregular incisure rose up to 14 (20,6%), seven of them with visible cystic lesions or hypoattenuated areas; all the included elbows were graded as 3 in the elbow dysplasia score, one dog with the presence of bilateral UAP, the rest with a concomitant FCP, except one elbow with a fissured coronoid.

Cystic lesions were generally very small and mostly observed in transverse views (Figure 29 A), except for one larger lesion better approachable in the sagittal view (Figure 28), in a female German shepherd dog affected by FCP and severe osteoarthrosis at 12 months old, while not present at 6 months.

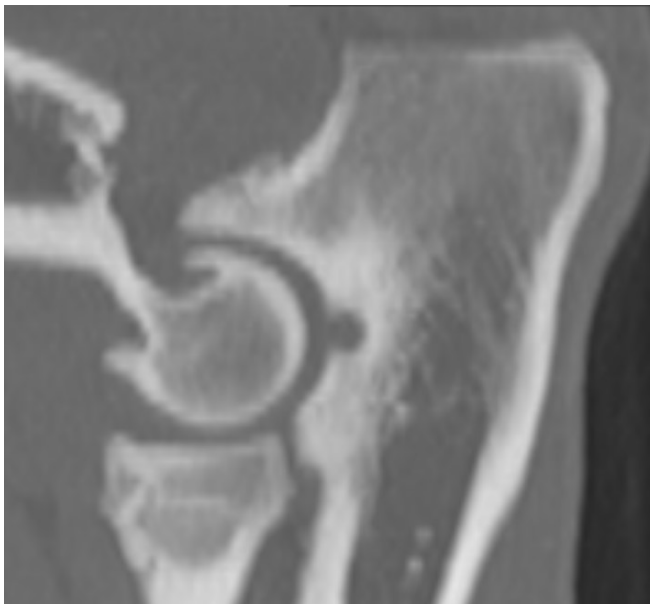

Figure 28. CT scan, sagittal view, right elbow joint of a female 12 months GSD. Subchondral cystic lesion in the middle part of the ulnar trochlear notch. From the Veterinary Science Department of the University of Parma

In the LRDs group, at 6 months of age we found 6 elbows (15%) with an irregular incisure of the ulna, of which 5 with hypoattenuated areas attributable to cysts. Half of them had a concomitant

FCP, while the other 3 were observed in grade 0 elbows (two in CED free elbows, one in an elbow contralateral to one with FCP).

At 12 months, 9 elbows (22,5%) showed irregularities of the incisure, 4 with cystic lesions (Figure 29 B); of these 9, only one elbow did not have any sign of medial coronoid disease, with a final ED score of 0.

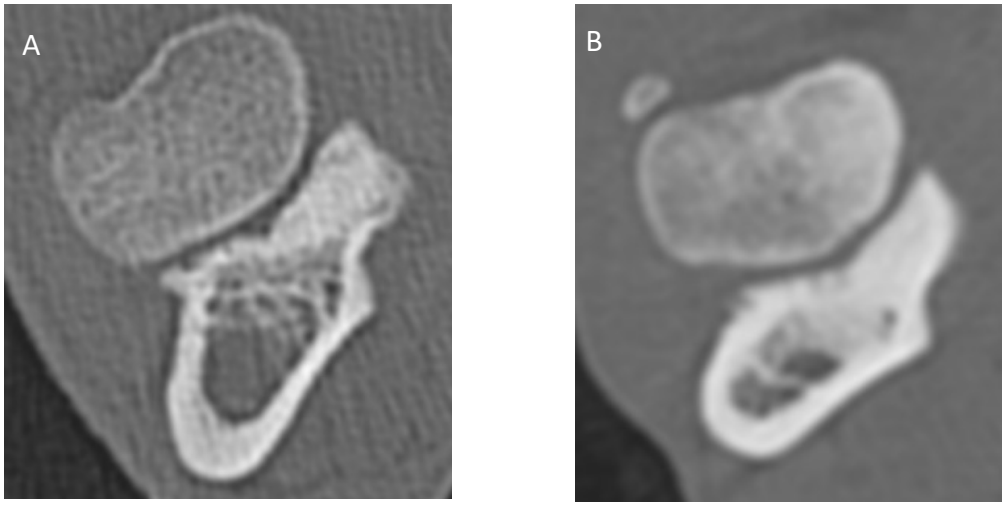

Figure 29. CT scans, transverse views, irregular radial incisure of the ulna with hypoattenuated and cystic-like lesions in a left elbow joint of a male 12 months GSD (A) and a right elbow joint of a 12 months LRD (B). From the Veterinary Science Department of the University of Parma

Elbow osteophytes

In both the examined populations, elbow osteophytes were found on the medial coronoid and anconeal process of the ulna, on the radial head and most commonly on the humeral condyle, almost exclusively in dysplastic elbow joints with an ED score equal or higher than 2, whether as initial or extensive arthrosis consequent to a MCD, UAP and/or IC disease.

At 6 months of age, 14 elbows (20,6%) in the GSDs group and only 2 (5%) in the LRDs group were positive for the presence of osteophytes, while at 12 months of age new bone formation was detected in 22 (32,3%) GSDs elbows and 7 (17,5%) LRDs elbows, as can be seen in Graph 3.

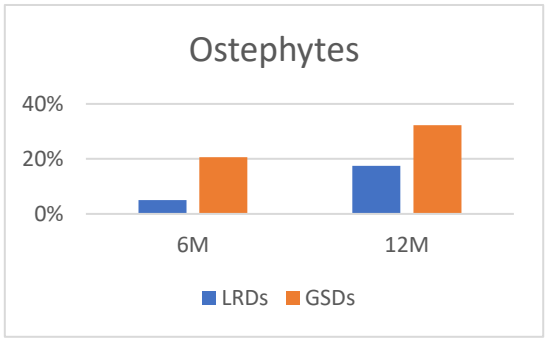

Graph 3. Frequency of osteophytes positive elbows at 6 and 12 months of age in GSDs and LRDs.

Only one joint of a sound female German shepherd dog, with no other signs of ED present bilaterally, was scored 1 due to elbow osteophyte grading, for the presence of small, millimetric bony fragments in the articular space (Figure 30 below).

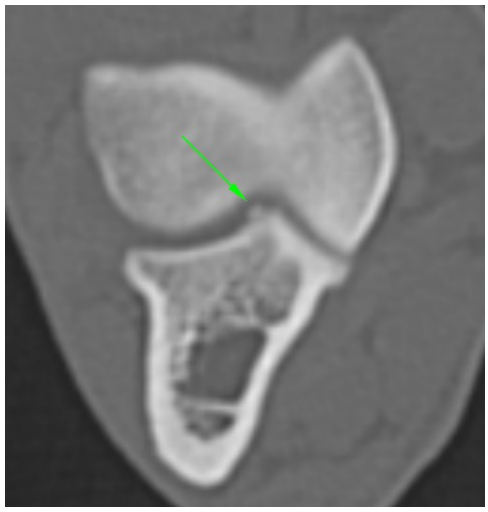

Figure 30. CT scan, transverse view, right elbow joint of a female 12 months GSD. Osteophytic fragment in the joint space in a rather healthy joint. From the Veterinary Science Department of the University of Parma

Ulnar subtrochlear sclerosis

The two breeds populations showed a similar frequency of ulnar subtrochlear sclerosis of the trochlear notch, with 32 elbows (47%) of the GSDs group and 18 elbows (45%) of the LRDs group resulting positive to this feature at 6 months of age, while respectively 37 (54,4%) in the GSDs and 22 (55%) in the LRDs at 12 months, as it is illustrated in Graph 4.

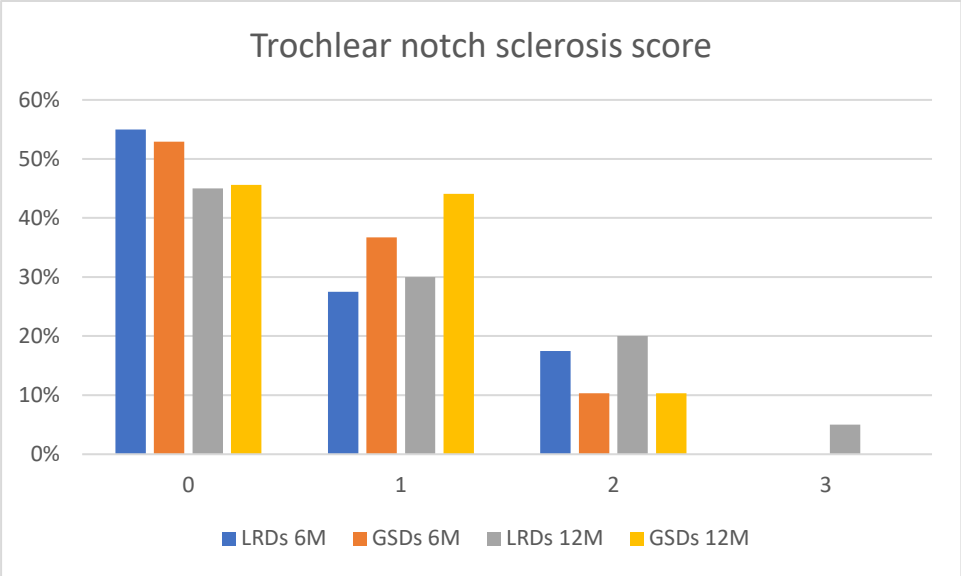

Graph 4. Distribution of the trochlear notch sclerosis scores according to tomographic examinations at 6 and 12 months of age in GSDs and LRDs.

Nonetheless, when compared to German shepherds scores, Labrador retriever dogs showed a similar frequency of sclerosis at both ages, but with more severe grades.

Evaluation of ulnar subtrochlear sclerosis quantitatively in specific ROIs

First, a pilot study on 19 of the German shepherd dogs included in this study was made on the evaluation of the Proximal and Distal ROI by three operators, a senior radiologist (SR), a Phd student (PhD) and a fifth-year student of Veterinary Medicine (ST) purposely trained for the task.

ROIs measurements were repeated three times in consensus by each operator independently and being unaware of the TNS score given.

ROIs	Age	GSDs	LRDs
Proximal ROI	6 months	699,6 HU	891,4 HU
	12 months	821,1 HU	1042,3 HU
Central ROI	6 months	782,6 HU	1315,1 HU
	12 months	875,9 HU	1462,8 HU
Distal ROI	6 months	841,4 HU	855,9 HU
	12 months	869,5 HU	1117,7 HU

Table 6. Mean HU values in Proximal, Central and Distal areas at 6 and 12 months of age; comparison between German shepherd dogs and Labrador retrievers.

In general, LRDs had higher HU values in comparison to the GSDs in all regions, but particularly in the central aspect of the trochlear notch (Table 6). Moreover, all HU values tended to increase with age.

Almost all taken measurements, checked with the Inter-Class Correlation (ICC) coefficient, as can be seen in the table 7, proved to have a good to high correlation, thus indicating their repeatability and reproducibility. Repeatability by the same operator was generally high. In the GSDs group, agreement between the operators was generally good to high, with values higher than 0,6, with the exception of the Distal ROI calculated at 12 months of age, in which we observed a high level of agreement between the two students, but a low agreement (<0,5) between both the students and the board-certified radiologist.

Age	Measurement	Operator	ICC values	Correlation
6 months	Proximal ROI	SR	0,71	Good
6 months	Distal ROI	SR	0,92	Excellent
12 months	Proximal ROI	SR	0,75	Excellent
12 months	Distal ROI	SR	0,93	Excellent
6 months	Proximal ROI	PhD	0,95	Excellent
6 months	Distal ROI	PhD	0,93	Excellent
12 months	Proximal ROI	PhD	0,96	Excellent
12 months	Distal ROI	PhD	0,92	Excellent
6 months	Proximal ROI	ST	0,79	Excellent
6 months	Distal ROI	ST	0,84	Excellent
12 months	Proximal ROI	ST	0,85	Excellent
12 months	Distal ROI	ST	0,87	Excellent
6 months	Proximal ROI	SR/PhD	0,79	Excellent
6 months	Distal ROI	SR/PhD	0,78	Excellent
6 months	Proximal ROI	SR/ST	0,8	Excellent
6 months	Distal ROI	SR/ST	0,75	Excellent
6 months	Proximal ROI	ST/PhD	0,61	Good
6 months	Distal ROI	ST/PhD	0,81	Excellent
12 months	Proximal ROI	SR/PhD	0,67	Good
12 months	Distal ROI	SR/PhD	0,43	Fair
12 months	Proximal ROI	SR/ST	0,78	Excellent
12 months	Distal ROI	SR/ST	0,49	Fair
12 months	Proximal ROI	ST/PhD	0,78	Excellent
12 months	Distal ROI	ST/PhD	0,88	Excellent

Table 7. Reproducibility of the Proximal and Distal ROIs measurements relative to the operators and between the operators.

The preliminary results from the ROC curves of this pilot study suggested that the Proximal ROI could have a certain predictive value at 6 months of age in relation to the ED grade at 12 months, at least in the German shepherd breed in our population. In fact, it appeared that a higher value in the HU of the given proximal area at 6 months of age was significantly correlated to the development of worse signs of osteoarthrosis 6 months later, at 12 months old.

Therefore, in order to verify these results, it was decided to increase to 31 subjects the number of dogs (excluding the UAP positive elbows), to add a Central ROI to the other measurements, and eventually perform the same study on a similar population of 20 growing Labrador retrievers, to make comparisons between the two breeds. The measurements were taken by two operators, a senior radiologist and a PhD student, three times each, as in the previous study.

Firstly, Central ROIs ICC was calculated and resulted in an excellent repeatability and reproducibility, as depicted in Table 8.

Age	Measurement	Operator	ICC values	Correlation
6 months	Central ROI	PhD	0,98	Excellent
12 months	Central ROI	PhD	0,97	Excellent
6 months	Central ROI	SR/PhD	0,76	excellent
12 months	Central ROI	SR/PhD	0,81	excellent

Table 8. Repeatability and reproducibility of the Central ROIs measurements.

Age	Measurement	Operator	ICC values	Correlation
6 months	Proximal ROI	SR/PhD/ST	0,78	Excellent
12 months	Proximal ROI	SR/PhD/ST	0,81	Excellent
6 months	Distal ROI	SR/PhD/ST	0,84	Excellent
12 months	Distal ROI	SR/PhD/ST	0,85	Excellent

Table 9. Reproducibility of Central and Distal ROIs measurements.

Proximal and distal ROIs HU values at 6 months of age were significantly higher in GSDs affected by ED (P:0,04 and P:0,003 respectively).

Consequently, Proximal, Central and Distal ROIs HU values (Table 9) were related to the final ED score at 12 months of the 31 GSDs and the same was performed for the 20 LRDs, by calculating the

ROC (Receiver Operating Characteristic) curves, and the respective AUCs (Area Under the Curve), in order to test their diagnostic accuracy, and an eventual cut-off value.

In contrast with the pilot study, in the extended group of the German shepherd dogs at 6 months of age the Proximal ROIs resulted in having a scarcer accuracy than the Distal ROI measurements. The Central ROI measures did not reveal diagnostic accuracy at the test. All the measurements did not show accuracy at 12 months. (Graphs 5 – 10)

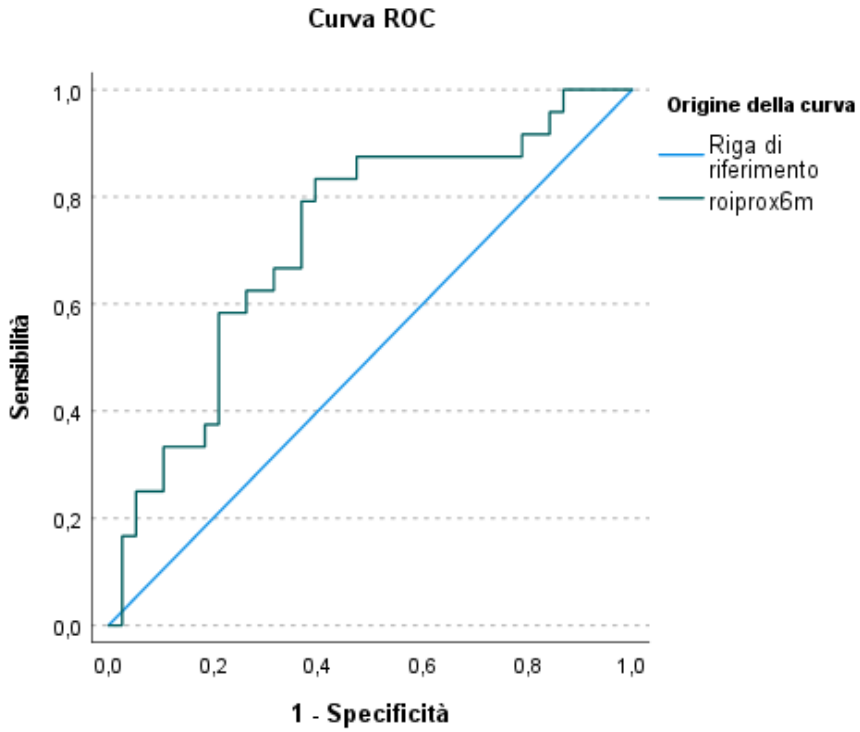

Graph 5. ROC curve relative to the Proximal ROI measurements of GSDs at 6 months with reference to their ED final scores. **AUC: 0,72 –** the test demonstrated a fair diagnostic accuracy. **Cut-off value: 680,43 HU (sensitivity 83%, specificity 61%)**

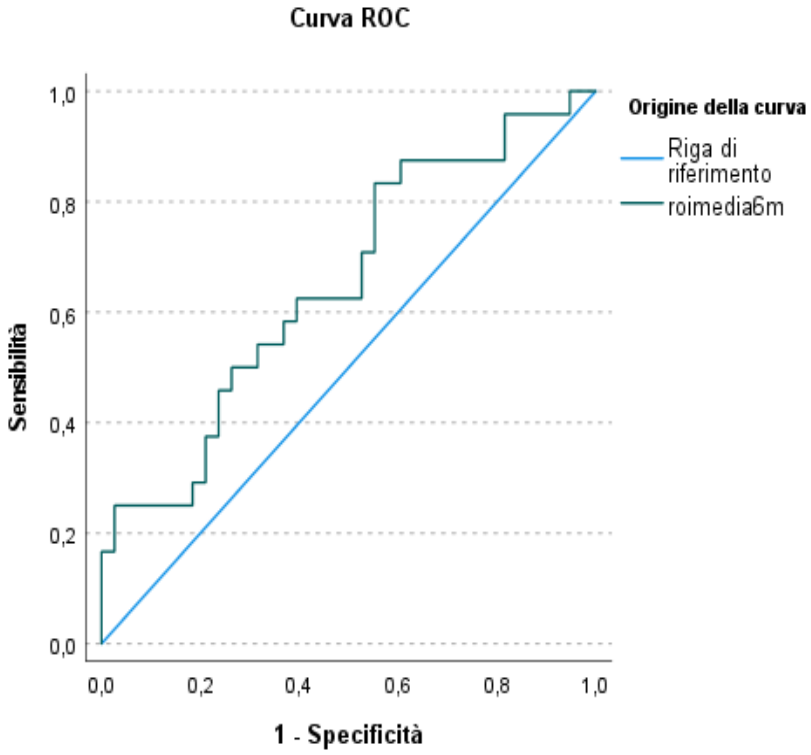

Graph 6. ROC curve relative to the Central ROI measurements of GSDs at 6 months with reference to their ED final scores. **AUC: 0,65 –** the test did not demonstrate diagnostic accuracy. **Cut-off value: 898,14 HU (sensitivity 83%, specificity 45%)**

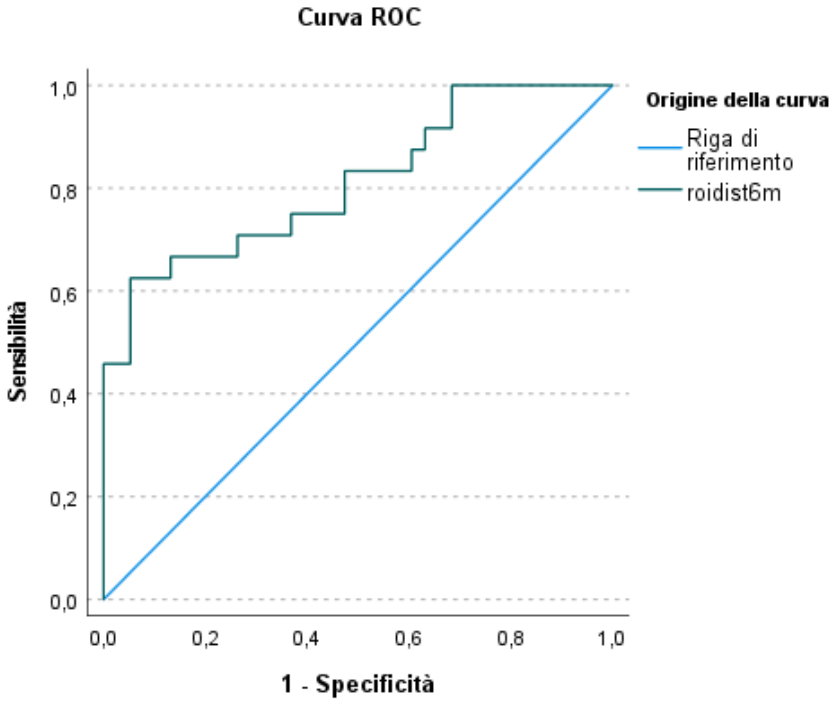

Graph 7. ROC curve relative to the Distal ROI measurements of GSDs at 6 months with reference to their ED final scores. **AUC: 0,81 –** the test demonstrated good diagnostic accuracy. **Cut-off value: 711,83 HU (sensitivity 62%, specificity 94,7%)**

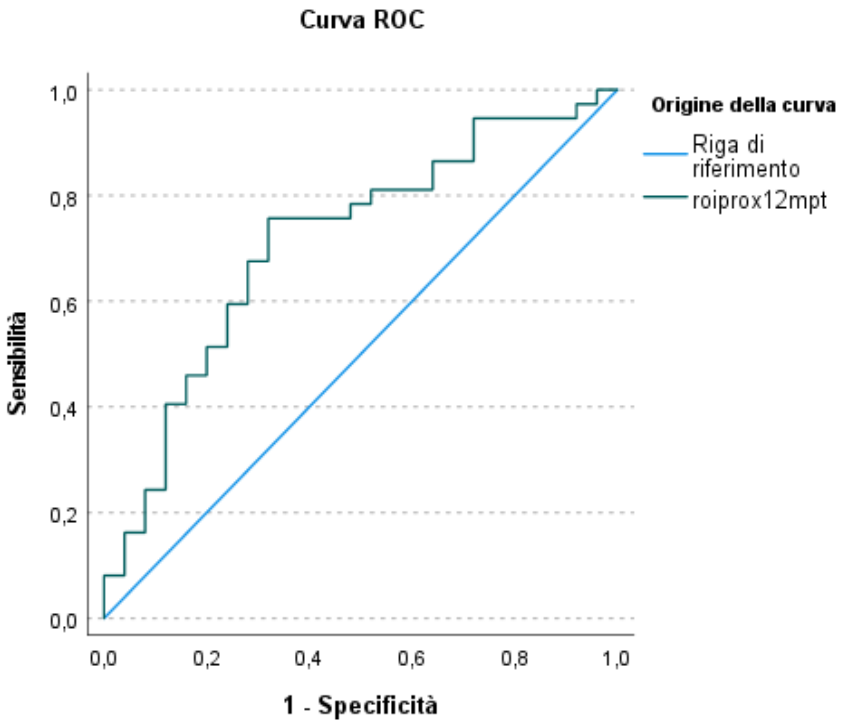

Graph 8. ROC curve relative to the Proximal ROI measurements of GSDs at 12 months with reference to their ED final scores. **AUC: 0,71 –** the test demonstrated scarce diagnostic accuracy. **Cut-off value: 740,65 HU (sensitivity 75%, specificity 68%)**

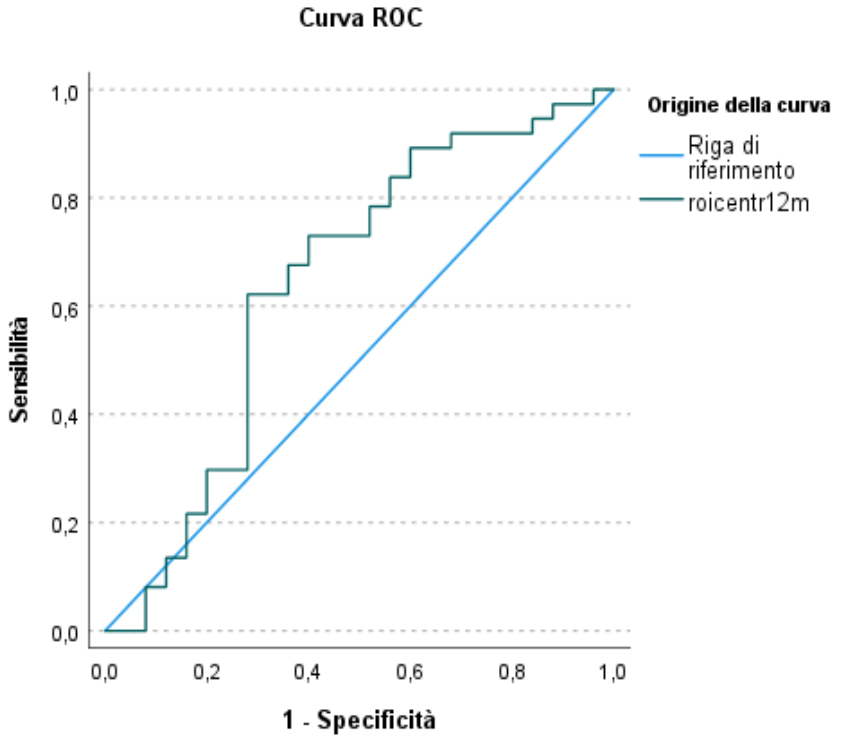

Graph 9. ROC curve relative to the Central ROI measurements of GSDs at 12 months with reference to their ED final scores. **AUC: 0,64 –** the test did not demonstrate diagnostic accuracy. **Cut-off value: 888,28HU (sensitivity 62%, specificity 72%)**

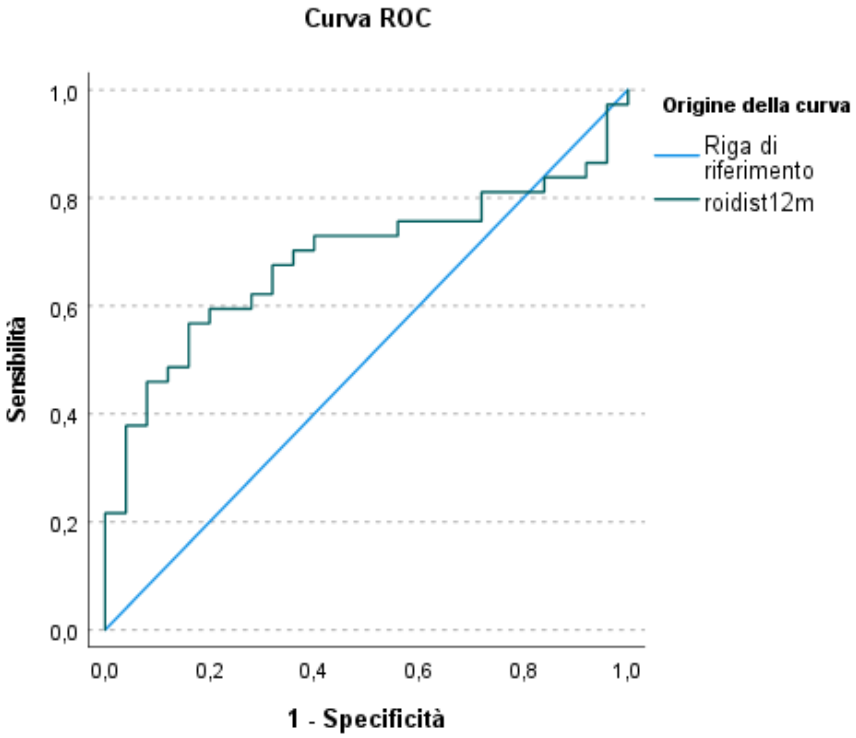

Graph 10. ROC curve relative to the Distal ROI measurements of GSDs at 12 months with reference to their ED final scores. **AUC: 0,68 –** the test did not demonstrate diagnostic accuracy. **Cut-off value: 914,07 HU (sensitivity 57%, specificity 84%)**

Contrariwise, in the Labrador retrievers the trochlear notch attenuation values at both ages resulted as generally more accurate in comparison with the GSDs. In fact, proximal and distal ROIs values at 6 and 12 months were higher in dogs with ED (P<0,001).

ROC curves are presented in Graphs 11 – 16. The best accuracy was achieved by the distal ROIs values at 6 and 12 months of age.

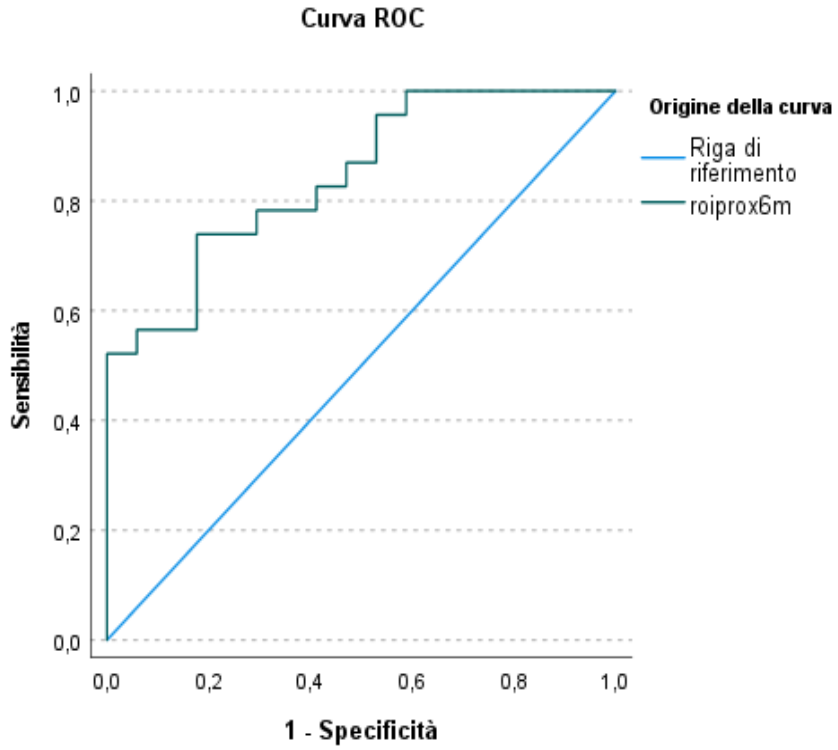

Graph 11. ROC curve relative to the Proximal ROI measurements of LRDs at 6 months with reference to their ED final scores. **AUC: 0,84 –** the test demonstrated good diagnostic accuracy. **Cut-off value: 804,16 HU (sensitivity 74%, specificity 83%)**

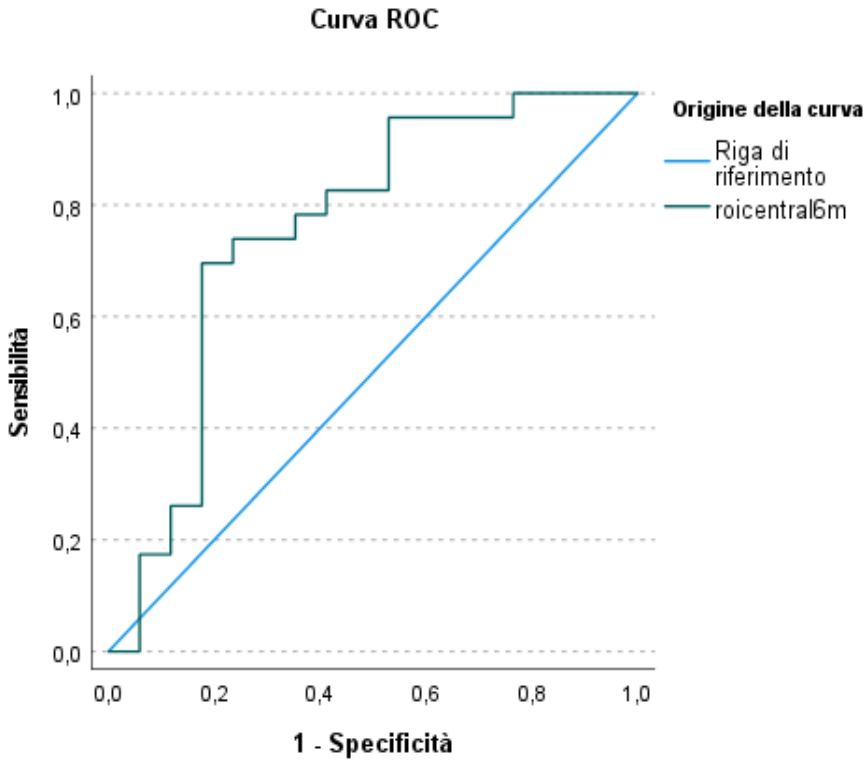

Graph 12. ROC curve relative to the Central ROI measurements of LRDs at 6 months with reference to their ED final scores. **AUC: 0,76 –** the test demonstrated fair diagnostic accuracy. **Cut-off value: 1290,98 HU (sensitivity 70%, specificity 83%)**

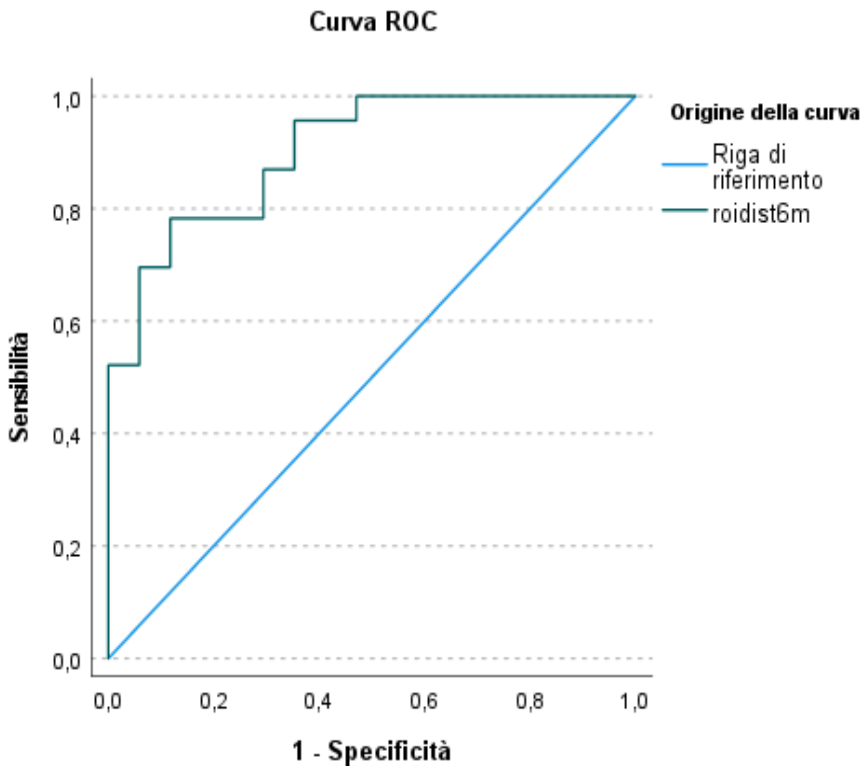

Graph 13. ROC curve relative to the Distal ROI measurements of LRDs at 6 months with reference to their ED final scores. **AUC: 0,90 –** the test demonstrated excellent diagnostic accuracy. **Cut-off value: 852,23 HU (sensitivity 78%, specificity 89%)**

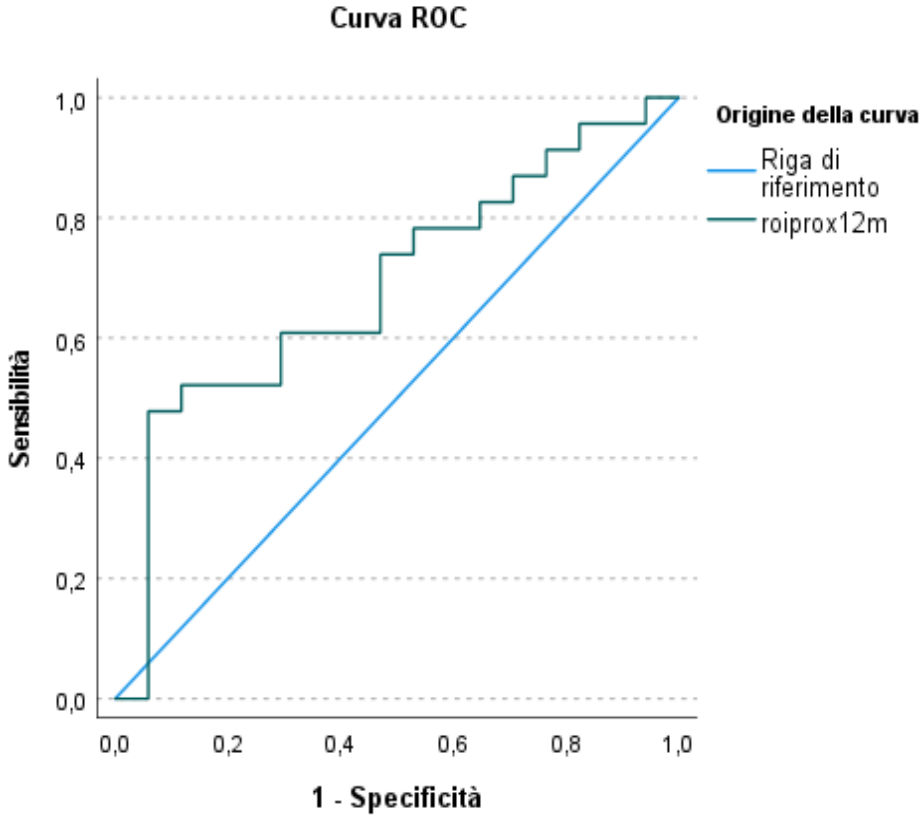

Graph 14. ROC curve relative to the Proximal ROI measurements of LRDs at 12 months with reference to their ED final scores. **AUC: 0,68 –** the test did not demonstrate diagnostic accuracy. **Cut-off value: 923,43 HU (sensitivity 48%, specificity 94%)**

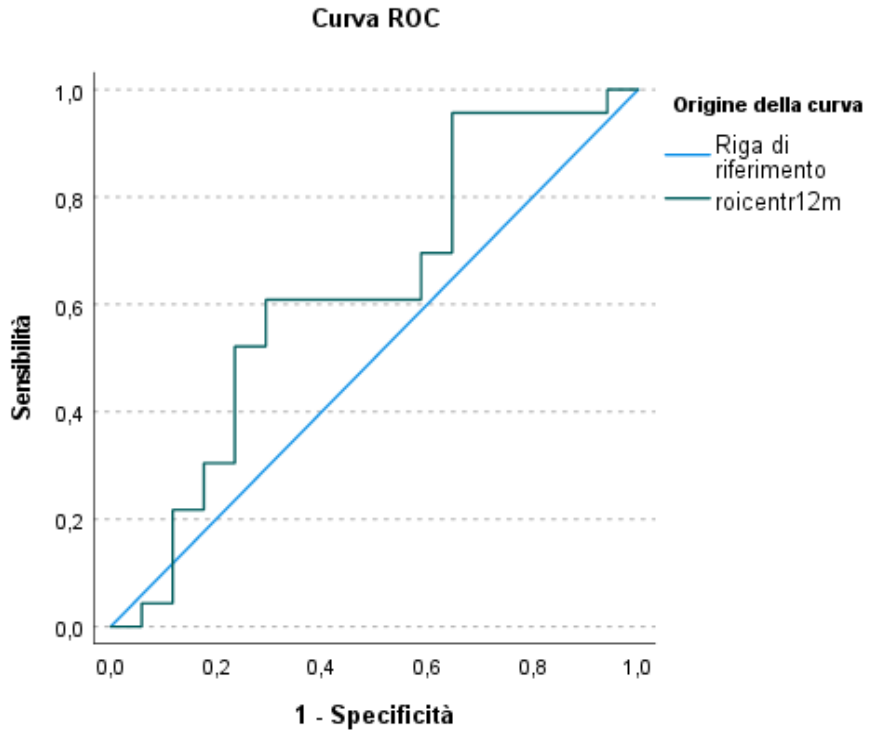

Graph 15. ROC curve relative to the Central ROI measurements of LRDs at 12 months with reference to their ED final scores. **AUC: 0,62 –** the test did not demonstrate diagnostic accuracy. **Cut-off value: 1478,01 HU (sensitivity 61%, specificity 71%)**

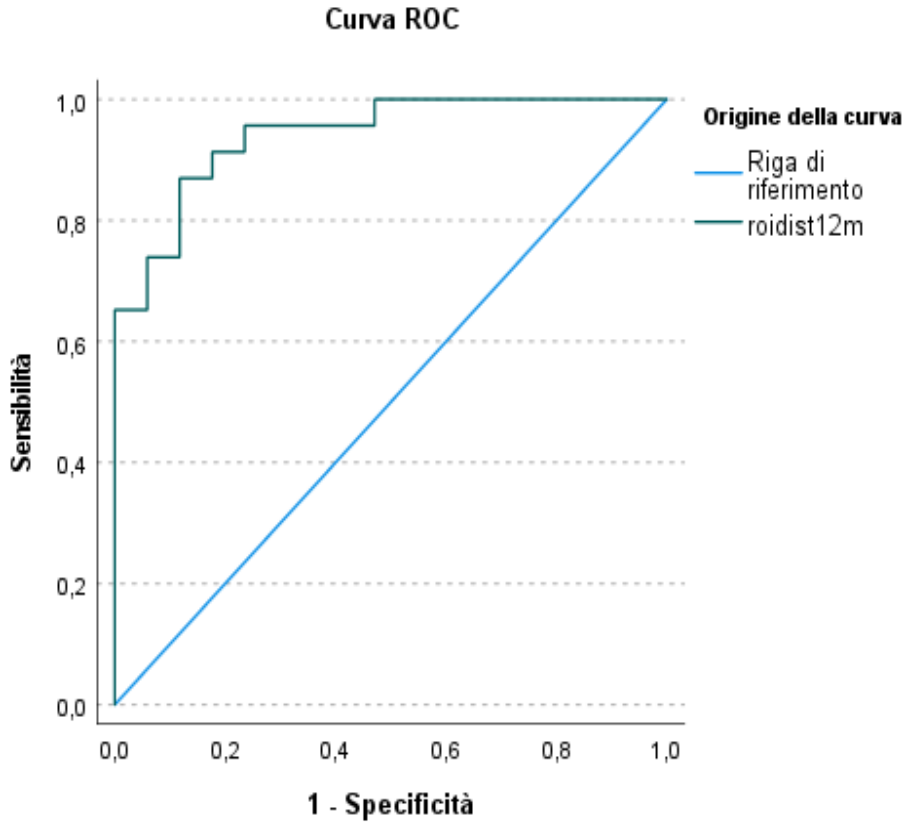

Graph 16. ROC curve relative to the Distal ROI measurements of LRDs at 12 months with reference to their ED final scores. **AUC: 0,94 –** the test demonstrated excellent diagnostic accuracy. **Cut-off value: 1087,01 HU (sensitivity 87%, specificity 88%)**

The values of Proximal, Central and Distal ROIs in the FCP positive elbows were significantly higher in LRDs (P value < 0.001), as seen in table 10.

ROIs	Age	GSDs	LRDs
Proximal ROI	12 months	866,5	1139,94
Central ROI	12 months	800,45	1435,96
Distal ROI	12 months	918,25	1395,4

Table 10. Mean HU values in Proximal, Central and Distal areas at 12 months of age in FCP elbows; comparison between German shepherd dogs and Labrador retrievers.

Joint incongruity grade

As explained before, each elbow has been evaluated subjectively for the presence of incongruence, and on the basis of the radio-ulnar joint space as measured in the sagittal view. (Graph 17, Figure 31)

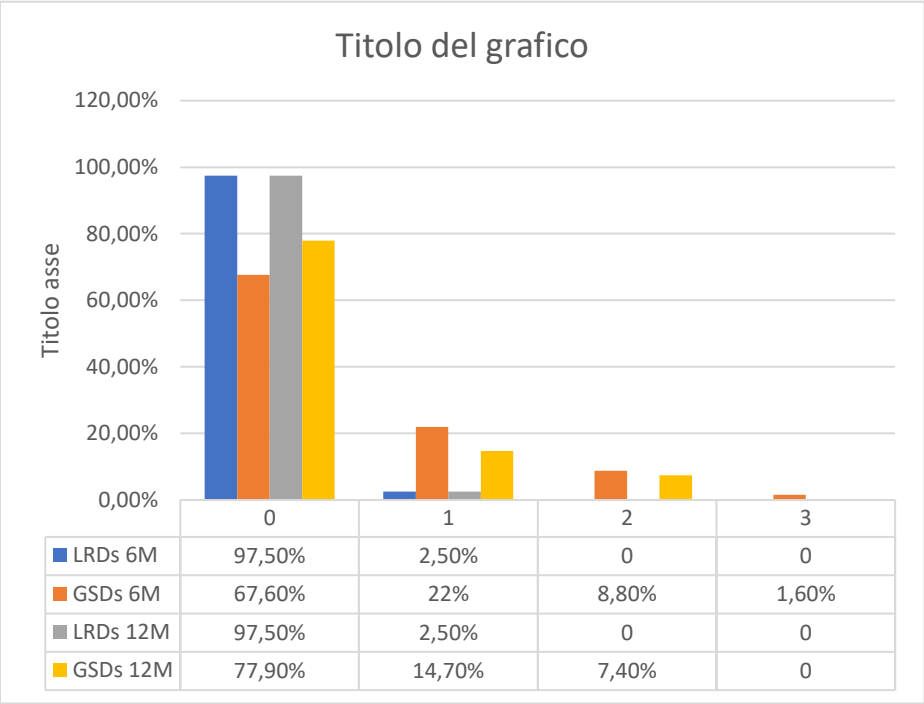

	0	1	2	3
LRDs 6M	97,50%	2,50%	0	0
GSDs 6M	67,60%	22%	8,80%	1,60%
LRDs 12M	97,50%	2,50%	0	0
GSDs 12M	77,90%	14,70%	7,40%	0

Graph 17. Distribution of the presence and extent of radio-ulnar incongruity according to tomographic examinations at 6 and 12 months of age in GSDs and LRDs.

Figure 31. CT scans, sagittal views, radio-ulnar step with a shorter radio in a left elbow joint of a female GSD, from 6 months old (A) to 12 months old (B). From the Veterinary Science Department of the University of Parma

In the GSDs population aged 6 months, a radio-ulnar step, evidence of a shorter radio, was detected in 24 elbows (70,6%), mostly between 1,5 to 2 mm; surprisingly, 8 of these steps resolved or improved over the given period, so that at 12 months of age 16 elbows (47%) were accounted for the presence of a quantifiable RUI.

It is also noticeable that in one dog with overt UAP a bilateral RUI was observed (Figure 32), but this time with a bilateral shorter ulna, so the radio-ulnar step was measured as negative and anyhow considered as grade 1.

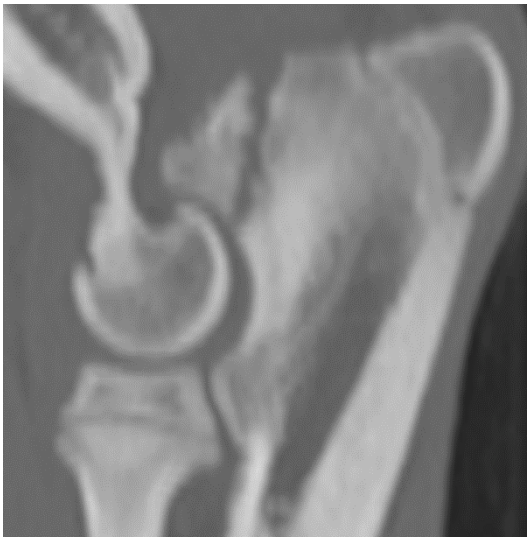

Figure 32. CT scans, sagittal views, radio-ulnar step with a shorter ulna in a left UAP elbow joint of a male 6 months old GSD. From the Veterinary Science Department of the University of Parma

IC	LRDs 6M	LRDs 12M	GSDs 6M	GSDs 12M
0	39	39	44	52
1	1	1	17	11
2	0	0	6	5
3	0	0	1	0
TOTALE	40	40	68	68

Table 11. Distribution of the radio-ulnar incongruity score according to tomographic examinations at 6 and 12 months of age in GSDs and LRDs.

At 12 months, out of the 15 elbows with the presence of a positive radio-ulnar step, 12 had a fragmentation of the medial coronoid process, of which 11 with also a concomitant elliptical ulnar

trochlear notch. Two were detected in the contralateral elbow of an FCP unilaterally affected dog, and the last one was found in a graded 2 sclerotic elbow.

Conversely, only one Labrador retriever dog showed a radio-ulnar step, lower than 2mm thus graded as 1, in an elbow with severe osteoarthrosis with concurrent FCP. (Table 11)

In both breeds, all the measurements of the radio-ulnar space were related to the final ED scores at 12 months by creating a ROC curve for each breed. Whereas no diagnostic accuracy was found in the LRDs group, the AUC in the GSDs group revealed a discreet accuracy. (Graphs 18-19)

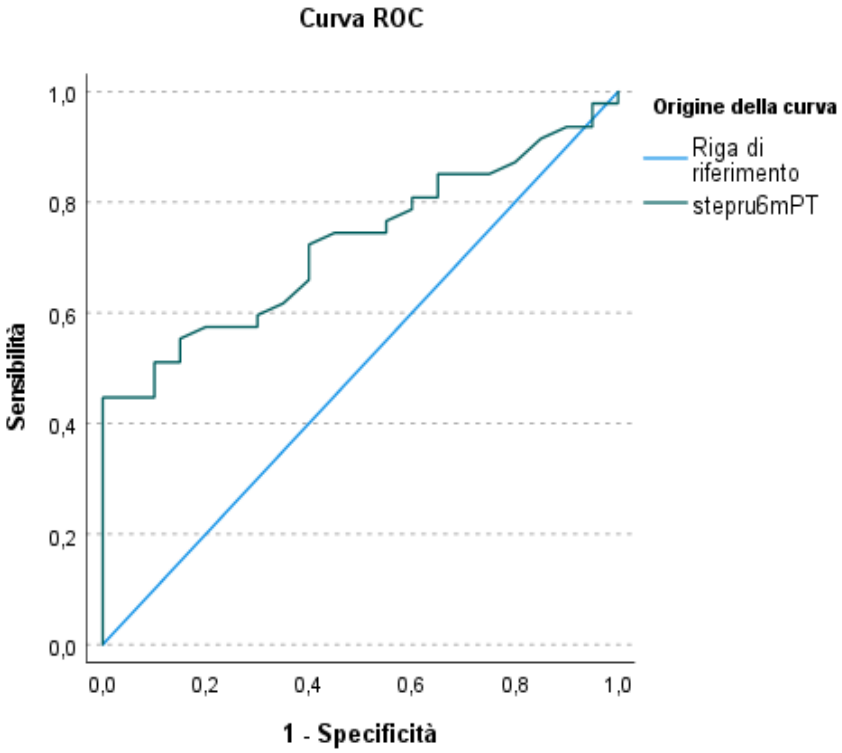

Graph 18. ROC curve relative to the radio-ulnar space measurements of GSDs at 6 months with reference to their ED final scores. **AUC: 0,72 –** the test demonstrated a fair diagnostic accuracy. **Cut-off value: 1,4 mm (sensitivity 45%, specificity 100%)**

Radio-ulnar steps at 6 months of age were significantly higher only in GSDs with the development of elbow dysplasia (P value of 0,004).

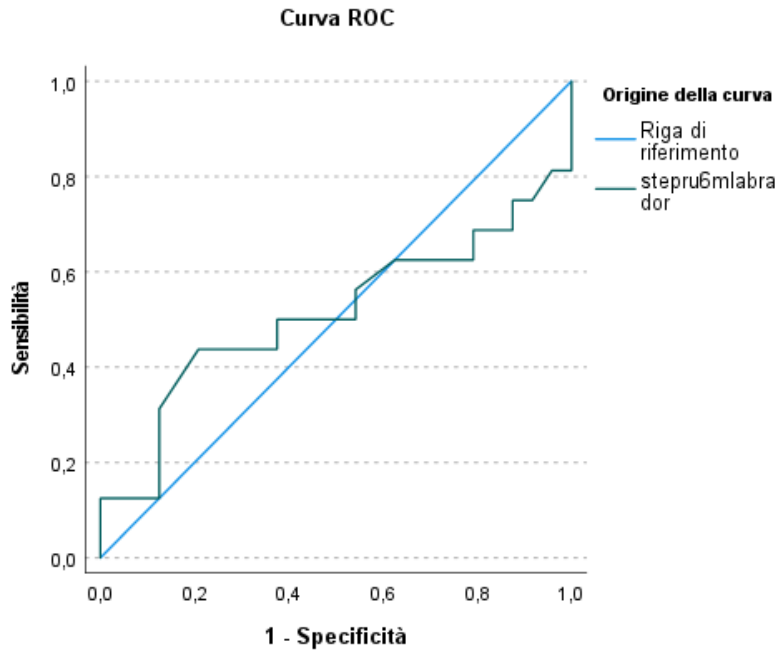

Graph 19. ROC curve relative to the radio-ulnar space measurements of LRDs at 6 months with reference to their ED final scores. **AUC: 0,51 –** the test did not demonstrate diagnostic accuracy. **Cut-off value: 0,99 mm (sensitivity 44%, specificity 80%)**

There was only a significant correlation between radio-ulnar steps and attenuation values of the Distal ROIs in LRDs at 12 months of age (low positive correlation, r: 0,33). Correlations are described in the graphs 20 - 37.

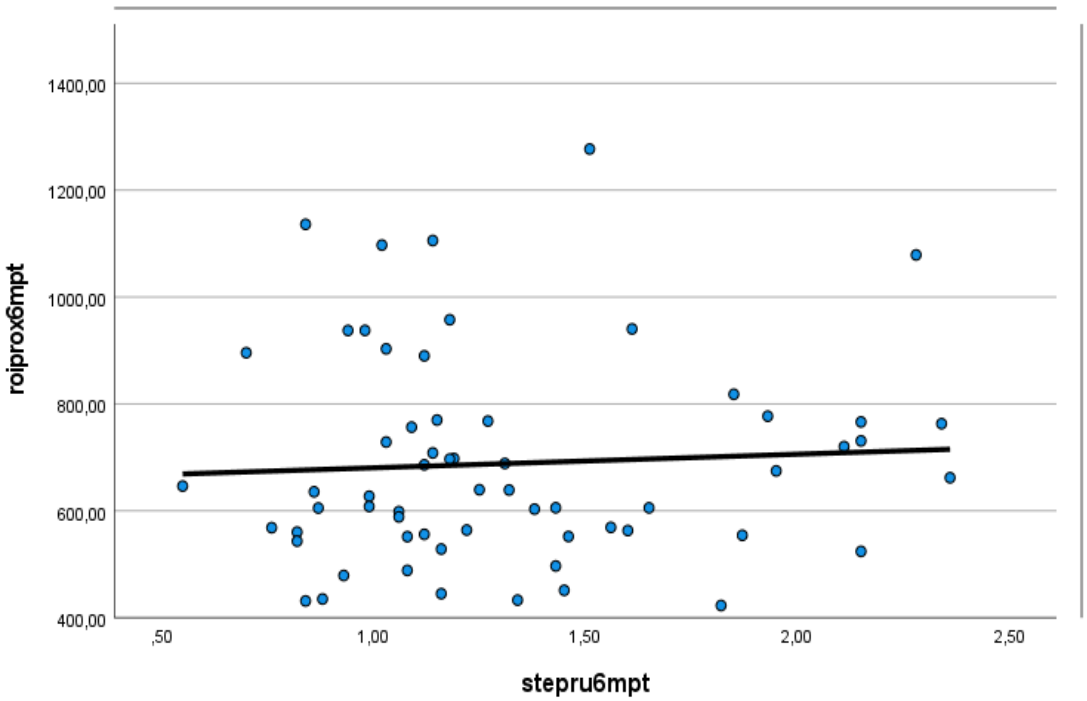

Graph 20. Correlation between Proximal ROIs values and radio-ulnar steps in 6 months old GSDs (r: 0,07).

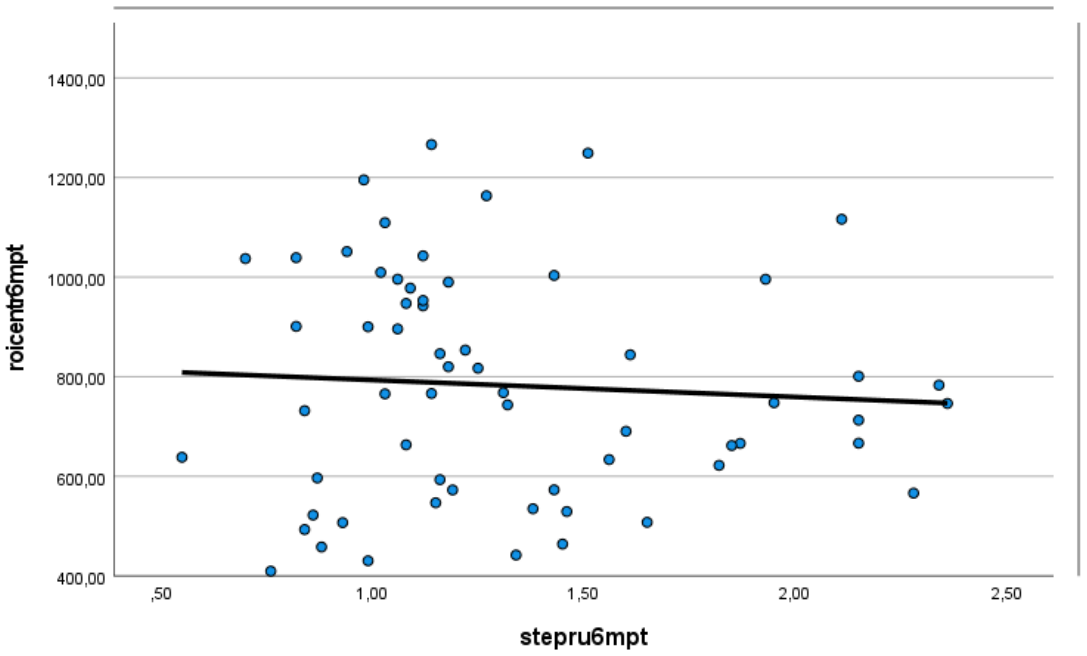

Graph 21. Correlation between Central ROIs values and radio-ulnar steps in 6 months old GSDs (r: -0,07).

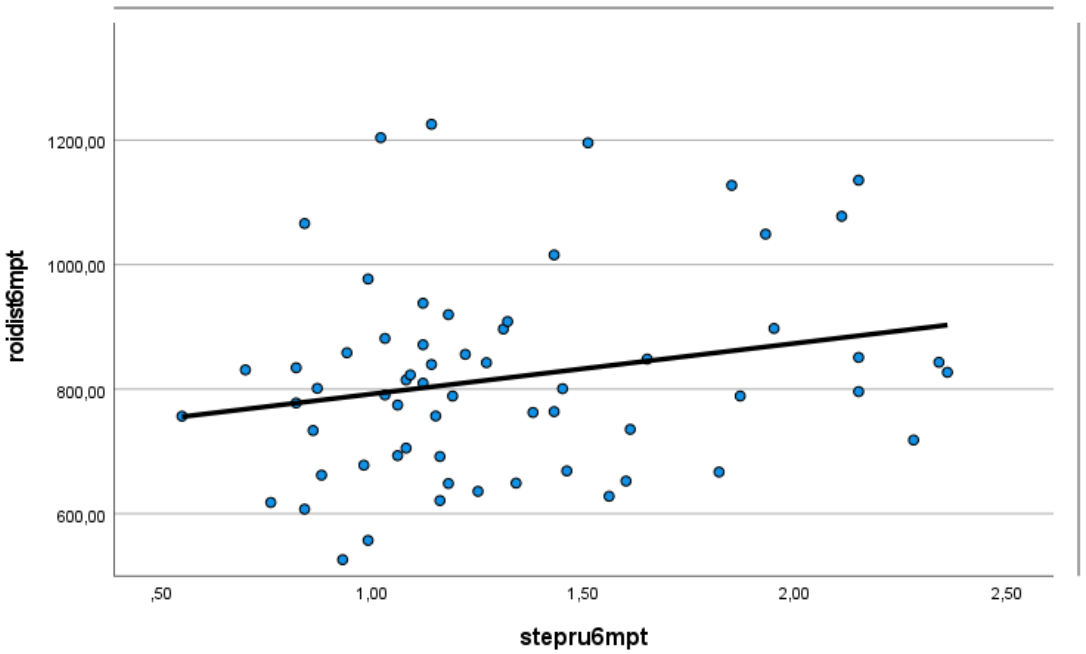

Graph 22. Correlation between Distal ROIs values and radio-ulnar steps in GSDs at 6 months (r: 0,22).

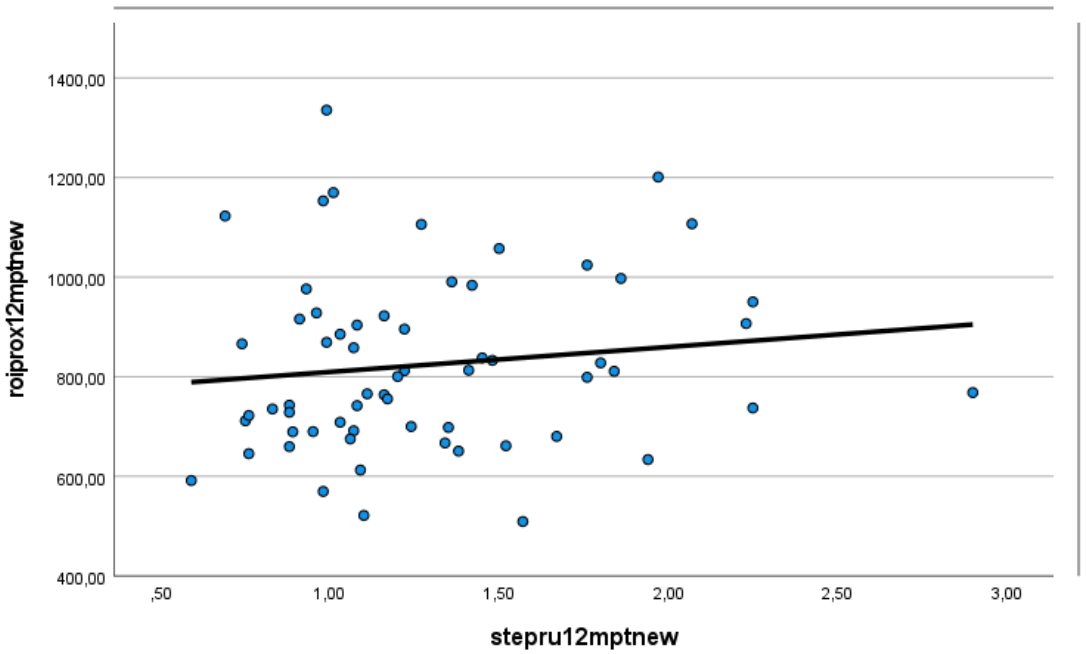

Graph 23. Correlation between Proximal ROIs values and radio-ulnar steps in GSDs at 12 months (r: 0,13)

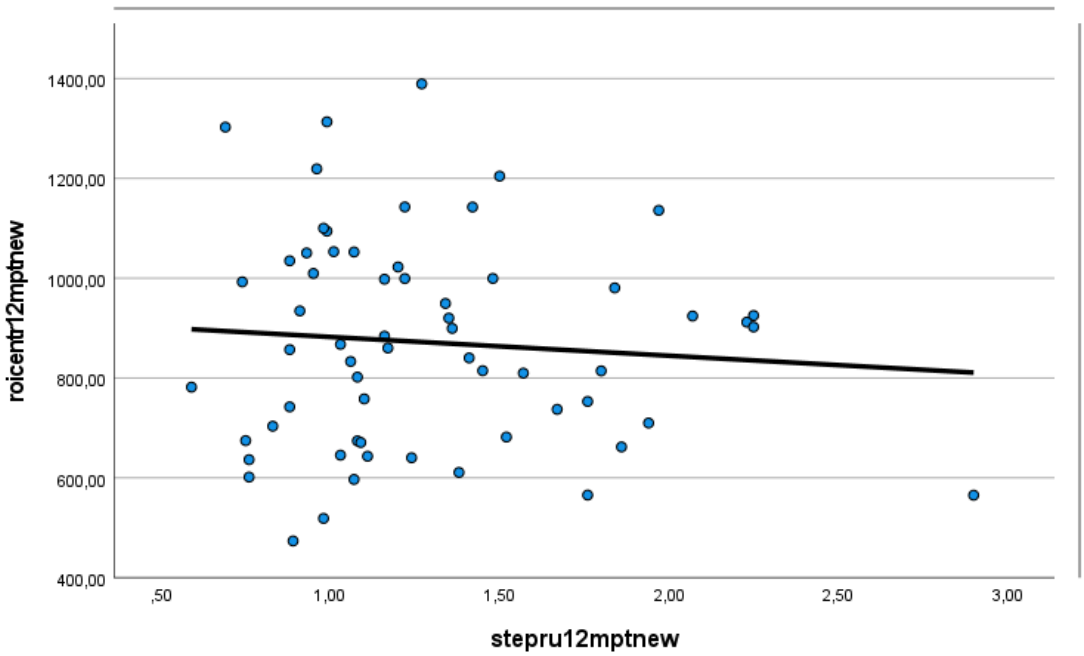

Graph 24. Correlation between Central ROIs values and radio-ulnar steps in GSDs at 12 months (r: -0,08).

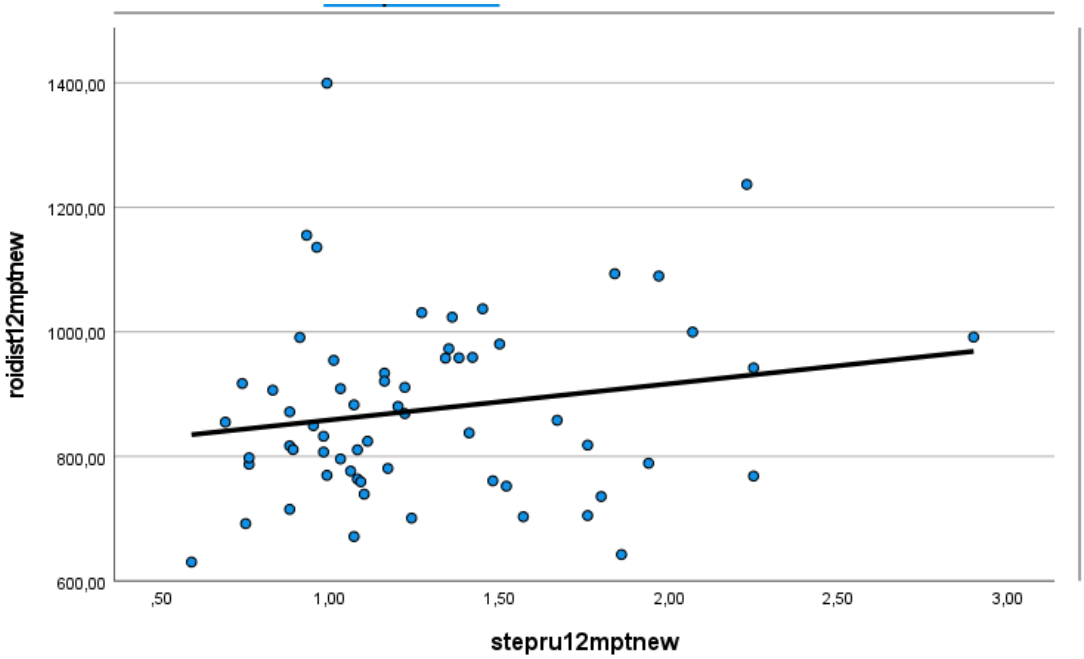

Graph25. Correlation between Distal ROIs values and radio-ulnar steps in GSDs at 12 months (r :0,15).

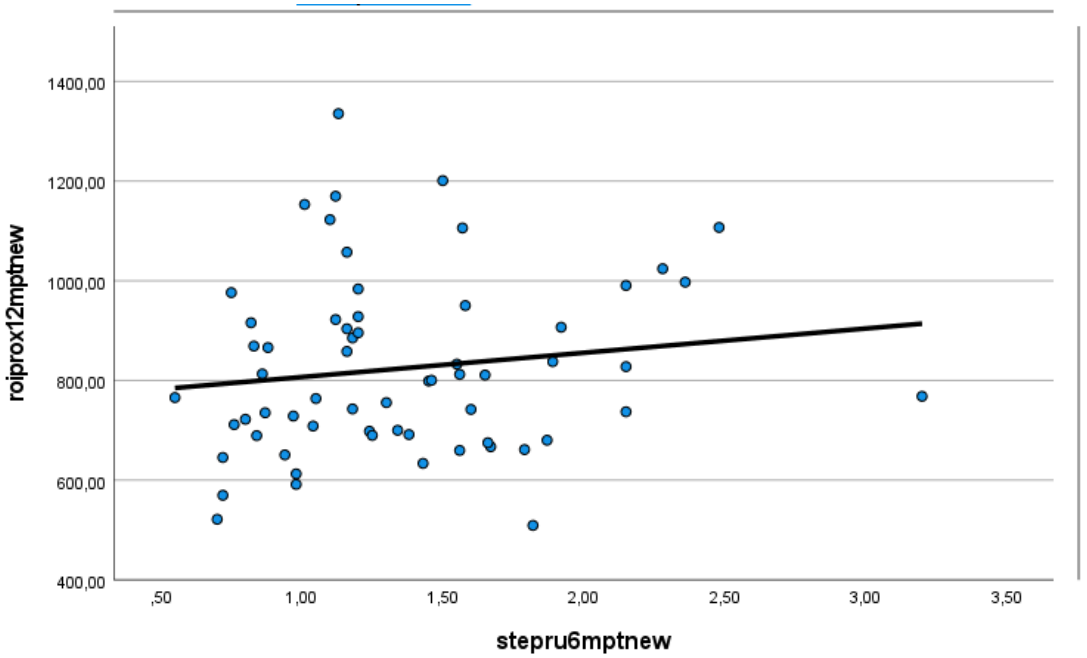

Graph 26. Correlation between Proximal ROIs values at 12 months and radio-ulnar steps at 6 months in GSDs (r:0,14).

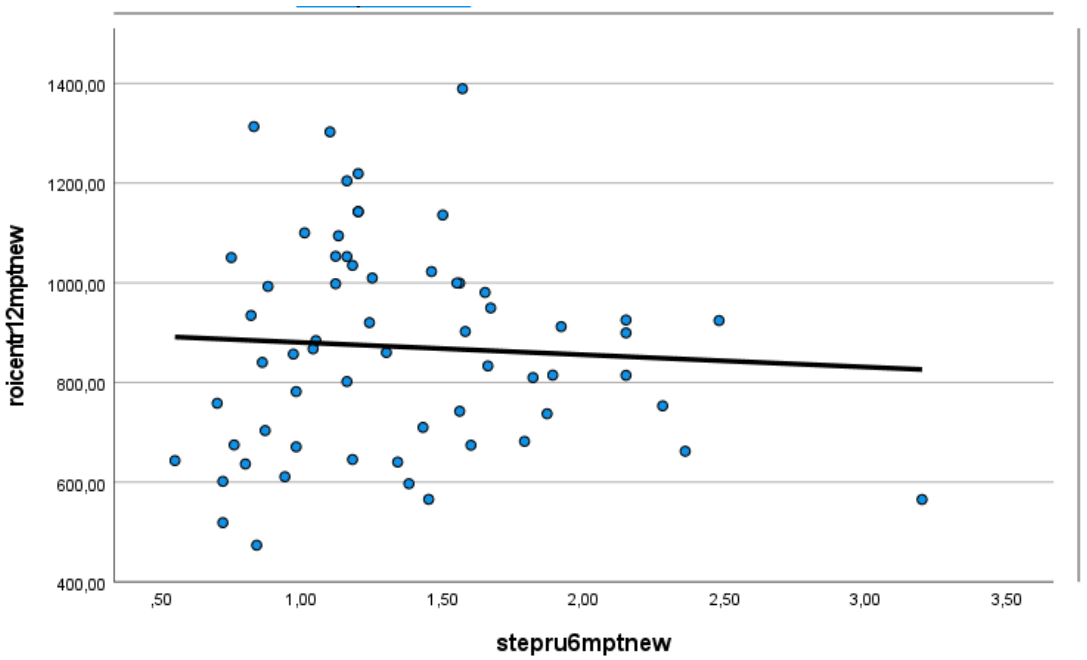

Graph 27. Correlation between Central ROIs values at 12 months and radio-ulnar steps at 6 months in GSDs (r: -0,06).

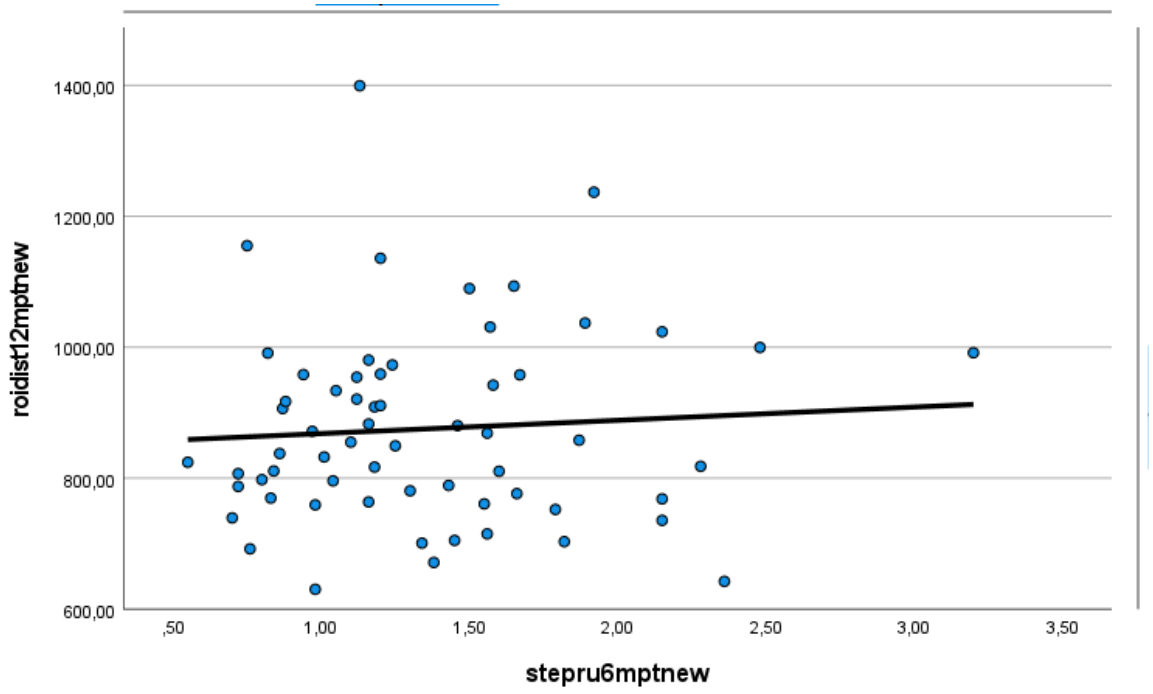

Graph 28. Correlation between Distal ROIs values at 12 months and radio-ulnar steps at 6 months in GSDs (r: 0,07).

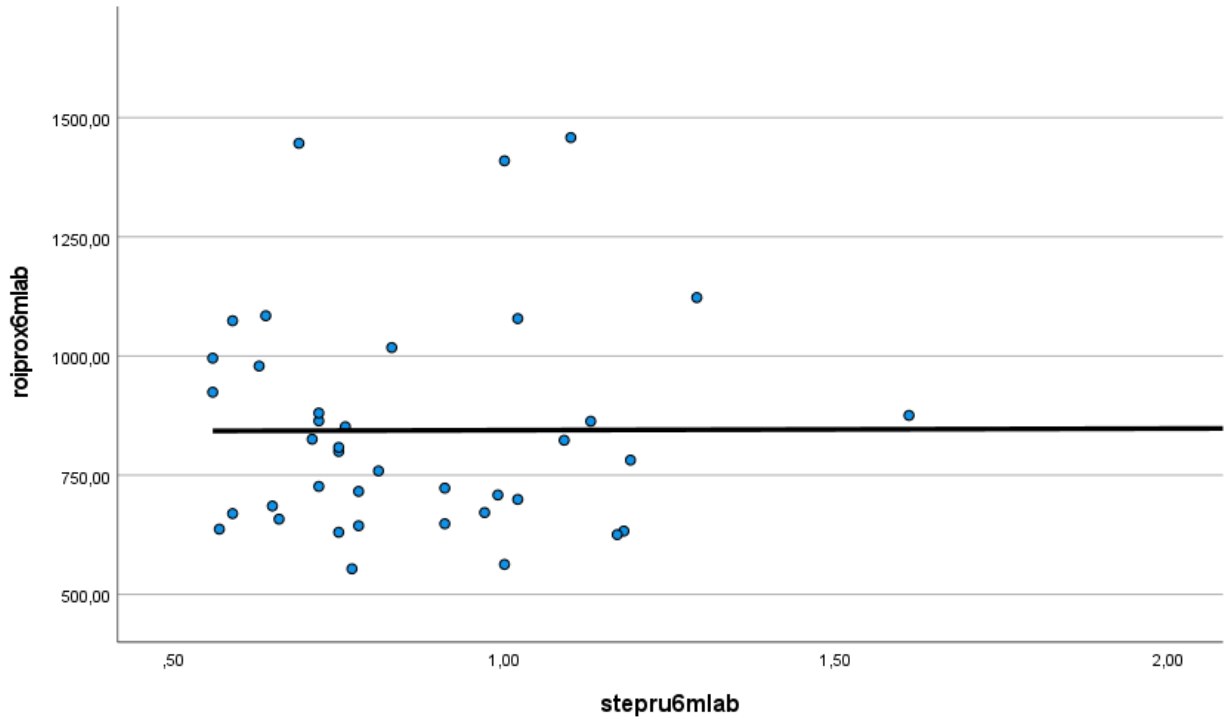

Graph 29. Correlation between Proximal ROIs values and radio-ulnar steps at 6 months in LRDs (r: 0,01).

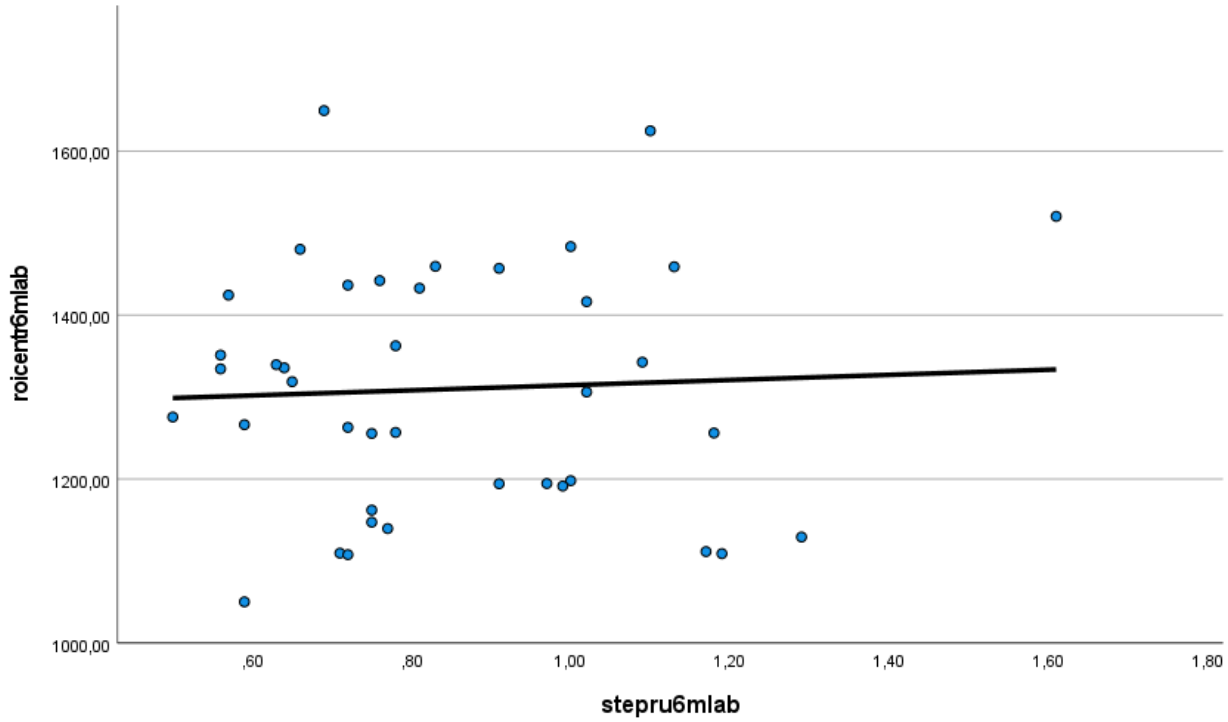

Graph 30. Correlation between Central ROIs values and radio-ulnar steps at 6 months in LRDs (r: 0,05).

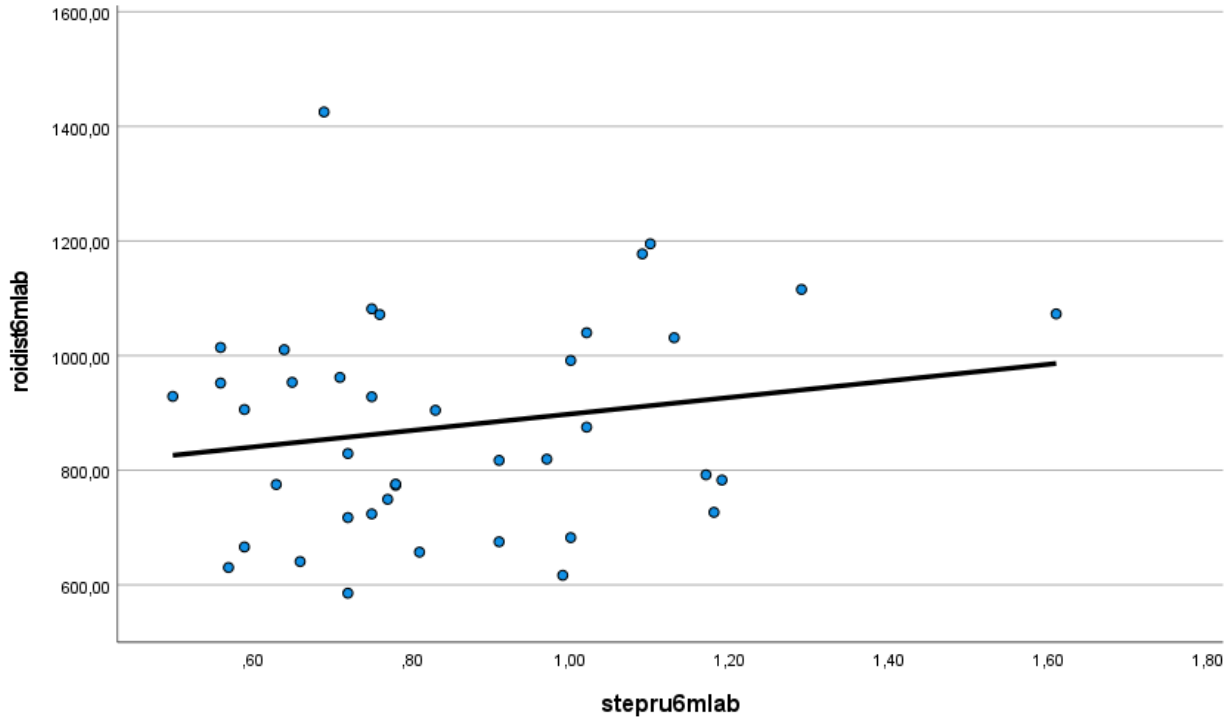

Graph 31. Correlation between Distal ROIs values and radio-ulnar steps at 6 months in LRDs (r: 0,15).

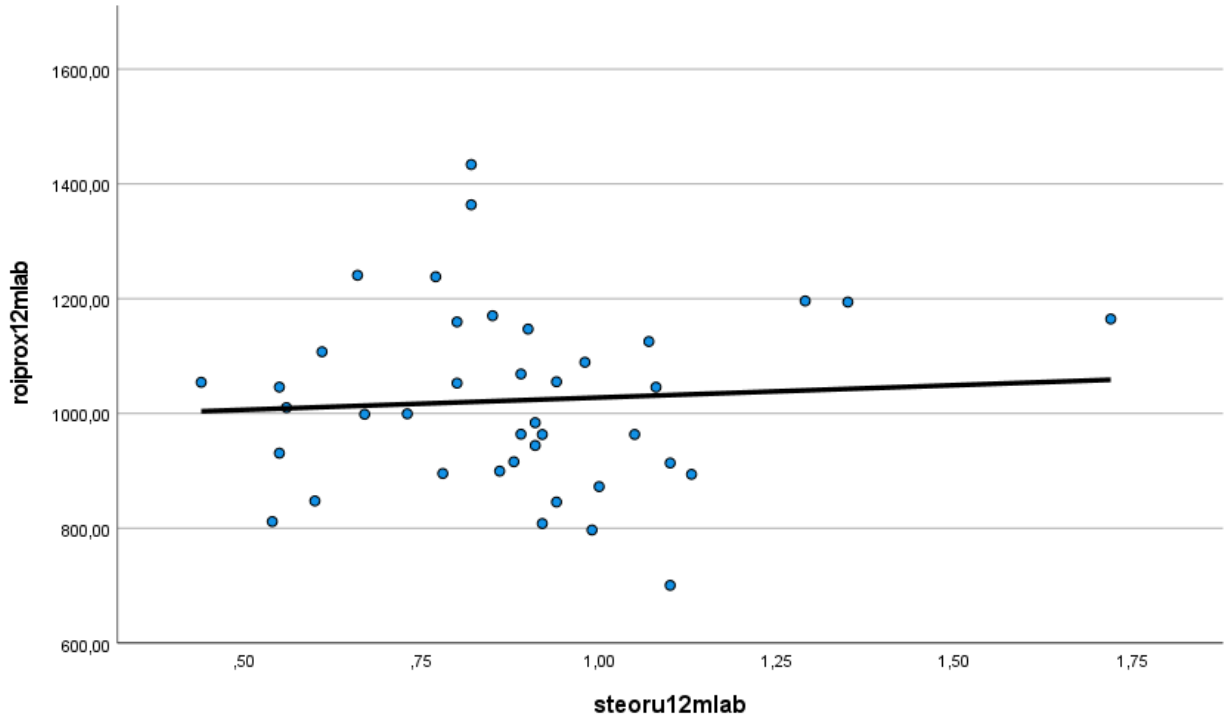

Graph 32. Correlation between Proximal ROIs values and radio-ulnar steps at 12 months in LRDs (r: 0,06).

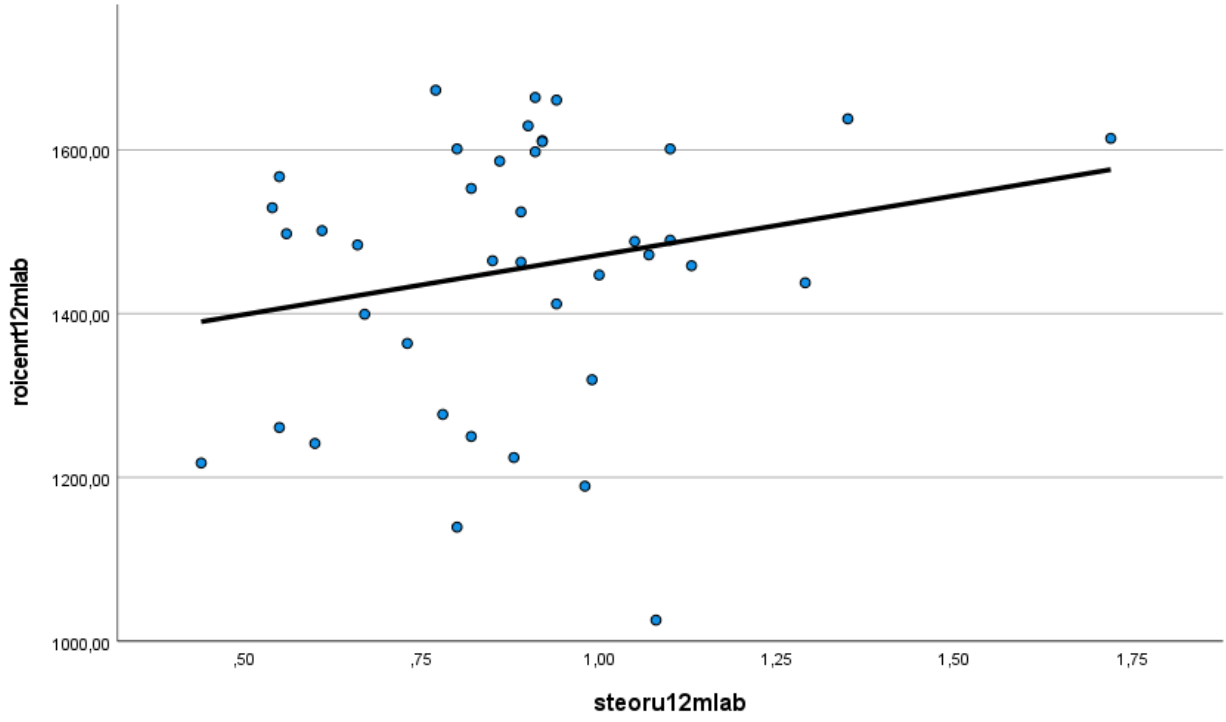

Graph 33. Correlation between Central ROIs values and radio-ulnar steps at 12 months in LRDs (r: 0,21).

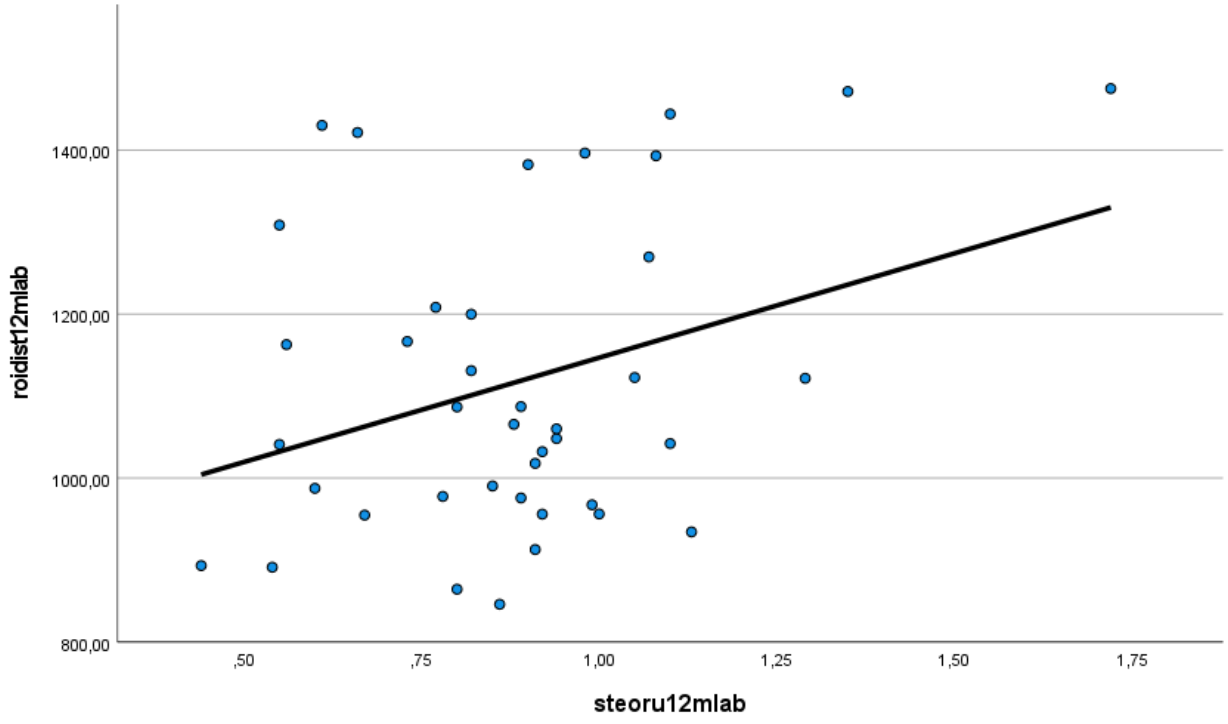

Graph 34. Correlation between Distal ROIs values and radio-ulnar steps at 12 months in LRDs (significant low positive correlation, r: 0,33, P:0.037).

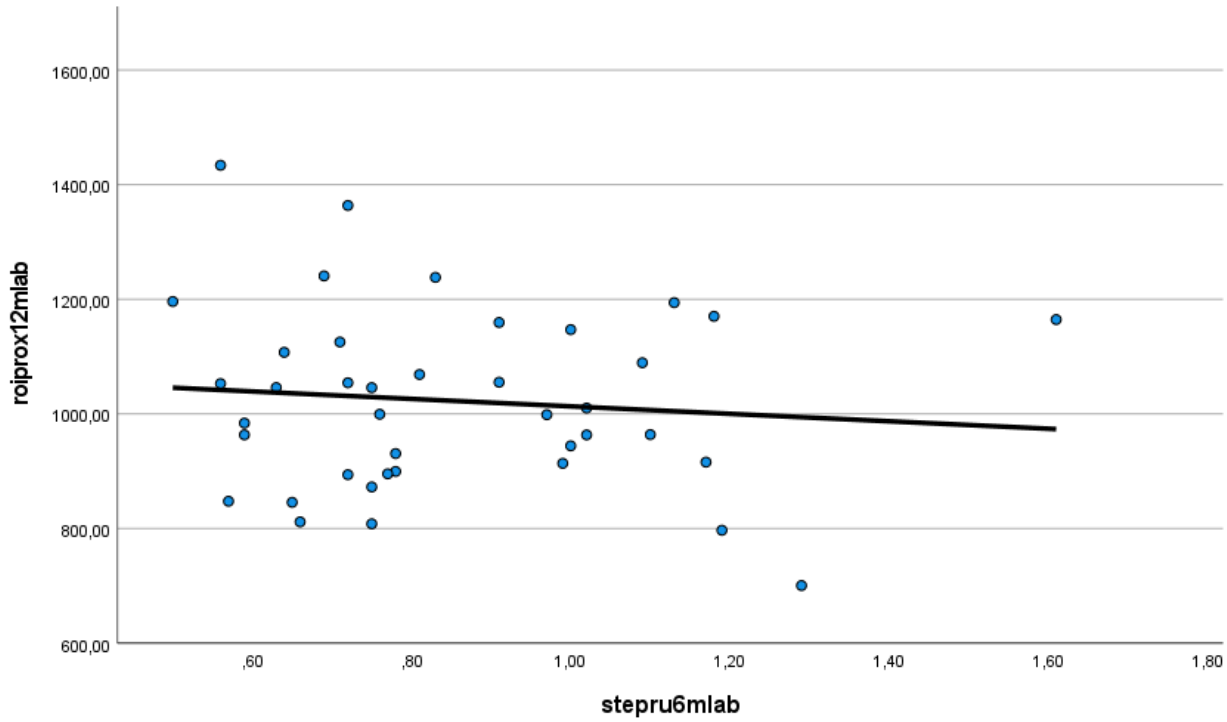

Graph 35. Correlation between Proximal ROIs values at 12 months and radio-ulnar steps at 6 months in LRDs (r: -0,09).

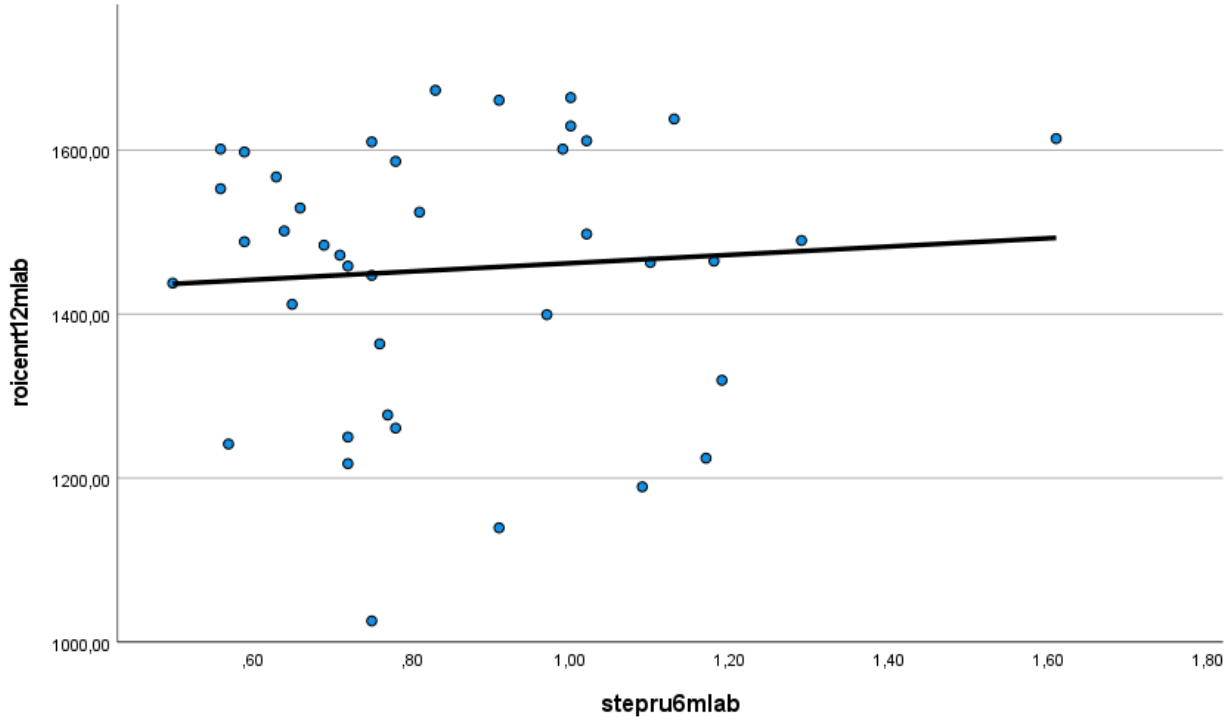

Graph 36. Correlation between Central ROI values at 12 months and radio-ulnar steps at 6 months in LRDs (r: 0,07).

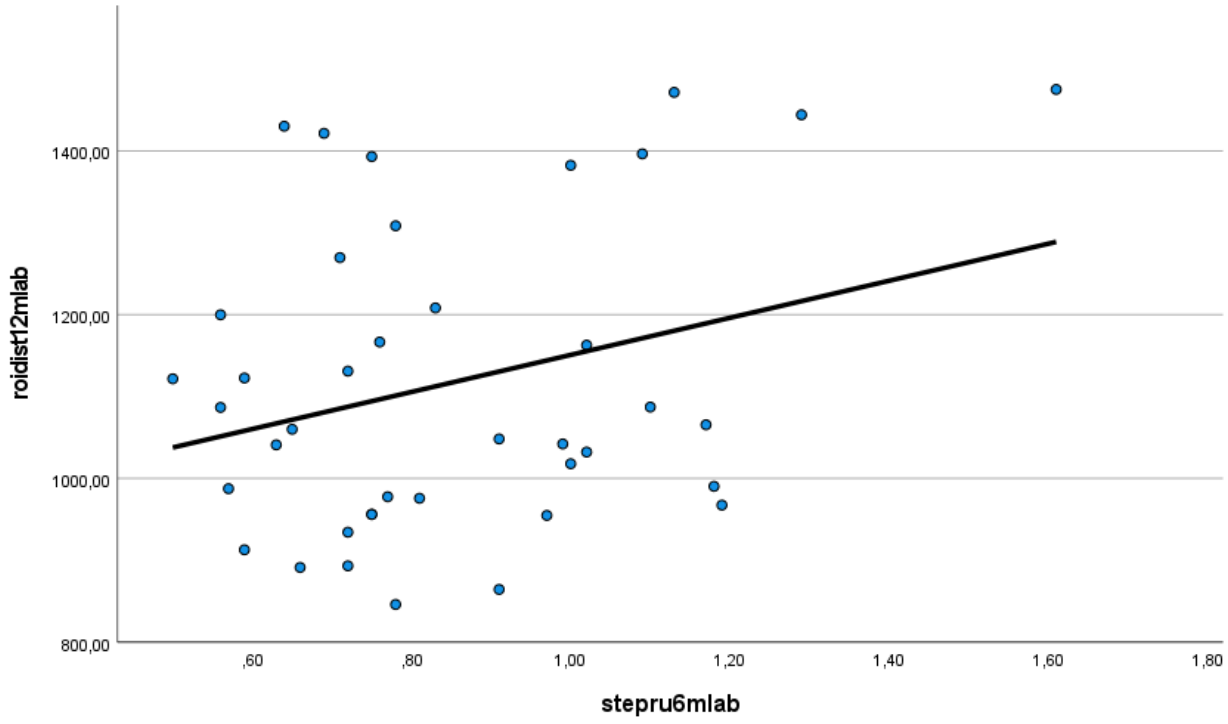

Graph 37. Correlation between Distal ROIs values at 12 months and radio-ulnar steps at 6 months in LRDs (r: 0,29).

Elliptical trochlear notch

The presence of a smaller, elliptical trochlear notch of the ulna, unfitting to accommodate a wider and rounder humeral trochlea, was mostly noticed in the German shepherd group, and as opposed to the other observed features, it did not change over time.

In fact, 27 elbows (39,7%) of GSDs at both 6 and 12 months of age presented an elliptical shaped notch, while only 3 (7,5%) elbows, two of the same subject, presented it in the LRDs population, all with concomitant FCP.

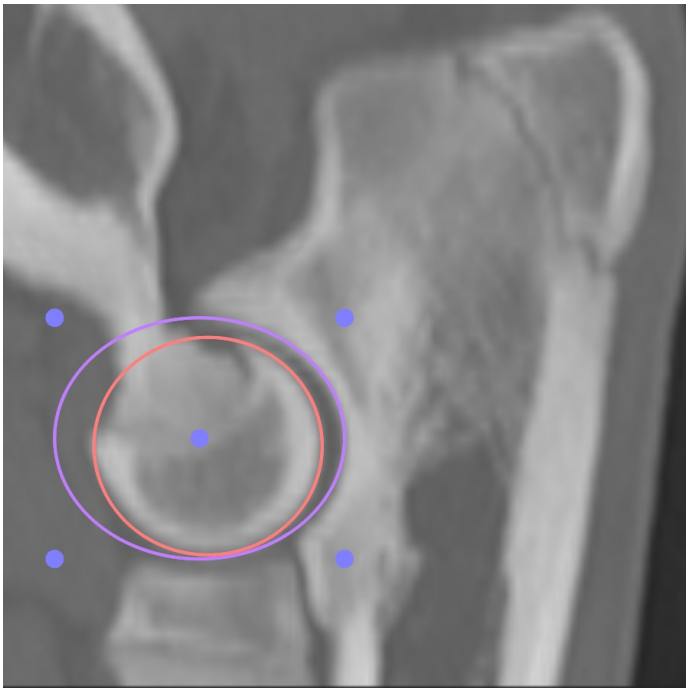

Figure 33. CT scan, sagittal view, elliptical trochlear notch in the left elbow joint of a male 6 months GSD. From the Veterinary Science Department of the University of Parma

An elliptical trochlear notch was found in 15 GSDs (44,1%), bilateral in 12 and unilateral in 3 of them. In 10 dogs (8 bilateral, 2 unilateral) it was concomitant to the presence of an FCP positive elbow – the same elbow among the 2 unilateral elliptical shaped subjects. (Figure 33)

The other elliptical trochlear notches were detected in 3 healthy dogs graded as 0 (2 bilateral, 1 unilateral), one dog graded as 1 and one dog graded as 2, bilaterally, both sclerotic.

The presence of an elliptical trochlear notch of the ulna was significantly associated with the development of elbow dysplasia in the GSDs population (P value: 0,017).

The radio-ulnar step was not significantly higher in dogs with elliptical trochlear notch.

Presence or absence of an ununited anconeal process

The presence of an ununited anconeal process (UAP) was found bilaterally in three German shepherd dogs, 2 males and 1 female, and observed at both ages, with a prevalence of 8,8% in our population. Two of these dogs had signs of radio-ulnar incongruency and an elliptical trochlear notch of different degree in both elbows. (Figure 34)

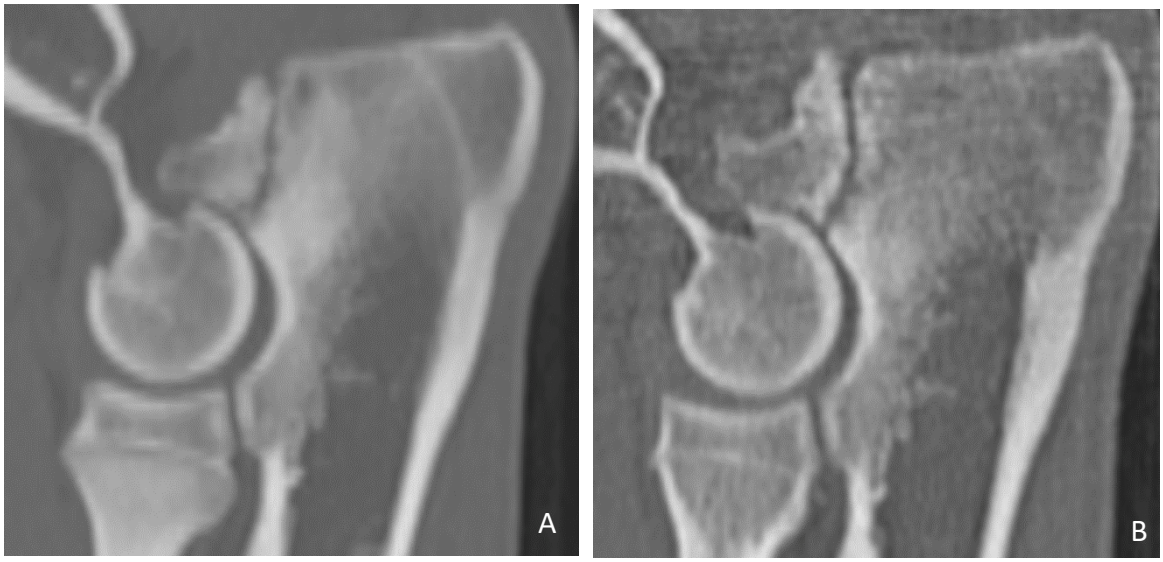

Figure 34. CT scans, sagittal views, left elbow joint of a female GSD affected by UAP from 6 month of age (A) to 12 months of age (B). From the Veterinary Science Department of the University of Parma

The third male GSD was presented at our clinic at 4 months of age with bilateral lameness and underwent radiologic examination that diagnosed bilateral UAP. The lameness was not present at 6 months old, and tomographic examination did not show a clear incongruence of the elbow joint bilaterally; in this patient, despite not having received any treatment, we observed an initial

spontaneous reunion of the anconeal process in both elbows, along with lower degrees in sclerosis and arthrosis in comparison with the other 4 UAP elbows. (Figure 35)

None of the Labrador retriever dogs showed any sign attributable to this pathology.

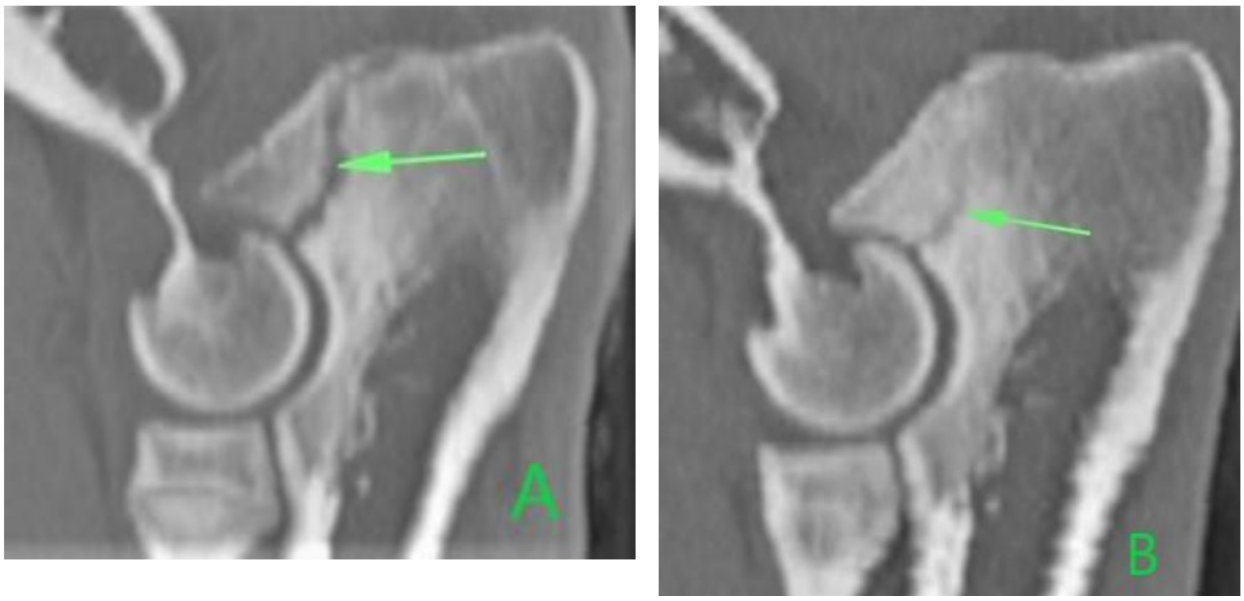

Figure 35. CT scans, sagittal views, left elbow joint of a male GSD affected by UAP, from 6 month of age (A) to 12 months of age (B); the green arrows indicate a radiolucent line that separate the anconeal process from the olecranon, only partially visible in figure B, where a partial spontaneous attachment of the anconeal process can be observed. From the Veterinary Science Department of the University of Parma

Elbow Dysplasia Score

The first whole tomographic evaluation at 6 months of age of the 68 elbow joints of the GSDs population and the 40 elbow joints of the LRDs population found respectively 24 GSDs elbows (35,3%) and 22 LRDs elbows (55%) negative for signs of CED. (Table 12 - 13 - 16)

Between the 44 (64,7%) positive GSDs joints, 12 (17,6%) were graded 3, 8 (11,7%) were graded 2 and 24 (35,9%) were graded 1.

In summary, of the 34 GSDs enrolled in this research, 24 (70,6%) were considered positive to ED changes at the tomographic evaluation at 6 months old; among these, 8 (23,5%) scored as 3, 3 (8,8%) scored as 2, and 13 (38,2%) scored as 1.

Between the 18 (45%) positive LRDs elbows, 4 (10%) were classified with an ED score of 3, 4 (10%) with an ED score of 2, and 10 (25%) with an ED score of 1.

Half of the 20 LRDs in this study had a positive ED score at 6 months of age, 3 (15%) graded 3, 2 (10%) graded 2, and the other 5 (25%) graded 1.

ED score at 6 months – LABRADOR RETRIEVERS		
ED SCORE	**N° patients**	**%**
Grado 0	10	50%
Grado 1	5	25%
Grado 2	2	10%
Grado 3	3	15%
TOTALE	20	

ED score at 6 months – GERMAN SHEPHERDS		
ED SCORE	**N° patients**	**%**
Grado 0	10	29,5%
Grado 1	13	38,2%
Grado 2	3	8,8%
Grado 3	8	23,5%
TOTALE	34	

Tables 12-13. Distribution of the Elbow Dysplasia score according to tomographic examinations at 6 months of age in GSDs and LRDs.

The final tomographic evaluation at 12 months of age of the 68 elbow joints of the GSDs population and the 40 elbow joints of the LRDs population found respectively 23 GSDs elbows (33,8%) and 18 LRDs elbows (45%) negative for signs of CED. (Table 14 - 15 - 16)

In the 45 (66,2%) positive GSDs elbows, 19 (27,9%) were graded as 3, 5 (7,3%) were graded as 2, and 21 (30,9%) as grade 1.

In particular, as at 6 months of age, 24 GSDs (70,6%) out of 34 had a positive final CED score at 12 months, but among these, up to 13 dogs (38,2%) scored as 3, 3 (8,8%) scored as 2, and 8 (23,6%) scored as 1.

At 12 months, twelve (80%) out of 15 males GSDs were positive, 5 with a grade 3 and 2 graded as 2. Of the 19 female GSDs, 12 (63,1%) had a positive score, of which 8 graded as 3 and 1 graded 2.

In the 22 (55%) positive LRDs elbows, 6 (15%) were graded as 3, 7 (17,5%) were graded as 2, and 9 (22,5%) had a grade 1.

The number of positive LRDs rose slightly up to 11 dogs (55%) out of 20 at 12 months, of which 5 (25%) scored as 3, 3 (15%) scored as 2, and finally 3 (15%) scored as 1.

At 12 months, seven (53,8%) out of 13 males LRDs were positive, 4 with a grade 3 and 2 graded as 2. Of the 7 female LRDs, 4 (57,1%) had a positive score, of which 1 graded as 3 and 1 graded 2.

ED score at 12 months – LABRADOR RETRIEVERS		
ED SCORE	**N° patients**	**%**
Grado 0	9	45%
Grado 1	3	15%
Grado 2	3	15%
Grado 3	5	25%
TOTALE	20	

ED score at 12 months – GERMAN SHEPHERDS		
ED SCORE	**N° patients**	**%**
Grado 0	10	29,5%
Grado 1	8	23,5%
Grado 2	3	8,8%
Grado 3	13	38,2%
TOTALE	34	

Tables 14-15. Distribution of the Elbow Dysplasia score according to tomographic examinations at 12 months of age in GSDs and LRDs.

German shepherd dogs	6 months	12 months	Labrador retriever dogs	6 months	12 months
1	3	3	1	3	3
2	3	3	2	1	2
3	3	3	3	0	1
4	0	0	4	0	0
5	1	3	5	1	2
6	0	0	6	1	0
7	1	0	7	0	0
8	1	3	8	1	3
9	1	0	9	1	0
10	3	3	10	0	1
11	1	3	11	2	2
12	2	3	12	2	3
13	0	1	13	3	3
14	3	3	14	0	0
15	0	0	15	0	0
16	2	2	16	0	1
17	0	0	17	3	3
18	1	1	18	0	0
19	1	1	19	0	0
20	1	1	20	0	0
21	1	1			
22	0	0			
23	2	3			
24	3	3			
25	1	1			
26	0	1			
27	3	3			
28	0	0			
29	1	2			
30	3	3			
31	1	1			
32	0	0			
33	0	0			
34	1	2			

Table 16. Elbow Dysplasia scores according to tomographic examinations at 6 and 12 months of age in GSDs and LRDs. Red cells represent female subjects, while blue cells represent male subjects.

8. DISCUSSION

The first aim of this research was to describe the computed tomographic features of healthy and CED affected elbow joints in a population of growing dogs of two different breeds, Labrador retriever and German shepherd, making, when possible, comparisons between the two breeds.

Labrador retrievers and German shepherds are well-known to have both a high prevalence of ED. In particular, the two breeds have reportedly been correlated and predisposed to specific manifestations of the condition, suggesting a different etiopathogenetic and pathophysiologic point of view. The high incidence of UAP in the German shepherd dog is well-known, although FCP is believed to have a high prevalence in this breed as well. On the other hand, the Labrador retriever has a higher occurrence of FCP, apparently most likely combined with OCD, and has been extensively studied for this pathology. (Kirberger and Fourie, 1998)

At 12 months of age, 24 out of 34 GSDs were given a CED positive grade, thus with a prevalence of the disease in this group of 70,6%; in particular, among these, 16 dogs (47%) had a score of 2 or 3.

In the LRDs group, at 12 months of age, the prevalence of CED positive subjects was 55% (11 dogs), with a 40% of dogs (8) graded as 2 or 3 due to already evident osteoarthrosis and/or sclerosis and the presence of a primary lesion.

Mean weight was similar in the two populations at both ages; it was a bit lower in the LRDs group at the mean age of 6 months as few 4 months old puppies were also included.

Males had generally a higher incidence of the pathology in the GSDs group, as according to literature. In the LRDs group the prevalence of positive dogs appeared slightly higher between females, but with lower grades and in a very small number of subjects.

While OCD lesions were not detected in any of the dogs of the present study, MCD was definitely the most represented pathology in our population, and we could observe a consistent prevalence of FCP in both breeds, surprisingly higher as up to 29,4% in GSDs, in contrast with a prevalence of 25% in LRDs.

On the other hand, UAP had a prevalence of 8,8% in our population of GSDs, while none was found in LRDs. Although this pathologic condition has been indicated as the most frequent form of elbow dysplasia in the German shepherd dog (Wind & Packard, 1986), its prevalence has progressively decrease in the recent years' reports, probably due to a relative ease in diagnosing this lesion by the standard ML flex projection of the screening protocol, thus consequent stricter breeding selection. Nonetheless, the GSD remains the most representative breed for the UAP.

Different forms of IC were observed in our GSDs group, in particular a radio-ulnar incongruity (RUI), mostly with what was interpreted as a shorter radius, and the presence of an elliptical trochlear notch. One of the dogs affected by bilateral UAP seemed to have a mild radio-ulnar incongruity with a shorter ulna, due to the absence of a step or even the presence of a "negative" step, while another had a visible elliptical notch.

Interestingly, the third UAP bilaterally affected German shepherd did not show any sign of RUI or alteration in the shape of the ulnar trochlear notch, ruling out IC as the underlying cause of the ununion of the anconeal process. In this patient, a spontaneous re-attachment of the process to the olecranon was witnessed at 12 months of age, without any treatment, in absence of lameness and with reduced signs of sclerosis and osteophytosis when compared to the other two UAP cases (Figure 35). Our hypothesis was that in this dog UAP manifested

primarily as a genetic condition and could undergo a partial spontaneous resolution properly in the absence of an incongruence or other underlying causes. A radiographic follow-up examination of this patient would be needed to better characterize its clinical evolution.

In regard to the incongruent joints, as described in the results, in some cases the radio-ulnar step appeared to be reduced at 12 months when compared to how it was perceived at 6 months (Figure 31). This finding could be caused by the concomitant fragmentation of the involved processes, either the medial coronoid process or the anconeal process, and consequent release of the pressure in the joint, that could therefore regain a better congruence.

The statistical analysis in the German shepherd group revealed a fair diagnostic accuracy in the detection of a radio-ulnar step. Even if the AUC result was acceptable, this finding was supported by a very significant U test in relation to the final ED score at 12 months of age, suggesting that the presence of a step in 6 months old GSDs could indicate a probable underlying MCD/FCP about to develop, if not already manifest.

Although this was not the aim of our study, it seems important to note that, as our population underwent radiographic examination at the same time of the computed tomographic exam, the radio-ulnar step appeared to be radiographically detectable in almost all the subjects where CT could identify it, even in absence of other findings. Therefore, our perception is that, whenever a radio-ulnar step is visible in an early radiographic screening of an elbow joint in this breed, it could be indicated to investigate it further by CT.

On the other hand, most of the measured steps were lower or slightly wider than 2 mm, so that ideally it was difficult to clearly link the MCD only to the presence of such thin steps, even though the elbow is a relatively small and tight joint. Except for one elbow with FCP, where only a radio-ulnar step graded as 2 was present, all the other elbows found positive for the fragmentation had also an elliptical trochlear notch. For this reason, our main

hypothesis was that in the GSDs group object of this study, IC of the elbow joint, and in particular the presence of an elliptical trochlear notch, was an important factor in the development of the other forms of elbow dysplasia, thus an underlying cause of either FCP or UAP in this breed population. In fact, the underdevelopment of the trochlear notch, already observed in the German shepherd dog by Wind (1986), can cause both FCP and UAP, sometimes even together, while increasing pressure over these processes, according to Hazewinkel & Lau (IEWG Proceedings, 2017). In fact, in our study the presence of an elliptical trochlear notch turned out to be statistically significative in the group of CED positive GSDs elbows. Our evaluation of the ulnar trochlear notch shape, though, was mostly subjective and based on outlining the notch in comparison with the drawn humeral trochlea circumference; a more objective method, that could eventually give additional information on the extent and the severity of an elliptical shape, may be needed to support our theory. Moreover, in the GSDs group, not all the elliptical trochlear notches were found in MCD elbows, but a lower prevalence was noted either in healthy elbows or sclerotic elbows with no signs of an evident radio-ulnar step. The rest of the elliptical trochlear notches were concomitant to both FCP and RUI, only one elbow with only FCP was noted.

In view of our results and all these past considerations, it was speculated that the compresence of an elliptical trochlear notch with even a small step could lead to the fragmentation of the coronoid process, therefore supposing a correlation between these two findings. But, surprisingly, no correlation could be found by the Pearson correlation coefficient test, leading to believe the two findings as independent.

In addition, all the operators found the MPR standardized positioning more difficult to obtain when evaluating the incongruent elbows of the GSDs, if compared to the normal, congruent joints. Also, in these elbows, when sclerosis was present, the pattern of subcortical sclerosis

was subjectively more inhomogeneous and ROIs measurements more difficult to achieve with a low standard deviation.

By contrast, in our population of Labrador retriever dogs, only one patient showed mild signs of incongruency in both its severely MCD affected elbows, and in fact neither the presence of radio-ulnar incongruity nor that of an elliptical trochlear notch were found significant in relation to the development of elbow dysplasia in this group of dogs. In fact, all the other evaluated elbows with MCD had a good congruence and, instead, all affected elbows had, as a main secondary sign of ED, principally an increased sclerosis of the ulnar trochlear notch.

This finding would be in accordance with what demonstrated by Lau et al. (2013) in a group of Labrador retriever puppies, where an alteration in subchondral ossification, thus osteochondrosis, was supposed as the main cause of FCP and MCD in this breed. Moreover, in a similar study (Lau et al., IEWG Proceedings, 2017), no difference in the length of radio and ulna was noticed between two groups of MCD positive and healthy Labrador retriever puppies, suggesting that IC is unlikely to play a role in MCD development in this breed.

In this framework, our study verted on the evaluation of specific ROIs of the ulnar trochlear notch in an attempt to find an objective, quantitative measurement method to define sclerosis of the subchondral bone through the tomographic examination.

Despite not having confirmed the predictive value found in the Proximal ROI in the preceding pilot study in the GSDs, it was interesting to observe the outstanding difference in the sclerosis distribution and extent in the two examined breeds.

In our evaluation of the ulnar trochlear notch ROIs, HU mean values of the LRDs group were in general consistently higher when compared to the GSDs group, especially in the central and distal regions (Table 6). This finding confirmed the results of a research by Villamonte-Chevalier et al. in 2016, where Labrador retriever dogs presented increased

values of HU and bone density (BD) in the MCP base and apex in comparison to Golden retriever dogs, suggesting the importance of a more breed-related approach. Moreover, as in this study, our canine population also showed HU values increasing with age in both breeds. On the other hand, while being significantly lower, HU values in the GSDs population appeared less predictable than LRDs values, especially in higher ED scored subjects. Whereas in LRDs an increased ED score, due to a fragmentation or fissuring of the coronoid, was usually linked to a dramatical increase in sclerosis as well, in the GSDs group this trend was far less present (Table 10) to the extent that, in few cases with a clear FCP, the trochlear notch sclerosis appeared less at 12 months when compared to 6 months in the same elbow. In our opinion, this appearance could be due to an eventual necrosis and/or rarefaction of the subchondral bone, consequent to the altered pressures inside the joint. Moreover, as previously described, most of the affected elbows in the GSDs group were also incongruent, and this characteristic made positioning more difficult, while the subchondral pattern appeared more inhomogeneous.

These considerations were confirmed by the statical analysis, where in the Labrador retrievers the trochlear notch sclerosis at both ages resulted as generally more significant in comparison with the GSDs. This could suggest that Distal ROIs, thus sclerosis in this particular area, could have a fair predictive value in the development of elbow dysplasia, according to our results.

In particular, in consensus with the literature, the Distal ROIs measurements, closer to the MCP, resulted in having a certain diagnostic accuracy at 6 months of age in both breeds, although with completely different HU values. However, in the LRDs group the accuracy was excellent and way more significative than in the other evaluated breed, as it was in fact confirmed by the significancy of the sclerosis also at 12 months in this same region.

In support to our results, a significant, even though low, positive correlation between radio-ulnar steps and attenuation values of the Distal ROIs was found in LRDs at 12 months of age; although RUI did not seem to play an important role in CED in this breed, this finding could confirm the potential value of sclerosis in the distal portion of the trochlear notch in the LRD.

Further studies on a larger number of dogs should be made to establish these measurements as possible early indicators of elbow dysplasia at 6 months. Even so, more than for their potential predictive value, the importance of these findings could be in determining a new method of studying subtrochlear sclerosis, making more objective comparisons between breeds. The evaluated measures appeared to have high reproducibility and repeatability between operators, regardless of experience level, and showed a very fast learning curve, so that they could be easily learned and performed. Therefore, they could be considered in view of a more breed-oriented etiopathogenetic research method.

In this context, morphologic conformations of the medial coronoid process were observed in the two breeds and several differences were noted.

GSDs had mostly narrower and pointy MCPs in comparison to LRDs, in which a round shaped, wider coronoid was most frequently seen.

In contrast to what affirmed by Klumpp et al. (2013), an irregular MCP was often seen in the GSDs, but only 4 out of the 13 observed at 6 months lead to a fragmentation over the given time. This type of conformation was not always linked to the presence of arthrosis, although graded as 1 in the medial coronoid disease score, but it was frequently involved in shape shifting of the MCP over time.

Changing of the conformation of the MCP were mostly observed in the GSDs population, but none of the observed shapes could be clearly associated with an increased risk of developing MCD; instead, it could be speculated, from this frequent changes, that the elbow

joint of the German shepherd is a more unstable joint when compared to Labrador retrievers, at least in our population, and more studies should be focused on gait distribution, joint contact patterns, and subchondral bone density distribution during growth in this breed.

In three Labrador retrievers' joints, a round MCP shifted to a flattened conformation over time. This finding was interpreted as a possible consequence of different pressures and gait distribution in the elbow joint in this breed, not necessarily associated to a pathologic development. In fact, it was noticed that the only elbow with a pointy MCP at 6 months underwent fragmentation at 12 months. From this finding we assumed that this rarely seen conformation in this breed could be more subject to pathological changes, as less resistant to an increased pressure on a narrower structure (as a pointy MCP visibly is compared to a round-shaped one), but further studies on a larger group of dogs are needed to verify this speculation.

In fact, in a study over the biomechanics in GSDs and LRDs by Humphries et al. (2020), the two breeds differed in terms of weight bearing and loading pattern on the joints, with the LRDs carrying almost 10% more of their weight on the forelimbs, and this could support our idea that in this breed, compared to the GSD, elbow joint pressures are more intense and differently borne.

Further studies could be made by measuring the mean HU values of the MCP area, or its bone density, in relation to the MCP different conformations.

The arthroscopic evaluation could also be useful to reveal the status of the overlying cartilage, adding more valuable information and better understanding on these CT findings.

As stated before, a better understanding of the gait analysis, loading distribution and contact patterns of elbow joints in different breeds, both healthy and affected, could help in deepening our knowledge in regard to the etiopathogenesis of elbow dysplasia.

Although there are several reports on computed tomographic evaluation of elbow joints in dogs, there is no standard protocol describing patient positioning, slice thickness and slice selection; in our study, patients of two different breeds at different ages underwent CT examination in sternal recumbency, with a slice thickness of 1mm and standard bone and soft tissue reconstruction, without showing any differences in the measurements and general evaluation or any artefact. No difference was noticed also between the CT scans from the single-slice scanner and those from the multi-slice scanner, although the use of a different machine in few cases could be considered a bias in our study.

Other limitations of this research are first of all the limited number of dogs tested, in particular in the Labrador retriever group, which may have influenced the representativeness of our study; on the other hand, although all dogs came from the same breeders and lived in a similar environment, with similar activity and feeding, an additive role of environmental factors on the development of elbow dysplasia cannot be completely excluded in our etiopathogenetic hypothesis. Lastly, the use of arthroscopy for supporting definitive diagnosis and evaluation of the elbow joints could have made our study more complete, and more accurate in discerning affected from sane at all ages and in detecting all specific alteration; in particular regarding joint incongruity, arthroscopy results to have the highest diagnostic value for this alteration compared to radiography and CT, allowing a direct joint inspection. Even so, the value of arthroscopy as a routine screening tool can be questioned, because of its invasive nature and the high experience needed to interpret the signs of incongruity. (Samoy et al., 2012)

9. CONCLUSIONS

Our results suggest that a more breed-oriented approach could be pivotal in the study of the elbow joint and consequently of elbow dysplasia etiopathogenesis and pathophysiology. In this context, computed tomography could have a central role by giving a clear overview of the joint surfaces without any superimposition, allowing tridimensional reconstructions, while being a minimally invasive procedure.

This study also allowed us to suppose an important role of computed tomography in the evaluation of elbow joints particularly at an early stage. An early diagnosis could then be fundamental in leading to a correct treatment plan and/or prognosis, and CT could therefore intervene whenever radiology results unclear, to better characterize the disease.

In the population of this study, FCP/MCD was the most frequent form of elbow dysplasia in both breeds. However, each group presented a different type of this disease, with characters and lesions specific of the breed. In the GSD, IC was the underlying condition and almost no sclerosis was present with lower HU values. On the other hand, in the LRD the most probable cause of FCP/MCD appeared to be the development of osteochondrosis, with subtrochlear sclerosis as the main manifestation and much higher HU values in the subchondral bone. According to our results, in the two evaluated groups of German shepherds and Labrador retrievers elbow dysplasia appear to have a completely different etiopathogenetic hypothesis, and this finding should be considered in future studies on these breeds.

In conclusion, further breed specific studies throughout growth and comparisons between canine breeds would be necessary to determine the potential role of CT as a diagnostic imaging technique complementary to radiology in the evaluation of canine elbow dysplasia, able to show specific characters and different manifestations of the same pathology especially at an early stage, and as a valuable method of improving the current understanding of this complex pathology, in particular regarding its etiopathogenesis, which still remains unclear.

BIBLIOGRAPHY

1. Alves-Pimenta, S., Ginja, M. M., & Colaço, B. (2019). Role of elbow incongruity in canine elbow dysplasia: advances in diagnostics and biomechanics. *Veterinary and Comparative Orthopaedics and Traumatology*, *32*(02), 087-096.
2. Barone R. (2004) Anatomia comparata dei mammiferi domestici. Vol I, Osteologia. Edagricole; 447-473
3. Barone R. (2004) Anatomia comparata dei mammiferi domestici. Vol.II parte 1, Artrologia. Edagricole; 116-128
4. Boroffka S.A.E.B. (2015) Dog Positioning for Radiology of the Elbow. Proceedings of 29° IEWG Meeting, Bangkok, p. 17-22.
5. Burton NJ,Warren-Smith CM, Roper DP, Parsons KJ. (2013) CT assessment of the influence of dynamic loading on physiological incongruency of the canine elbow. *J Small Anim Pract*; 54(06):291–298
6. Burton, N. J., Comerford, E. J., Bailey, M., Pead, M. J., & Owen, M. R. (2007). Digital analysis of ulnar trochlear notch sclerosis in Labrador retrievers. *Journal of Small Animal Practice*, *48*(4), 220-224.
7. Burton, N. J., Perry, M. J., Fitzpatrick, N., & Owen, M. R. (2010). Comparison of bone mineral density in medial coronoid processes of dogs with and without medial coronoid process fragmentation. *American journal of veterinary research*, *71*(1), 41-46.
8. Burton, N., & Owen, M. (2008). Canine elbow dysplasia 1. Aetiopathogenesis and diagnosis. *In practice*, *30*(9), 508-512.
9. Carmichael. S. (1998) Fractures in skeletally immature animals. In A. Coughlan, A. Miller "BSAVA Manual of Small Animal Fracture Repair and Management*",*103-109.

10. Caron A, Caley A, Farrell M, Fitzpatrick N. (2014) Kinematic gait analysis of the canine thoracic limb using a six degrees of freedom marker set. Study in normal Labrador Retrievers and Labrador Retrievers with medial coronoid process disease. *Vet Comp Orthop Traumatol*; 27(06):461–469
11. Cook, C. R., & Cook, J. L. (2009). Diagnostic imaging of canine elbow dysplasia: a review. *Veterinary Surgery*, *38*(2), 144-153.
12. Coppieters, E., Gielen, I., Verhoeven, G., Van Vynckt, D., & Van Ryssen, B. (2015). Erosion of the medial compartment of the canine elbow: occurrence, diagnosis and currently available treatment options. *Veterinary and Comparative Orthopaedics and Traumatology*, *28*(01), 9-18.
13. Debruyn, K., Peremans, K., Vandermeulen, E., Van Ryssen, B., & Saunders, J. H. (2013). Evaluation of semi-quantitative bone scintigraphy in canine elbows. *The Veterinary Journal*, *196*(3), 424-430.
14. DeCamp CE, Soutas-Little RW, Hauptman J, Olivier B, Braden T, Walton A. (1993) Kinematic gait analysis of the trot in healthy greyhounds. *Am J Vet Res*; 54(04):627–634
15. Dickomeit MJ, Böttcher P, Hecht S, Liebich HG, Maierl J. (2011) Topographic and age-dependent distribution of subchondral bone density in the elbow joints of clinically normal dogs. *Am J Vet Res*; 72(04):491–499
16. Draffan, D., Carrera, I., Carmichael, S., Heller, J., & Hammond, G. (2009). Radiographic analysis of trochlear notch sclerosis in the diagnosis of osteoarthritis secondary to medial coronoid disease. *Veterinary and Comparative Orthopaedics and Traumatology*, *22*(01), 7-15.

17. Eckstein, F., Lohe, F., Muller-Gerbl, M., Steinlechner, M., & Putz, R. (1994). Stress distribution in the trochlear notch. A model of bicentric load transmission through joints. *The Journal of bone and joint surgery. British volume*, *76*(4), 647-653.

18. Evans, Howard E., and Alexander De Lahunta. (2013) Miller's Anatomy of the Dog. 4th ed. Elsevier Health Sciences; 169; 42

19. F. M. Martini. (2006) Patologie articolari nel cane e nel gatto. Poletto Editore; 133-154

20. Fitzpatrick, Noel, and Russell Yeadon. "Working algorithm for treatment decision making for developmental disease of the medial compartment of the elbow in dogs." *Veterinary Surgery* 38.2 (2009): 285-300

21. Franklin, S. P., Burke, E. E., & Holmes, S. P. (2017). Utility of MRI for characterizing articular cartilage pathology in dogs with medial coronoid process disease. *Frontiers in veterinary science*, *4*, 25.

22. Gasch E.G., Labruyère J.J., Bardet J.F. (2012) Computed tomography of ununited anconeal process in the dog. *Veterinary and Comparative Orthopaedics and Traumatology*, 25, Nr. 6; 498–505

23. Gemmill, T. J., Mellor, D. J., Clements, D. N., Clarke, S. P., Farrell, M., Bennett, D., & Carmichael, S. (2005). Evaluation of elbow incongruency using reconstructed CT in dogs suffering fragmented coronoid process. *Journal of small animal practice*, *46*(7), 327-333.

24. Gielen I. and Villamonte-Chevalier A. (2018) Strength and limitations of radiography, scintigraphy, ultrasound, CT, MRI and arthroscopy to diagnose Elbow Dysplasia in lame dogs. Proceedings of 32° IEWG Meeting, Barcelona, p. 13-16

25. Gielen I., Villamonte-Chevalier A., Broeckx B.J.G., van Bree H. (2017) Different imaging modalities in ED; what is their specific added value? Proceedings of 31° IEWG Meeting, Verona, p. 5-8.
26. Hazewinkel H.A.W. (2018) Prevalence of elbow dysplasia, and pathogenesis of FCP in young Labradors. Proceedings of 32° IEWG Meeting, Barcelona, p. 5-11.
27. Hazewinkel H.A.W. & Lau S.F. (2017) Early development of FCP and the value of radiology and CT to detect FCP. Proceedings of 31° IEWG Meeting, Verona, p. 9-14
28. Hebel, M., Panek, W. K., Ruszkowski, J. J., Nabzdyk, M., Niedzielski, D., Pituch, K. C., Pomorska-Mól, M. (2021). Computed tomography findings in a cohort of 169 dogs with elbow dysplasia-a retrospective study. *BMC Veterinary Research*, *17*(1), 1-12.
29. Heng H.G. (2015) Dog Radiograph for FCP, OCD, UAP and Elbow Incongruity, Additional Value of Extra Views or Other Imaging Modalities. Proceedings of 29° IEWG Meeting, Bangkok, p. 25-26.
30. Hosmer D.W., Lemeshow S. (2000) Applied Logistic Regression, 2nd Ed. Chapter 5, John Wiley and Sons, New York, NY, pp. 160-164
31. How K.L. (2016) Clinical signs of Elbow Dysplasia and Osteoarthritis. Proceedings of 30° IEWG Meeting, Vienna, p. 5-7.
32. Humphries, A., Shaheen, A. F., & Álvarez, C. G. (2020). Different conformations of the German shepherd dog breed affect its posture and movement. *Scientific reports*, *10*(1), 1-16.
33. Humphries, A., Shaheen, A. F., & Gómez Álvarez, C. B. (2020). Biomechanical comparison of standing posture and during trot between German shepherd and Labrador retriever dogs. *PloS one*, *15*(10), e0239832.
34. Kealy, R. D., Lawler, D. F., Ballam, J. M., Lust, G., Biery, D. N., Smith, G. K., & Mantz, S. L. (2000). Evaluation of the effect of limited food consumption on radiographic

evidence of osteoarthritis in dogs. *Journal of the American Veterinary Medical Association*.

35. Kirberger, R. M., & McEvoy, F. J. (2016). *BSAVA manual of canine and feline musculoskeletal imaging* (No. Ed. 2). British Small Animal Veterinary Association.
36. Kirberger, R. M., and S. L. Fourie. (1998) "Elbow dysplasia in the dog: pathophysiology, diagnosis and control: review article." *Journal of the South African Veterinary Association* 69.2: 43-54.
37. Klumpp, S., Karpenstein, H., Tellhelm, B., Failing, K., & Kramer, M. (2013). Computed tomography morphology and anatomy of the elbow joint of specific dog breeds focusing on the medial coronoid process in ED 0 scored dogs. *Kleintierpraxis*, *58*(2), 57-64.
38. König, Horst Erich, Hans-Georg Liebich, and Hermann Bragulla. (2004) Veterinary anatomy of domestic mammals: textbook and colour atlas. *Schattauer Verlag*; 150-152
39. Kramer, A., Holsworth, I. G., Wisner, E. R., Kass, P. H., & Schulz, K. S. (2006). Computed tomographic evaluation of canine radioulnar incongruence in vivo. *Veterinary Surgery*, *35*(1), 24-29.
40. L. Nardella. (2010) “Disturbi di crescita dell’avambraccio del cane. Esperienze di terapia con l’apparato di Ilizarov.” Scuola di Dottorato di Ricerca in Scienze Cliniche e Farmaco-Tossicologiche Veterinarie. Università degli Studi di Napoli Federico II
41. Lappalainen, A. K., Hyvärinen, T., Junnila, J., & Laitinen-Vapaavuori, O. (2016). Radiographic evaluation of elbow incongruity in Skye terriers. *Journal of Small Animal Practice*, *57*(2), 96-99.
42. Lau S.F. (2015) The etiology of Medial Coronoid Disease. Proceedings of 29° IEWG Meeting, Bangkok, p. 31-33.

43. Lau S.F. and Voorhout G. (2015) Dog Positioning for CT Scanning of the Elbow Joints. Proceedings of 29° IEWG Meeting, Bangkok, p. 23-24.
44. Lau S.F., Hazewinkel H.A.W., Voorhout G. (2017) Radiographic and CT assessment of postnatal development of antebrachia and elbow joints in Labrador Retrievers. Proceedings of 31° IEWG Meeting, Verona, p. 15
45. Lau SF, Hazewinkel HA, Voorhout G. (2015) Radiographic and computed tomographic assessment of the development of the antebrachia and elbow joints in Labrador Retrievers with and without medial coronoid disease. *Vet Comp Orthop Traumatol*; 28(03):186–192
46. Lau, S. F., Wolschrijn, C. F., Hazewinkel, H. A. W., Siebelt, M., & Voorhout, G. (2013). The early development of medial coronoid disease in growing Labrador retrievers: radiographic, computed tomographic, necropsy and micro-computed tomographic findings. *The Veterinary Journal*, *197*(3), 724-730.
47. Lewis D.D., Parker R.B., Hager D.A. (1989) Fragmented medial coronoid process of the canine elbow. *Compendium on Continuing Education for the Practicing Veterinarian (Small Animals)* 11: 703–715
48. Lusetti, Filippo. (2014) "La displasia di gomito nel cane approccio preventivo." Aivpa Journal 3.4: 30-37.
49. Manfredi, S., Di Ianni, F., Di Girolamo, N., Canello, S., Gnudi, G., Guidetti, G., Miduri, F., Fabbi, M., Daga, E., Parmigiani, E., Centenaro, S., & Volta, A. (2018). Effect of a commercially available fish-based dog food enriched with nutraceuticals on hip and elbow dysplasia in growing labrador retrievers. *Canadian Journal of Veterinary Research*, 82(2), 154–158.
50. Michelsen, J. (2013). Canine elbow dysplasia: Aetiopathogenesis and current treatment recommendations. *Veterinary Journal*, *196*(1), 12–19.

51. Moores, Andrew P., Livia Benigni, and Christopher R. Lamb. (2008) Computed tomography versus arthroscopy for detection of canine elbow dysplasia lesions. *Veterinary Surgery* 37.4: 390-398.
52. Murino, C. (2017). Esame TC in corso di Displasia del gomito del cane.
53. Nap R.C. (1995) Pathophysiology and clinical aspects of canine elbow dysplasia. Proceedings of 7° IEWG, Constance, Germany, p.6-8
54. Narojek, T., Fiszdon, K. & Hanysz, E. (2008). Canine elbow dysplasia in different breeds. *Bulletin of the Veterinary Institute in Puławy*, *52*(1).
55. Olsson S.E. (1983) The early diagnosis of fragmented coronoid process and osteochondritis dissecans of the canine elbow joint. *Journal of the American Animal Hospital Association* 19: 616–626
56. Ondreka N. and Tellhelm B. (2017) Explanation of grading according to IEWG and discussion of cases. Proceedings of 31° IEWG Meeting, Verona. p. 17-22
57. Ondreka, N., Von Pückler, K., & Tellhelm, B. (2016) Canine elbow dysplasia CT based assessment and grading. In *Proceedings of the 30th International Elbow Working Group Meeting, Vienna, Austria* (pp. 19-32).
58. Padgett G.A., Mostosky U.V., Probst C.W., Thomas M.W., Krecke C.F. (1995) The inheritance of osteochondritis dissecans and fragmented coronoid process of the elbow joint in Labrador retrievers. *Journal of the American Animal Hospital Association* 31, 327–330.
59. Palmer, R. (2015). Arthroscopic evaluation and treatment of the dysplastic elbow. Proceedings of 29° IEWG Meeting, Bangkok. p. 11-14.
60. Palmer, R. (2018). Surgical Treatment of Canine Elbow Dysplasia (MCPD, UAP, OCD, EI). Proceedings of 33° IEWG Meeting, Singapore. p. 14-21.

61. Preston CA, Schulz KS, Kass PH. (2000) In vitro determination of contact areas in the normal elbow joint of dogs. Am J Vet Res; 61(10):1315–1321

62. Reichle J.K., Park R.D., and Bahr A.M. (2000) “Computed tomographic findings of dogs with cubital joint lameness.” *Veterinary Radiology & Ultrasound*, 41.2, 125-130.

63. Reichle, Jean K., and Frédéric Snaps. (1999) "The elbow." Clinical techniques in small animal practice 14.3, 177-186.

64. Remy, D., Neuhart, L., Fau, D., & Genevois, J. P. (2004). Canine elbow dysplasia and primary lesions in German shepherd dogs in France. *Journal of Small Animal Practice*, *45*(5), 244–248.

65. Roush, J. K., Dodd, C. E., Fritsch, D. A., Allen, T. A., Jewell, D. E., Schoenherr, W. D., Richardson, D. C., Leventhal, P. S., & Hahn, K. A. (2010). Multicenter veterinary practice assessment of the effects of omega-3 fatty acids on osteoarthritis in dogs. *Journal of the American Veterinary Medical Association*.

66. Rycke, L. M. D., Gielen, I. M., Bree, H. V., & Simoens, P. J. (2002). Computed tomography of the elbow joint in clinically normal dogs. *American Journal of Veterinary Research*, *63*(10), 1400-1407.

67. Sallander, M. H., Hedhammar, Å., & Trogen, M. E. H. (2006). *Diet, Exercise, and Weight as Risk Factors in Hip Dysplasia and Elbow Arthrosis in Labrador Retrievers*. *136*(8), 1935–1939.

68. Samoy, Y., Gielen, I., Saunders, J., van Bree, H., & Van Ryssen, B. (2012). Sensitivity and specificity of radiography for detection of elbow incongruity in clinical patients. *Veterinary Radiology & Ultrasound*, *53*(3), 236-244.

69. Samoy, Yves, et al. (2006) "Review of the literature Elbow incongruity in the dog." *Veterinary and Comparative Orthopaedics and Traumatology* (VCOT) 19.1, 1-8.

70. Schulz K. (2013) “Diseases of the joints”, in Fossum, T.W. ed: Small animal surgery textbook. Elsevier Health Sciences, 1143-1309.

71. Sjostrom, L., H. Kasstrom, and M. Kallberg. (1995) Ununited anconeal process in the dog. Pathogenesis and treatment by osteotomy of the ulna. *Veterinary and comparative orthopaedics and traumatology*: VCOT.

72. Sjöström, L., Kasström, H., & Källberg, M. (1995). Ununited Anconeal Process in the Dog. Pathogenesis and Treatment by Osteotomy of the Ulna. *Veterinary and Comparative Orthopaedics and Traumatology*.

73. Slater, M. R., Scarlett, J. M., Donoghue, S., Kaderly, R. E., Bonnett, B. N., Cockshutt, J., & Erb, H. N. (1992). Diet and exercise as potential risk factors for osteochondritis dissecans in dogs. *American Journal of Veterinary Research*, 53(11), 2119–2124.

74. Snaps FR, Balligand MH, Saunders JH, Park RD, Dondelinger RF (1997): Comparison of radiography, magnetic resonance imaging, and surgical findings in dogs with elbow dysplasia. *American Journal of Veterinary Research* 58, 1367–1370.

75. Theyse L.F.H. (2018) Clinical, diagnostic and pathological findings in Canine Elbow Dysplasia. Proceedings of 32° IEWG Meeting, Barcelona. p. 17-18.

76. Tobias, Karen M., and Spencer A. Johnston. (2013) Veterinary surgery: small animal: 2-Volume Set. Elsevier Health Sciences.

77. Todd Trostel, C., Pool, R. R., & McLaughlin, R. M. (2003). Canine Lameness Caused by Developmental Orthopedic Diseases: FCP and UAP. *Compendium on Continuing Education for the Practicing Veterinarian*, *25*(4), 282–293.

78. Válega, A., Alves-Pimenta, S., McEvoy, F. J., Nielsen, D. H., & Ginja, M. (2021). Digital analysis of subtrochlear sclerosis in elbows submitted for dysplasia screening. *Frontiers in veterinary science*, *8*.

79. Vandeweerd, J. M., Coisnon, C., Clegg, P., Cambier, C., Pierson, A., Hontoir, F., Saegerman, C., Gustin, P., & Buczinski, S. (2012). Systematic Review of Efficacy of Nutraceuticals to Alleviate Clinical Signs of Osteoarthritis. In *Journal of Veterinary Internal Medicine*.

80. Vannini, R. (2015). Treatment Strategies in the Growing and Adult Dog with Elbow Disease. Proceedings of 29° IEWG Meeting, Bangkok 2015. p. 27-30.

81. Vezzoni, A., & Benjamino, K. (2021). Canine Elbow Dysplasia: Ununited Anconeal Process, Osteochondritis Dissecans, and Medial Coronoid Process Disease. *Veterinary Clinics: Small Animal Practice*, *51*(2), 439-474.

82. Villamonte-Chevalier, A., Dingemanse, W., Broeckx, B. J. G., Van Caelenberg, A., Agut, A., Duchateau, L., van Bree H. & Gielen, I. (2016). Bone density of elbow joints in Labrador retrievers and Golden retrievers: Comparison of healthy joints and joints with medial coronoid disease. *The Veterinary Journal*, *216*, 1-7.

83. von Pückler, K. H., Ondreka N., Tellhelm B. (2016) Elbow Dysplasia: Computed tomography standards, protocols and quality assurance. Proceedings of 30° IEWG Meeting, Vienna. p. 17-18

84. Wind P., Packard M. E. (1986) Elbow incongruity and developmental elbow diseases in the dog: Part II. *Journal of the American Animal Hospital Association* 22: 725–735

85. Zweifel, R. T., DiDonato, P., Hartmann, A., Kramer, M., & von Pückler, K. H. (2020). Improved computed tomography accuracy with a 1-mm versus 2-or 3-mm slice thickness for the detection of medial coronoid disease in dogs. *Veterinary and Comparative Orthopaedics and Traumatology*, *33*(01), 045-050.